



THESIS APPROVAL
GRADUATE SCHOOL, KASETSART UNIVERSITY

Master of Engineering (Chemical Engineering)

DEGREE

Chemical Engineering

FIELD

Chemical Engineering

DEPARTMENT

TITLE: Study of Kinetic Rate of Heterogeneous Catalysts for Biodiesel Production

NAME: Mr. Kasamar Petchtabtim

THIS THESIS HAS BEEN ACCEPTED BY

THESIS ADVISOR

(Associate Professor Thongchai Srinophakun, Ph.D.)

DEPARTMENT HEAD

(Associate Professor Paisan Kongkachuichay, Ph.D.)

APPROVED BY THE GRADUATE SCHOOL ON _____

DEAN

(Associate Professor Gunjana Theeragool, D.Agr.)

THESIS

STUDY OF KINETIC RATE OF HETEROGENEOUS CATALYSTS
FOR BIODIESEL PRODUCTION

KASAMAR PETCHTABTIM

A Thesis Submitted in Partial Fulfillment of
the Requirements for the Degree of
Master of Engineering (Chemical Engineering)
Graduate School, Kasetsart University

2009

Kasamar Petchtabtim 2009: Study of Kinetic Rate of Heterogeneous Catalysts for Biodiesel Production. Master of Engineering (Chemical Engineering), Major Field: Chemical Engineering, Department of Chemical Engineering. Thesis Advisor: Associate Professor Thongchai Srinophakun, Ph.D. 149 pages.

Kinetic rate equation of the transesterification of palm olein with methanol (biodiesel production) is reported. Firstly, the effect of mass transfer resistance on the kinetic rate was investigated using a different speed of agitator that is 500, 700 and 1000 rpm. For the kinetic study, both Pseudo-homogeneous (PH) and Langmiur-Hinshelwood (LH) kinetic models were used and evaluated to find the suitable model that could be described the kinetic rate data. The experiments were carried out at 328, 333 and 338 K by a strontium oxide as solid catalysts. In order to estimate related parameters, the genetic algorithm (GA) was used to find the chemical reaction rate constant. The values of operator in GA were tune to address the best performance.

Overall, the mass transfer resistance was not shown the effect on the reaction rate while the reaction temperature played the more effect on the reaction rate. The reaction rate was increased with increasing the temperature. Both kinetic models showed the suitable results to explain and predict the kinetic results. In case of PH model, the activation energy of hydrolysis triglyceride, diglycerides, monoglycerides and reversible of monoglycerides were 70.28, 33.34, 250 and – 85.24 kJ/mol; respectively. The best value of population size, generation number, crossover fraction, mutation rate, migration fraction and hybrid function for GA operators were 100, 100, 0.8, 0.01, 0.2 and none, respectively.

Student's signature

Thesis Advisor's signature

____ / ____ / ____

ACKNOWLEDGMENTS

I would like to express my sincere gratitude to my advisor, Assoc. Prof. Dr. Thongchai Srinophakun for his encouragement and valuable suggestions to this work.

Furthermore, I would like to express gratitude to Miss Peesamai Jenvanitpanjakul, Deputy Governor Research & Development, Thailand Institute of Scientific and Technological Research (TISTR), for giving me a big chance in my life and suggestion with love. I would like to sincerely thank to Mr. Yoothana Thanmongkhon and Mrs. Panida Thepkhun who is a researcher at energy department of TISTR, for our help and support throughout my master's degree.

Finally, I would like to express gratitude to my parents, brother, sisters, and my friends for giving me a chance and recommendation with love.

Kasamar Petchtabtim

November 2008

TABLE OF CONTENTS

	Page
TABLE OF CONTENTS	i
LIST OF TABLES	ii
LIST OF FIGURES	v
LIST OF ABBREVIATIONS	ix
INTRODUCTION	1
OBJECTIVES	3
LITERATURE REVIEW	5
MATERIALS AND METHODS	58
Materials	58
Methods	60
RESULTS AND DISCUSSION	75
CONCLUSIONS AND RECOMMENDATIONS	112
Conclusion	112
Recommendation	113
LITERATURE CITED	115
APPENDICES	119
Appendix A Experimental results from gas chromatograph	120
Appendix B Standard solution of gas chromatography	123
Appendix C Estimation of TG, DG and MG molecular weight in palm olein oil	126
Appendix D Genetic algorithm tool user manual	128
Appendix E Analysis method for biodiesel sample	131
Appendix F MATLABTM code for pseudo-homogeneous model	140
Appendix G MATLABTM code for pseudo-homogeneous model	144
CIRRICULUM VITAE	149

LIST OF TABLES

Table		Page
1	Term in the generalized formulation of Langmuir-Hinshewood kinetic model	25
2	Sample of data matrix	28
3	Two-way analysis of variance	31
4	The different characteristics between the conventional optimization and GA method	34
5	The decimal number of the binary number	39
6	The position of mutated genes in mutated chromosomes	51
7	The experimental data of transesterification that showed the effect of agitator speeds and reaction times on the diglyceride and triglyceride concentration.	77
8	The experimental data of transesterification that showed the effect of agitator speeds and reaction times on the glyceride and monoglyceride concentration.	78
9	The two-way analysis of variance of triglyceride concentration by MATLAB statistic toolbox at the speed of 500, 700 and 1000 rpm	79
10	The two-way analysis of variance of diglyceride concentration by MATLAB statistic toolbox at the speed of 500, 700 and 1000 rpm	80
11	The two-way analysis of variance of monoglycerides concentration by MATLAB statistic toolbox at the speed of 500, 700 and 1000 rpm	81
12	The two-way analysis of variance of monoglycerides concentration by MATLAB at the agitator speed of 700 and 1000 rpm	82

LIST OF TABLES (Continued)

Table		Page
13	GA parameters and results of population size value for the kinetic rate constant of PH model at $T = 65^{\circ}\text{C}$	84
14	GA parameters and results of population size value for the kinetic rate constant of LH model at $T = 65^{\circ}\text{C}$	84
15	GA parameters and results of generation number for the kinetic rate constant of PH model at $T = 65^{\circ}\text{C}$	85
16	GA parameters and results of generation number for the kinetic rate constant of LH model at $T = 65^{\circ}\text{C}$	86
17	GA parameters and results of crossover fraction value for the kinetic rate constant of PH model at $T = 65^{\circ}\text{C}$	87
18	GA parameters and results of crossover fraction value for the kinetic rate constant of LH model at $T = 65^{\circ}\text{C}$	87
19	GA parameters and results of mutation fraction value for the kinetic rate constant of PH model at $T = 65^{\circ}\text{C}$	88
20	GA parameters and results of mutation fraction value for the kinetic rate constant of LH model at $T = 65^{\circ}\text{C}$	89
21	GA parameters and results of migration fraction value for the kinetic rate constant of PH model at $T = 65^{\circ}\text{C}$	90
22	GA parameters and results of migration fraction value for the kinetic rate constant of LH model at $T = 65^{\circ}\text{C}$	90
23	GA parameters and results of migration fraction value for the kinetic rate constant of PH model at $T = 65^{\circ}\text{C}$	99

LIST OF TABLES (Continued)

Table		Page
24	GA parameters and results of migration fraction value for the kinetic rate constant of LH model at $T = 65^{\circ}\text{C}$	92
25	The fitness value ($\times 10^3$) of LH model of type 1 and 2 that based on the irreversible reaction and reversible reaction in step 3 at 65°C of reaction temperature	105
26	The fitness value ($\times 10^3$) of PH and LH type 1 model that based on the irreversible reaction and reversible reaction in step 3 at 65°C of reaction temperature	107
27	The kinetic reaction rate constants of PH model with FAME concentration at various temperatures	108
28	Energy of activation (J/mol) of transesterification reaction	111
29	The kinetic reaction rate constants of LH model type 1 with FAME concentration at various temperatures	111

Appendix Table

A1	Results from gas chromatography	121
B1	Standard solution of gas chromatography	124
C1	Fatty acid molecular weight	128
C2	Summary of the estimated molecular weight of TG, DG and MG in palm olein oil.	129
C3	The estimated molecular weight of palm olein oil.	130
D1	Total area of fatty acid composition	132

LIST OF FIGURES

Figure		Page
1	Overall reaction of transesterification of vegetable oil	17
2	The stepwise reaction of transesterification of vegetable oils	
	(a) triglycerides reaction step	
	(b) diglycerides reaction step	
	(c) monoglycerides reaction step	18
3	The general structure of GA	33
4	The standard GA	36
5	The general structure of crossover	47
6	The general structure of mutation	50
7	Strontium oxide powder with 99.9 of purity	59
8	Three neck-glass flask as a slurry reactor	61
9	The procedure flowchart of kinetic study of catalytic transesterification of palm olein oil over SrO	74
10	The sampling mixture at various reaction time from transesterification at 65 °C of reaction temperature, 1000 rpm of agitator speed	
	(a) 5 min	
	(b) 10 min	
	(c) 15 min	
	(d) 20 min	75
11	Experiment results at 65 °C of reaction temperature, 1000 rpm of agitator speed (% wt)	93
12	Experiment results at 60 °C of reaction temperature, 1000 rpm of agitator speed (% wt)	94
13	Experiment results at 55 °C of reaction temperature, 1000 rpm of agitator speed (% wt)	94

LIST OF FIGURES (Continued)

Figure		Page
14	Experiment results at 65 °C of reaction temperature, 1000 rpm of agitator speed (mole/g-catalyst)	95
15	Experiment results at 60 °C of reaction temperature, 1000 rpm of agitator speed (mole/g-catalyst)	96
16	Experiment results at 55 °C of reaction temperature, 1000 rpm of agitator speed (mole/g-catalyst)	96
17	Transesterification at T = 65 °C; Experimental data and calculated of PH model (reversible reaction in all step) with FAME concentration	97
18	Transesterification at T = 65 °C; Experimental data and calculated of PH model (irreversible reaction) with FAME concentration.	98
19	Transesterification at T = 65 °C; Experimental data and calculated of PH model (irreversible reaction) with FAME concentration.	98
20	Transesterification at T = 65 °C; Experimental data and calculated of PH model (reversible reaction in step 3) without FAME concentration	99
21	Transesterification at T = 65 °C; Experimental data and calculated of PH model (reversible reaction in step 3) with FAME concentration	100
22	Transesterification at T = 60 °C; Experimental data and calculated of PH model (reversible reaction in step 3) with FAME concentration	100
23	Transesterification at T = 55 °C; Experimental data and calculated of PH model (reversible reaction in step 3) with FAME concentration	102
24	Transesterification at T = 65 °C; Experimental data and calculated of LH model type 1 (irreversible reaction) without FAME concentration.	102

LIST OF FIGURES (Continued)

Figure		Page
25	Transesterification at $T = 65\text{ }^{\circ}\text{C}$; Experimental data and calculated of LH model type 1 (irreversible reaction) with FAME concentration.	103
26	Transesterification at $T = 65\text{ }^{\circ}\text{C}$; Experimental data and calculated of LH model type 1 (reversible reaction in step 3) without FAME concentration	104
27	Transesterification at $T = 65\text{ }^{\circ}\text{C}$; Experimental data and calculated of LH model type 1 (reversible reaction in step 3) with FAME concentration	104
28	Transesterification at $T = 65\text{ }^{\circ}\text{C}$; Experimental data and calculated of LH model type 2 (irreversible reaction) without FAME concentration	105
29	Transesterification at $T = 65\text{ }^{\circ}\text{C}$; Experimental data and calculated of LH model type 2 (irreversible reaction) with FAME concentration.	106
30	Transesterification at $T = 65\text{ }^{\circ}\text{C}$; Experimental data and calculated of LH model type 2 (reversible reaction in step 3) without FAME concentration	107
31	Arrhenius plot for transesterification reaction rate constants between $\ln(k_1)$ and $1/T\text{ (K}^{-1}\text{)}$, $R^2=0.8611$	109
32	Arrhenius plot for transesterification reaction rate constants between $\ln(k_2)$ and $1/T\text{ (K}^{-1}\text{)}$, $R^2=0.8592$	109
33	Arrhenius plot for transesterification reaction rate constants between $\ln(k_3)$ and $1/T\text{ (K}^{-1}\text{)}$, $R^2=0.9781$	110

LIST OF FIGURES (Continued)

Figure		Page
34	Arrhenius plot for transesterification reaction rate constants between $\ln(k_4)$ and $1/T$ (K^{-1}), $R^2=0.9146$	110
Appendix Figure		
B1	Standard solution graph of gas chromatography	125
C1	Chemical structure of triglyceride	127

LIST OF ABBREVIATIONS

C	=	Concentration (mole/g-catalyst)
DG	=	Diglycerides
E	=	Activation energy (J/mol^{-1})
GA	=	Genetic algorithm
GC	=	Gas chromatography
GL	=	Glycerides
FAME	=	Fatty acid methyl ester
k	=	reaction rate constant
K	=	adsorption equilibrium constant
LH	=	Langmuir-Hinschwood
MG	=	Monoglycerides
MS	=	Mean squares
PH	=	Pseudo-homogeneous
r	=	reaction rate ($\text{mole/g}^{-1}\text{min}^{-1}$)
SS	=	Sum of squares
T	=	Temperature (K)
TG	=	Triglycerides

STUDY OF KINETIC RATE OF HETEROGENEOUS CATALYSTS FOR BIODIESEL PRODUCTION

INTRODUCTION

Recently, biomass has been highlighted as an energy source because of the limited and fast diminishing resource of fossil fuels, increasing crude oil price and environmental problems. Biodiesel is one of the groups of biomass that has very attractive as an alternative energy and friendly for environment in the present time. Biodiesel consists of alkyl ester of long chain fatty acids originating from a renewable resource such as vegetable oils. In Thailand, there are many materials to produce biodiesel such as palm oil, sun flower, coconut and Jatropha oil. Biodiesel can be used in usual diesel engines and presents some advantages compared to traditional petroleum-based diesel. Biodiesel is an environment-friendly compound, non-toxic and emits less carbon monoxide, sulphur compounds, particular matter and unburned hydrocarbons than traditional diesel. However, NO_x emissions are 10% higher compared to petroleum-based diesel.

Biodiesel is commonly produced by the transesterification of plants oil or animal fat with short chain alcohols such as methanol or ethanol, in the presence of alkali such as NaOH or KOH, alkali alkoxides such as sodium methoxide or sodium butoxide and acid catalysts such as H₂SO₄. However, base catalysts are preferred to acid catalysts because of the higher reaction rates and the lower process temperature as compared to acid catalysts transesterification.

However, the use of homogeneous base catalysts requires neutralization and separation the reaction mixture that leading to a series of environmental problems. This is the main reasons that have been led to heterogeneous catalyst. Heterogeneous solid catalysts, able to substituted an alkali homogeneous catalyst. They can be easily separate from the reaction mixture, show easy regeneration, and have a less corrosive character. Many different heterogeneous catalysts have been developed to catalyze the transesterification of vegetable oils to prepare fatty acid methyl ester. These catalysts

have been found to be efficient heterogeneous catalysts for the transesterification of vegetable oils. However, there are quite expensive and complicated to prepare, which limits their industrial application. Thus it is desired to find more efficient and cheap catalysts. Recently, numerous studies have been performed to investigate the use of heterogeneous base compounds as catalysts for transesterification reactions. This includes the use of catalysts such as alkaline-earth oxides

The kinetics study of the heterogeneous catalyzed process that is very interesting to investigate the possibility to replace the homogeneous catalysts. Although several authors studied the kinetics of transesterification by homogeneous catalysts, there is very little information concerning the kinetics of heterogeneous catalysts

In this work, the kinetics study of heterogeneous catalyst was investigated that base on Pseudo-homogeneous and Langmuir-Hinshelwood kinetic models to describe transesterification reaction. The purpose is to find the best suitability kinetic model that could be related the result from the experiment over the investigated range of experimental conditions. The parameter estimation of chemical kinetic rates was performed by genetic algorithm (GA). It is powerful searching algorithms.

OBJECTIVES

1. To develop a kinetic model that describes the transesterification reaction of vegetables oil using heterogeneous catalysts.
2. To investigate the suitable condition of the reaction for the biodiesel production.
3. To implement a GA for estimation of chemical kinetic rate constant.

Scope of Work

1. The kinetic was investigated in the laboratory scale using strontium oxide as solid catalysts for transesterification of palm olein oil.
2. To compare performance of Pseudo-homogeneous (PH) and Langmuir-Hinshelwood (LH) model that was used to describe the kinetic experiment data.
3. To investigate the effect of temperature on the reaction rate of vegetable oil transesterification
4. To study the effect of mass transfer resistance on the transesterification of vegetable oil
5. The parameter estimation of kinetic models are performed by GA tool of MATLAB (R2007b)

Expected Results

1. The suitable model that used to describe the transesterification of palm olein oil over strontium oxide.
2. The chemical kinetic rate from suitable model that cloud be used to predict the performance of chemical reactor.

LITERATURE REVIEW

1. Homogeneous catalysts of transesterification

Freedman *et al.* (1986) investigated both acid- and alkaline - catalyzed transesterification of soybean oil with methanol and butanol. They found that the alkaline-catalysts could catalyze the reaction at a faster rate as compared to acid catalysts. They determined the reaction rate constants by varying the temperature, molar ratio of alcohol to soybean oil and catalyst type and concentration. They also estimated the activation energy for all forward and reverse reactions which are ranging from 8 – 20 kcal/mol.

Fukuda *et al.* (2001) present the comparing of base-catalyzed transesterification, acid-catalyzed transesterification is more suitable for glycerides that have relative high free fatty acid contents and more water because in alkaline-catalyzed transesterification, water can causes soap formation, which consumes catalyst and reduce catalyst efficiency.

Vincent *et al.* (2003) compared the effect of four basis catalysts on the transesterification reaction of refined sunflower oil such as sodium methoxide, potassium methoxide, sodium hydroxide and potassium hydroxide. He showed the methyl ester concentrations were near 100 wt.% in all catalysts, but biodiesel yields after the separation and purification steps were higher than 98 wt.% for the methoxide catalysts, because the yields losses due to triglycerides saponification and methyl ester dissolution in glycerol were negligible. However, methoxide catalysts were more expensive and difficult to manipulate. The temperature and catalysts concentration could be used to improve the high yield of biodiesel. Obtained biodiesel met the specifications, European Union draft standard, except the iodine value.

Meng *et al.* (2008) studied the biodiesel production from waste cooking oils (WCO), which contain large amounts of free fatty acids produced in restaurants. Experiments have been performed to determine the optimum condition for the transesterification process. The optimum experimental conditions, which were obtained from the orthogonal test, were methanol/oil molar ratio 9:1, with 1.0 wt.% sodium hydroxide, temperature of 50 °C and 90 min. Verified experiments showed methanol/oil molar ratio 6:1 was more suitable in the process, and under that condition WCO conversion efficiency led to 89.9% .

2. Heterogeneous catalysts of transesterification

Furuta *et al.* (2006) used solid super-acid catalysts of sulfated tin and zirconia oxides and tungstates as catalysts that for the transesterification at 200-300 °C and the esterification at 175-200 °C. Tungstates zirconia-alumina is a promising solid acid catalyst for the production of biodiesel fuels from soybean oil, the conversion over 90% for the both of the esterification and the reuse of these catalysts showed the conversion over 85% for 50 hr on stream.

Furuta *et al.* (2004) studied the effect of catalysts on the transesterification of soybean oil with methanol at 250 °C and the esterification of *n*-octanoic acid with methanol at 175-200 °C. Amorphous zirconia, titanium-, aluminium-, and potassium-doped zirconias were used in the both reaction that showed the good results and suitable for biodiesel production. Titanium- and aluminum-doped zirconias are promising solid catalysts for the production because of their high performance, with over 95 % conversion in the both of the reaction.

Suppes *et al.* (2003) investigated with NaX, NaY faujasite zeolite, ETS-10 zeolite (Titanosilicate structure-10) as catalyst for the transesterification of soybean oil with methanol. The ETS-10 catalysts provided higher conversion than the other zeolite type catalysts. The increased conversions were attributed to the basicity

of EST-10 zeolite and larger pore structure. Methyl ester yield increased with an increase in temperature. The second experimental is study the effect of the material of the reactor on the conversion of methyl ester. Nickel was the most catalytic of the metal evaluated and potentially could be configured to promote commercial reaction.

Peter *et al.* (2002) used metal salts of amino acids as catalysts to synthesize fatty acid esters by methanolysis of palm oil. They found that the salts containing a quaternary amino or a highly basic group e.g. zing salt of argininie, carnitine or histidine have catalytic activity in alcoholysis. These salts are insoluble in oil as well as in alcohol and are suitable for heterogeneous catalytic transesterification. Investigation of the effect of temperature and methanol concentration in the vegetable oil phase on the rate of reaction was also done. They found that the reaction increases strongly with increasing with temperature and depend on the methanol concentration in the fat phase.

Sercheli *et al.* (1999) studied the effect of the homegenerous compare with heterogeneous catalysts such as alkylguanidine (TBD), trisubstituted alkylguanidine (TCG) and there catalysts were anchored to modified polystyrene or siliceous MCM-41, encapsulates in the supercages of zeolite Y, or entrapped in SiO₂ sol-gel matrices. The catalytic adtivity of these catalysts showed that the yields of methyl esters can be obtained with the guanidine anchored to the supports after longer reaction times. The catalysts prepared by immobilization of alkylguanidines in microporous systems showed diffusion restriction.

In addition, the heterogeneous catalysts of transesterification had been very interested in other flied, not only in biodiesel process. Several investigations had shown the sustainable result.

Sankar *et al.* (2006) used alkali and alkaline-earth tungstates such as sodium-, calcium- and potassium tungstates for the transesterification of the ethylene carbonate to dimethyl carbonate and ethylene glycol. Sodium tungstate provided higher conversion and yield than the other catalysts at the temperature are 50 °C and atmospheric pressure. The transesterification reaction over the recovered catalyst gave nearly the same results as the fresh catalyst with no loss in its activity.

Serio *et al.* (2004) studied the effect of the heterogeneous basic catalyst on the synthesis of Poly ethylene terephthalate (PET). It was shown that both the calcines Al-Mg hydrotalcites and magnesium oxides are active in the dimethyl terephthalates (DMT) transesterification with ethylene glycol but magnesium oxide has higher activities in both reaction and is much more simple to prepare compared to calcined hydrotalcite.

Choudary *et al.* (2000) showed the high reactivity in transesterification, Mg-Al-O-*t*-Bu hydrotalcite appears as a fairly strong heterogeneous base.

Mayer and Hoelderich (1998) are to investigate the behavior of the basic zeolite catalysts in transesterification of methyl benzoate and dimethyl terephthalate with ethylene glycol. The results provide excellent in a discontinuous batch reaction, the easy removal of a heterogeneous catalyst as well as the higher activity in the reaction with zeolite Cs₂O/CsX as catalyst.

Gorzawski and Hoelderich (1998) provided the result of the investigated superbases can nicely be used in transesterification reaction as demonstrated. It could be shown that the superbases Cs_xO/γ-Al₂O₃ and Na/NaOH/γ-Al₂O₃ are efficient catalysts in the transesterification of methyl benzoate and dimethyl terephthalate with ethylene glycol.

However, there are shown the good results that could be used to substitute the homogeneous catalysts both biodiesel and non-biodiesel. It is not a conventional for the production in large-scale of process. Some researchers have reported the used of commercial heterogeneous for the reaction

Zajdlewicz (2001) reported that there are five commercially available catalysts that are active for transesterification of soybean oil. Valfor, ZSMS, β -Zeolite, MCM-41, Zeolite-Y and calcium carbonate (CaCO_3) were used as catalysts. The most active of these catalysts was Valfor (sodium alumina silicate).

Marchetti *et al.* (2006) in this work, basic resin is studied as catalyst for the esterification of frying oils with ethanol. The resin showed the value that is suitable for the esterification of oil with high amount of free fatty acids, Dowex monosphere 550A resin showed higher final conversion than the other, but the reuse resin gave lower conversion than the first time.

Lui *et al.* (2007) used the solid base, SrO, as catalyst for the transesterification. The results showed that the yield of biodiesel produced with SrO was in excess of 95 % at temperature below 70 °C within 30 min. this catalyst has a long catalyst lifetime and could maintain sustained activity even after being repeatedly used for 10 cycles.

3. Kinetic models

Lee *et al.* (2007) studied the kinetic of transesterification of soybean used frying oil (SBO) in the presence of KOH as a catalyst. A kinetic study was performed in two ways; firstly, the overall reaction was measured in terms of the amount of glycerol formed. Second, quantification of the formed esters was performed. From the Arrhenius plots of both case, they found that the transesterification reaction fitted better to a pseudo-first order reaction than to a second-order reaction. In case of the kinetic parameter estimation, the values of the activation energies of first-order was 7.05 kcal/mol for overall reaction, 116.84 kcal/mol for methyl linoleate from SBO.

First – order reaction:

$$k = 1/t \ln(C_o / C)$$

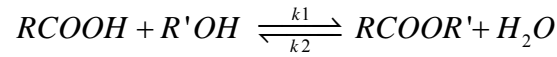
$$k = 1/t \ln(a / a - x)$$

Where

a = initial concentration

a-x = unreacted after time t

Wu *et al.* (2008) investigated biodiesel production using the cation-exchange resin as a heterogeneous acid-catalyzed, under varying catalyst loading (3.65 – 53.6 % w/w), reaction temperature (333-353 K) and methanol/FFAs molar ratio (1:1 to 20:1). A pseudo-homogeneous kinetics model coupling the effects of catalyst loading, reaction temperature and molar ratio of methanol to FFAs was developed. The reaction mechanisms are as follows:



A good agreement between reference value and calculated values was observed and correlation coefficient of 0.95 was evaluated. The optimal operating condition for obtaining equilibrium FFAs conversion of 0.985 at temperature 372.15 K, molar ratio of feeding reactant of 14.9:1 and 9.5 h required for reaction.

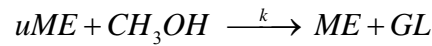
$$\frac{dx}{dt} = k_1 \cdot C_{RCOOH,0} \left[(1-x)(\theta-x) - \frac{x^2}{K_e} \right]$$

Where

$$K_e = \frac{k_1}{k_2} = \frac{x_e^2}{(1-x_e)(\theta-x_e)}$$

Huayang *et al.* (2007) studied the kinetic of soybean oil transesterification without a catalyst in subcritical and supercritical methanol was made at pressure between 8.7 and 36 MPa. It was found that the conversion of soybean oil into the corresponding methyl ester was enhanced considerably in the supercritical methanol. The apparent activation energies of the transesterification are different with subcritical and supercritical states of methanol, which are 11.2 and 56.0 kJ/mol (molar ratio of methanol to oil; 42, pressure; 28 MPa), respectively.

In this research, the components were grouped into four species, methanol (MeOH), methyl ester (ME), glycerin (GL), unsesterified compounds (uME) including triglyceride, diglyceride, monoglyceride and unreacted free fatty acids. The reaction can be model as:



The reaction equation can be expressed as

$$\ln[uME_0] - \ln[uME_t] = k \cdot t$$

Noureddini and Zhu (1997) presented the soybean oil kinetic study of homogeneous transesterification in the presence of NaOH as a catalyst. The kinetic differential equation that based on the three steps reaction;

$$\frac{d[TG]}{dt} = -k_1 [TG][A] + k_2 [DG][A] - k_7 [TG][A]^3 + k_8 [A][GL]^3$$

$$\frac{d[DG]}{dt} = k_1 [TG][A] - k_2 [DG][A] - k_3 [DG][A] + k_4 [MG][E]$$

$$\frac{d[MG]}{dt} = k_3 [DG][A] - k_4 [MG][E] - k_5 [MG][A] + k_6 [GL][E]$$

$$\begin{aligned}\frac{d[E]}{dt} &= k_1 [TG][A] - k_2 [DG][E] + k_3 [DG][A] - k_4 [MG][E] \\ &\quad + k_5 [MG][A] - k_6 [GL][E] + k_7 [TG][A]^3 - k_8 [GL][E]^3 \\ \frac{d[GL]}{dt} &= k_5 [MG][A] - k_6 [GL][E] + k_7 [TG][A]^3 - k_8 [GL][E]^3 \\ \frac{d[A]}{dt} &= -\frac{d[E]}{dt}\end{aligned}$$

Hitoshi *et al.* (2007) investigated the kinetic of palm oil via the non-catalytic transesterification. The superheated methanol was used in the reaction that has been carried out at 523-563 K. Evaluation on the reaction kinetic based on changes of the uME concentration shows that reaction rate constant at 523, 543 and 563 was 0.0034, 0.0051 and 0.0056 min⁻¹, respectively, activation energy was 31 kJ/mol and frequency factor was 4.2.

Royae *et al.* (2008) presented a kinetic model that was used to describe for the methanol to dimethylether dehydration reaction. In this research, a differential fixed bed reactor was selected to investigation in the presence of clinoptilolite-zeorite catalyst. Considering the rate controlling step, the kinetic rate model as follows:

$$-(r_M) = \frac{k_r K_M^2 P_M^2 - k_r' K_W P_D P_W}{\left(1 + K_M P_M + K_W P_W + K_N K_M P_M^{m+1} + K_{NN} K_M P_M P_W^n\right)^2}$$

It showed the better solution that could be explained the experimental results.

Moradi *et al.* (2008) investigated the intrinsic kinetics study of the three-phase dimethylether synthesis over a bi-functional catalyst in a slurry reactor. The kinetic rate equations for methanol synthesis and dehydration as follow:

$$r_{CO} = \frac{k_1 K_{CO} \left[f_{CO} f_{H_2}^{3/2} - f_{CH_3OH} / \left(f_{H_2}^{1/2} K_{f_{CO}} \right) \right]}{\left(1 + K_{CO} f_{CO} + K_{CO_2} f_{CO_2} \right) \left[f_{H_2}^{1/2} + \left(K_{H_2O} / K_{H_2}^{1/2} \right) f_{H_2O} \right]}$$

$$r_{MeOH} = \frac{k_2 K_M^2 \left(C_M^2 - C_D C_W / K_{f_{DME}} \right)}{\left(1 + 2 \left(K_M C_M \right)^{1/2} + K_W C_W \right)^4}$$

4. Genetic algorithm

Booker (1993) presented that the GA was loosely based on the principles of genetic variation and natural selection. The theory of mathematical genetics had not played a large role in most analyses of GA. This paper reviewed some well known results in mathematical genetics. That used probability distributions to characterize the effects of recombination to GA research was illustrated by quantifying certain inductive biases associated with crossover operators. The potential significance of this work for the theory of GA was also discussed.

Miki *et al.* (1999) presented paper to introduce an alternative approach to relieving of choosing optimal mutation and crossover rates by using a parallel and distributed GA with distributed environments. It was shown that the best mutation and crossover rates depended on the population sizes and the problems, and those were different between a single and multiple populations. The proposed distributed environment GA used various combinations of the parameters as the fixed values in the subpopulations. The excellent performance of the new scheme was experimentally recognized for a standard test function. It was concluded that the distributed environment GA was the fastest way to gain the good solution under the given population size and uncertainty of the appropriate crossover and mutation rates.

Yu *et al.* (2000) presented the new algorithm GA/SA (genetic algorithms/simulated annealing) for solving a large-scale system energy integration problem, which was difficult to solve on the total process system level directly by traditional

algorithm. Using OCX (orthogonal crossover) and EC (effective crowding) operators have improved the general GA, and the improved GA is combined effectively with a SA algorithm to avoid the common defect of early convergence. Numerical calculation results show that the new algorithm can converge faster than either SA or GA algorithm alone and has much more probability of locating a global optimum. The convergence proof of the new algorithm is also given. GA/SA has been used to solve a 167- stream problem. A good result is achieved for improving the total process retrofit efficiency.

Moon *et al.* (2001) presented the traveling sales man problem with precedence constraints (TSPPC) is one of the most difficult combinatorial optimization problems. An efficient GA to solve the TSPPS was presented. The key concept of the proposed GA was a topological sort (TS), which is defined as an ordering of vertices in a directed graph. Also, a new crossover operation is developed for the proposed GA. The results of numerical experiments show that the proposed GA produces an optimal solution shows superior performance compared to the traditional algorithms.

5. Estimation of kinetic parameter

The catalytic reduction of NO hydrogen was studied (Ayen and Peter, 1962) using a flow reactor operated differentially at atmospheric pressure. Two reactions were found to be important. Data were taken at 375 °C, 400 °C and 425 °C for NO and hydrogen partial pressure of 0.005 to 0.05 atm using nitrogen as the diluents. The total flow rate was held at 2000 cc per minute. Mechanisms were postulated for there reactions, rate and adsorption constants were evaluated from the data for the corresponding rate equations. This paper used the method of least squares to find the values of constants.

Bellman (1967) presented technique for estimated chemical rate constants from raw kinetic data. Such problems were viewed as nonlinear multipoint boundary value problems for systems of nonlinear ordinary differential equation, for which the quasilinearization procedure offered an effective means of numerical solution. The

method was illustrated using kinetic data on some gas phase reactions of nitrogen and oxygen.

Eftaxias *et al.* (2002) proposed the performance of simulated annealing (S-A) in nonlinear kinetic parameter estimation was studied and compared with the classical Levenberg-Marquardt (L_M) algorithm. Both methods were tested in the estimation of kinetic parameters using a set of three kinetic models of progressively higher complexity. The models described the catalytic wet air oxidation of phenol carried out on a small-scale trickle bed reactor. The first model only considered the phenol disappearance reaction, while the other two included oxidation intermediate compounds. The number of model parameters involved increased from 3 to 23 and 38, respectively, for the three models. Both algorithms gave good results for the first model, algorithm the L_M was superior in term of computation time. In the second case the algorithms achieved convergence, but S_A resulted in a better criterion and kinetic parameters with physical meaning. In the more complex model, only S_A was capable of achieving convergence, whereas the L_M failed. For the second and third model the solution of S_A could be further improved, when used as an initial guess for the L_M algorithm.

6. Genetic algorithm and estimation of kinetic parameter

Hibber (1992) present GA described to optimize the rate coefficients for the hydrolysis of adenosine 5-triphosphate by fitting a kinetic model to concentration versus time data. A simple GA was compared with one in which the genes were real variables, and to one that operates with the so-called incest prevention algorithm of Eshelman and Schaffer. The faster convergence to a good optimum was achieved by a hybrid GA in which a steepest descent, pseudo-Newton procedure was iterated with an incest preventing GA, each providing a starting point for the other. The best optimum was one of the results of using a pseudo-Newton routing on each of the converged population of a GA (not necessarily the best from the GA). This approach gave good results for problems having a multimodal response surface when there was

no good initial guess for a traditional optimization algorithm. After a small number of generations a GA gave a good starting points for steepest ascent optimizes.

Moros *et al.* (1996) applied of GA for generating initial parameter estimation for the kinetic models of a catalytic process (oxidative methane dehydrodimerization) was described. The aim was to provide suitable starting points for the applied combination of an integration process and a locally converging nonlinear parameter estimation algorithm. The influence of the control parameter of this GA (Number of individuals, the mutation rates and the second methods) was studied. Additional, studies of kinetics model parameters for two different Pb_0 /alumina catalysts were carried out. The suggested method could be used to estimate suitable values for the model parameters of a complex mathematical model.

Transesterification of vegetable oils

In the transesterification of vegetable oils, a triglyceride reacts with an alcohol in the presence of a catalyst such as homogeneous or heterogeneous, producing a mixture of fatty acids alkyl esters and glycerol. The overall process is a sequence of three consecutive and reversible reactions, in which diglycerides and monoglycerides are formed as intermediates. The stoichiometric reaction requires 1 mol of a triglyceride and 3 mol of the alcohol. However, an excess of the alcohol is used to increase the yield of the alkyl esters and to allow its phase separation from the glycerol formed.

Several aspects, including the type of catalyst, alcohol/vegetable oil ratio, temperature, purity of the reactants and free fatty acid content have an influence on the course of transesterification that based on the catalyst used such as homogeneous i.e. acid or base, or heterogeneous

The alcohol/vegetable oil molar ratio is one of the main factors that influence the transesterification. An excess of the alcohol favors the formation of the products. On the other hand, an excessive amount of alcohol makes the recovery of the glycerol difficult.

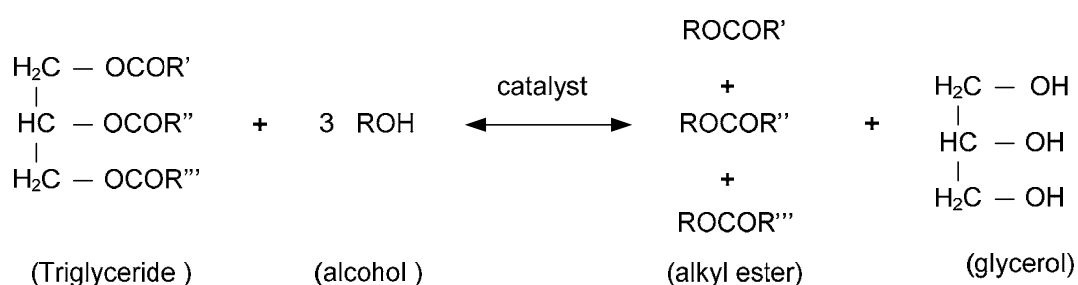


Figure 1 Overall reaction of transesterification of vegetable oils.

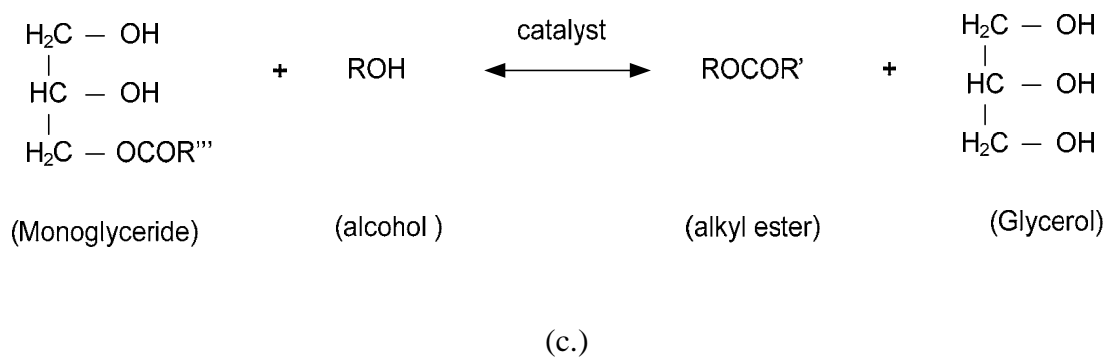
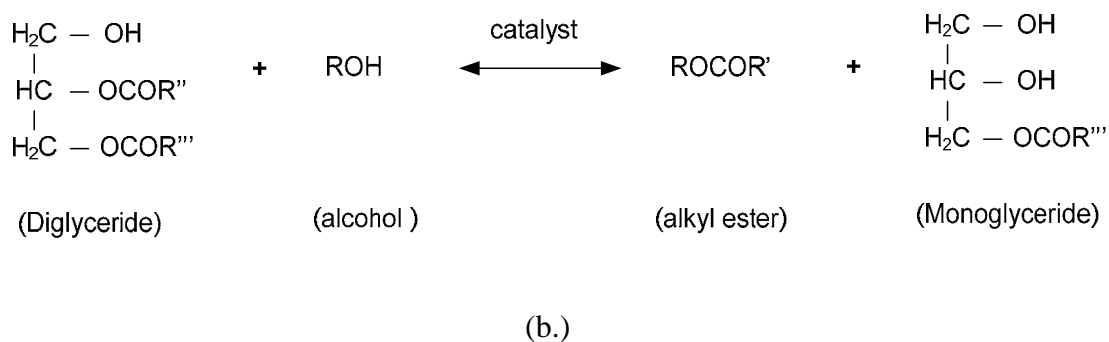
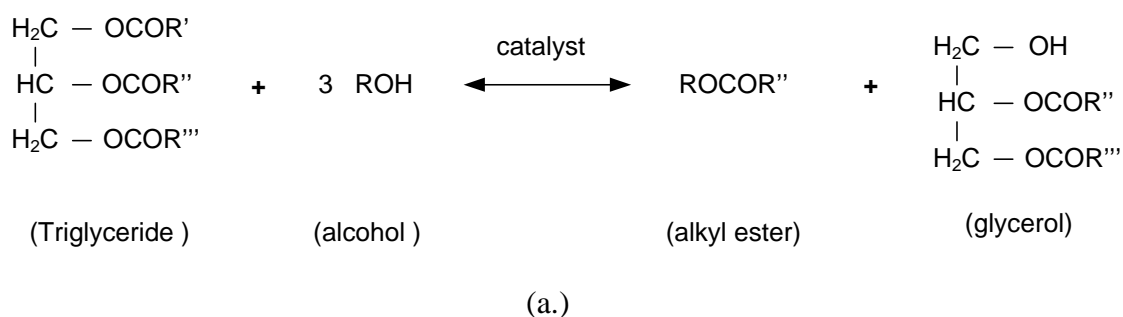


Figure 2 The stepwise reaction of transesterification of vegetable oils,
 (a.) triglycerides reaction step (b.) diglycerides reaction step
 (c.) monoglycerides reaction step

Kinetic models of catalytic reaction

Correlations of rate data may be sought for any of several purposes. The process engineering may wish to develop a model for a specific reaction so as to be able to predict the effect of reactor operating changes on performance. A study of the detail kinetics of one particular reaction has been a traditional approach to obtaining some understanding, even though indirect, of its mechanism. Regardless of the objective, the investigator desires a mathematic model to represent the data.

Consider a reaction occurring between a fluid and a porous solid catalyst. In order for reaction to occur, the reactants in the fluid must first be transported to the outer surface of the solid, and then they must diffuse through the pores of the solid to catalytically active sites. At least one of the reactant species must usually be chemisorbed onto the surface of the solid. Subsequently, reaction occurs among chemisorbed species or between a chemisorbed species and another species that is either physically adsorbed or that collides with the chemisorbed species directly from the fluid phase. After reaction, products are desorbed and diffuse out through the pores of the catalyst to the bulk fluid. Because the rates of these various steps respond in a different way to experimental variables such as pressure, temperature, bulk-fluid velocity, and chemical and physical structure of the catalyst, they can be conveniently classified as follows:

1. Mass transfer of reactants and products by counter diffusion between the bulk fluid and the outer surface of the catalyst particle.
2. Mass transfer of reactants and products by counter diffusion through the porous structure of the catalyst.
3. Adsorption of reactants onto the catalyst surface and desorption of products.
4. Chemical reaction involving one or more chemisorbed species.

One or more of these steps may be rate-limiting in the sense that it consumes the major portion of the chemical potential available for carrying out the process.

The true mechanism in all its details is not known for the simplest catalytic reaction. The closer a model reflects actuality, of course, the more reliable it is, but an attempt to allow for the complex nature of a heterogeneous reaction may easily lead to a complicated formulation containing many parameters that must be empirically adjusted. The process engineering may find it adequate to use an essentially empirical correlation that is pseudo-homogeneous model. It is expressed with power functions of reactant concentrations, the exponents being arbitrary adjustable constants. The second one is heterogeneous kinetic model, Langmuir-Hinshelwood model. This model was based on the physical theory of adsorption and desorption of chemical species on surface of catalyst, following with chemical reaction.

In this research, two kinetic models were selected to find a suitable model that described transesterification of palm oil over strontium oxide as solid catalyst.

1. Pseudo-Homogeneous model

The rate of an elementary bimolecular reaction between species A and B is given by

$$rate = \frac{\text{molecules reacted}}{(\text{time})(\text{area})}$$

$$rate = k_0 e^{-E/RT} \cdot f(C_A C_B)$$

Where, k_0 is taken to be independent of temperature and surface area of the catalyst. The function of the concentrations which usually is easiest to use in correlating rate data, consists of simple power function: C_A^a and C_B^b where a and b are empirically adjusted constants.

Hence

$$-r = k_0 e^{-E/RT} \cdot C_A^a C_B^b$$

More generally, this may be expressed as

$$-r = k \prod_i C_i^{a_i}$$

Where a_i is termed the order of the reaction with respect to C_i

For this research, the rate of reaction of transesterification that based on the pseudo-homogeneous model, the set of differential equations characterizing the stepwise reaction involved in the transesterification of palm oils as follows:

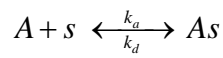
2. Langmuir-Hinshelwood model

Pseudo-homogeneous model is similar to power-law model that can frequently be used to quantify homogeneous reactions. However, many reactions occur among species in different phases (gas, liquid and solid). Reaction rate equations in such heterogeneous system often become more complicated to account for the movement of material from one phase to another. An additional complication arises from the different ways in which the phases can be contracted with each other. Many important industrial reactors involve heterogeneous systems. One of the more common heterogeneous systems involves liquid-solid reactions such as slurry reactor.

One approach to describe the kinetics of such system involves the use of various resistances to reaction. If we consider an irreversible reaction $A \rightarrow B$ that occurs in the presence of a solid catalyst pellet, we can postulate seven different steps required to accomplish the chemical transformation. First, we have to remove the reactant A from the bulk fluid to the surface of catalyst particle. Hence, the reactant A must diffuse from the surface reaches an active site, where it must be adsorbed onto the surface. The chemical transformation of reactant into product occurs on this active site. The product B must desorb from the active site back to the bulk fluid. The

product B must diffuse from inside the catalyst pore back to the surface. Finally, the product molecule must be moved from the surface to the bulk fluid.

To look at the kinetics in the heterogeneous systems, we consider the step of adsorbing a molecule A onto an active site s to form an adsorbed species As . The adsorption rate constant is k_a . The process is reversible, with a desorption rate constant k_d .



We usually write the rate of adsorption in terms of the concentration of A . The net rate of adsorption and desorption is

$$r = k'_a C_A C_S - k'_d C_{AS}$$

Where C_S is the concentration of open active sites and C_{AS} is the concentration of sites occupied by an adsorbed molecule of A . The total number of sites (C_T) is fixed and is the sum of the open and occupied sites:

$$C_T = C_S + C_{AS}$$

If we define θ as the fraction of total sites covered by the adsorbed molecules, then

$$\theta = \frac{C_{AS}}{C_T}$$

We can rewrite these equation and combine constant parameters into the following rate expression:

$$r = k_a C_A (1 - \theta) - k_d \theta$$

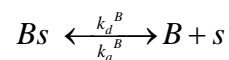
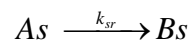
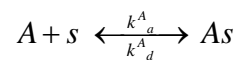
At equilibrium the net rates is zero, and we can define an adsorption equilibrium constant (K_A) to produce the following expression that define what is typically called

Langmuir isotherm behavior:

$$K_A = \frac{k_a}{k_d}$$

$$\theta = \frac{K_A C_a}{1 + K_A C_A}$$

We now consider the irreversible reaction $A \rightarrow B$, the reaction occurs on a solid catalyst. We can consider three steps to the mechanism: the adsorption of reactant A onto the surface, the transformation of A into B on the catalyst surface, and finally the desorption of product B from the surface:



The assumption of which step is slowest governs the form of the final kinetic expression. For the purposes of this simple example, we assume that the second step is the slowest and is first-order with respect to the adsorbed A species. Therefore the rate r is determined by a rate constant and the concentration of A absorbed on the surface (C_{AS}) according to standard power-law models:

$$r = k_{sr} C_{AS}$$

We can write the absorption equilibrium coefficients for A and B in term of concentrations

$$K_A = \frac{C_{AS}}{C_A C_S} = \frac{k_a^A}{k_d^A}$$

$$K_B = \frac{C_{BS}}{C_B C_S} = \frac{k_a^B}{k_d^B}$$

The total concentration of sites is a constant (C_T) and is the sum of open and occupied sites. We can express this it in terms of the equilibrium constants under the assumption that the transformation step is the slowest:

$$C_T = C_S + C_{AS} + C_{BS} = C_S (1 + K_A C_A + K_B C_B)$$

We can write the overall reaction rate as

$$r = \frac{k_T C_A}{(1 + K_A C_A + K_B C_B)}$$

Where k_T is a kinetic rate constant that is a function of temperature.

In catalytic reaction, the kinetic models was formulated that based on the rate-controlling step. It consisted of adsorption, desorption or surface reaction. The various mechanism and rate-controlling step considered lead to many difference model.

A useful generalized way of formulation various cases are presented. The rate equation is expressed in the general form:

$$-r = \frac{(\text{kinetic term})(\text{potential term})}{(\text{adsorption term})^n}$$

The summary table was presented to give the expression for each of the three terms and n for various adsorption or desorption process as the rate-limiting step, with or without dissociation, and for surface reaction as the rate-controlling step.

Table 1 Term in the generalized formulation of Langmuir-Hinshewood Kinetic model

	Reaction			
	$A \rightleftharpoons R$	$A \rightleftharpoons R + S$	$A + B \rightleftharpoons R$	$A + B \rightleftharpoons R + S$
Kinetic term, with or without dissociation of A	$k_s K_A$	$k_s K_A$	$k_s K_A K_B$	$k_s K_A K_B$
Potential term	$P_A - P_R / K$	$P_A - P_R P_S / K$	$P_A P_B - P_R / K$	$P_A P_B - P_R P_S / K$
Value of n A				
undissociated	1	2	2	2
A dissociated	2	2	3	3

Source: Satterfield (1991)

Table 1 gives the expressions for Langmuir-Hinshewood model where all reactants are taken to be adsorbed, adsorption/desorption is taken to be in equilibrium, and all species are assumed to complete for the same sites. K is the equilibrium constant for a reversible reaction, and driving force is expressed in term of partial pressure. The adsorption term is, in the most general case,

$$\left[1 + K_A P_A + K_B P_B + K_R P_R + K_S P_S + K_X P_X \right]^n$$

3. Temperature dependent on kinetic models

For many reactions, the rate expression can be written as a product of a temperature term and a composition term as following

$$\begin{aligned} r &= f_1(\text{temperature}) \cdot f_2(\text{composition}) \\ &= k \cdot f_2(\text{composition}) \end{aligned}$$

The reaction rate constant that has been found in practically all cases to be well represented by Arrhenius's law

$$k = k_0 e^{-E/RT}$$

where

k_0 is the pre-exponential factor

E is the activation energy of the reaction

Analysis of variance

1. Fundamental of analysis of variance

The technique known as analysis of variance (ANOVA) uses tests based on variance ratios to determine whether or not significant differences exist among the means of several groups of observations, where each group follows a normal distribution. The analysis of variance technique extends the t-test used to determine whether or not two means differ to the case where there are three or more means.

The analysis of variance is used very widely in the biological, social and physical sciences. The technique was first developed by R.A. Fisher and his colleagues in England in the 1920s. This statement points out that the statistical principle underlying the analysis of variance are quite simple; but the calculations can become quite involved, so that they require careful and systematic arrangement.

Analysis of variance is particularly useful when the basic difference between the groups cannot be stated quantitatively. For example, suppose we wish to determine whether there are any differences among the effects of four polymerization catalysts on the setting time of a particular plastic. We make several runs under identical conditions with each catalyst. We can then determine whether the mean setting times for the four catalysts are different by using a one-way analysis of variance to determine the effect of one independent variable (type of catalyst) on the dependent variables (setting time). However, we cannot describe the type of catalyst by a quantitative relationship. On the other hand, we must run a similar experiment in which we use four different concentrations of a single catalyst. Now we can relate the four groups quantitatively by concentration of catalyst. We could still use the analysis of variance to see whether a change in concentration had any effect.

Although the principles of analysis of variance are simple, the notation and arithmetic can be quite confusing at first contact. For this reason, we begin by discussing a few conversions in notation and arithmetic that we will use later. Support we have the following matrix:

Table 2 Sample of data matrix

Column		1	2	.	.	j	.	.	J
	1	X_{11}	X_{12}	.	.	X_{1j}	.	.	X_{1J}
	2	X_{21}	X_{22}	.	.	X_{2j}	.	.	X_{2J}

	i	X_{i1}	X_{i2}	.	.	X_{ij}	.	.	X_{iJ}

	I	X_{I1}	X_{I2}	.	.	X_{Ij}	.	.	X_{IJ}
Sums	I	$X_{\bullet 1}$	$X_{\bullet 2}$.	.	$X_{\bullet j}$.	.	$X_{\bullet J}$
Means		$X_{\bullet 1}$	$X_{\bullet 2}$.	.	$X_{\bullet j}$.	.	$X_{\bullet J}$

Source: Zivorad (2004)

Each data point is subscripted, first to identify its column location and second to identify its row location. Thus, X_{32} (read 'X' three two) is the data point in the third column and second row. Each column may be regarded as size I random sample drawn from the normal population. This matrix might represent the example of one-way analysis of variance given earlier. The column would be the four catalyst and the rows would simply identify the successive runs made at identical conditions.

In two way example, the column would again be the four catalysts, the rows would be the three temperatures, and each X would be a single value of the setting time for a given temperature and catalysts. Thus, X_{32} is the setting time using the third catalyst and the second temperature.

We designate a general location in the matrix of data as X_{ij} , where i refers to the column, and j to the row. The sum of values in the i -th column is:

$$X_{j\cdot} = \sum_{j=1}^J X_{ij}$$

The dot refers to the direction that has been summed. The mean of the values in the i -th column is then:

$$\bar{X}_{i\cdot} = \frac{X_{i\cdot}}{J}$$

Similarly, the sum for any row j is:

$$X_{\cdot j} = \sum_{i=1}^I X_{ij}$$

And the mean is:

$$\bar{X}_{\cdot j} = \frac{X_{\cdot j}}{I}$$

The sum of all values in the matrix is designated by $\bar{X}_{\cdot\cdot}$ where:

$$X_{\cdot\cdot} = \sum_{i=1}^I \sum_{j=1}^J X_{ij} = \sum_{i=1}^I X_{i\cdot} = \sum_{j=1}^J X_{\cdot j}$$

The mean of all the values in the matrix is call the grand mean $\bar{X}_{\cdot\cdot}$ where:

$$\bar{X}_{\cdot\cdot} = \frac{X_{\cdot\cdot}}{IJ}$$

From here on, to simplify the equations, we will designate:

$$\sum_{i=1}^I = \sum_i ; \sum_{j=1}^J = \sum_j$$

The same as before, capital letters denote random variable and the small ones the concrete value of the variable.

2. Two-way analysis of variance

If we desire to study the effects of two independent variables (factors) on one dependent factor, we will have to use a two-way analysis of variance. For this case the columns represent various values or levels of one independent factor and the rows represent levels or values of the other independent factor. Each entry in the matrix of data points then represents one of the possible combinations of the two independent factors and how it affects the dependent factor. Here, we will consider the case of only one observation per data point. We now have two hypotheses to test. First, we wish to determine whether variation in the column variable affects the column means. Secondly, we want to know whether variation in the row variables has an effect on the row means. To test the first hypothesis, we calculate a ‘between columns’ sum of squares, and to test the second hypothesis, we calculate a ‘between rows’ sum of squares. The between-rows means mean square is an estimate of the population variance, providing that the row means are equal. If they are not equal, then the expected value of the between-rows mean square is higher than the population variance. Therefore, if we compare the between-rows mean square with another unbiased estimate of the population variance, we can construct an F test to determine whether the row variable has an effect. Definition and calculation formulas for these quantities are given in Table 3.

Table 3 Two-way analysis of variance

Source of variance	Degree of freedom	Sum of squares-definition	Sum of squares practical calculation	Mean squares	Test statistic
Between columns	J-1	$SS_C = I \sum_j (\bar{X}_{.j} - \bar{X}_{..})^2$	$SS_C = \frac{\sum_j \bar{X}_{.j}^2}{I} - \frac{\bar{X}_{..}^2}{IJ}$	$MS_C = \frac{SS_C}{J-1}$	$\frac{MS_C}{MS_E}$
Between rows	I-1	$SS_R = J \sum_i (\bar{X}_{i.} - \bar{X}_{..})^2$	$SS_R = \frac{\sum_i \bar{X}_{i.}^2}{J} - \frac{\bar{X}_{..}^2}{IJ}$	$MS_R = \frac{SS_R}{I-1}$	$\frac{MS_R}{MS_E}$
Residual variance-error	(I-1)(J-1)	$SS_E = \sum_i \sum_j (X_{ij} - \bar{X}_{i.} - \bar{X}_{.j} + \bar{X}_{..})^2$	$SS_E = SS_T - SS_C - SS_R$	$MS_E = \frac{SS_E}{(I-1)(J-1)}$	
Total	IJ-1	$SS_T = \sum_i \sum_j (\bar{X}_{i.} - \bar{X}_{..})^2$	$SS_T = \sum_i \sum_j \bar{X}_{ij}^2 - \frac{\bar{X}_{..}^2}{IJ}$		

Source: Zivorad (2004)

Genetic algorithm

1. Fundamental of genetic algorithm

Goldberge (1989) described the usual form of GA. GA is stochastic search technique based on the mechanism of natural selection and natural genetics. GA, differing from conventional technique, starts with an initial set of the random solutions called population. Each individual in the population is called chromosome representing a solution to the problem at hand. A chromosome is a string of symbols; it is usually, but not necessarily, a binary bit string. The chromosome evolves through successive iterations, call generations. During each generation, the chromosome is evaluated, using some measure of fitness. To create the next generation, new chromosome, called offspring, are formed by either (a) merging two chromosomes from current generation using a crossover operator or (b) modifying a chromosome using a mutation operator. A new generation is formed by (a) selecting, according to the fitness values, some of the parents and offspring and (b) rejecting others so as to keep the population size constant. Filter chromosomes have higher probabilities of being selected. After several generations, the algorithms converge to the best chromosome, which hopefully represents the optimum or sub optimal to problem. Let $P(t)$ and $C(t)$ be parents and offspring in current generation t ; the general structure of GA (see Figure 1) is described as follows:

Procedure: GA

Begin

$t \leftarrow 0$;

Initialize $P(t)$;

evaluate $P(t)$;

While (not termination condition) do

Recombine $P(t)$ to yield $C(t)$;

Evaluate $C(t)$;

Selection $P(t+1)$ from $P(t)$ and $C(t)$;

$t \leftarrow t+1$

end

end.

Figure 3 The general structure of GA

Source: Gen and Cheng (1996)

Usually, initialization is assumed to be random. Recombination typically involves crossover and mutation to yield offspring. In face, there are only two kinds of operations in GA:

1. Genetic operations: crossover and mutation
2. Evolution operation: selection

The genetic operations mimic the process of heredity of genes to create new offspring at each generation. The evolution operations mimic the process of Darwinian evolution to create population from generation to generation. This description differs from the paradigm given by Holland (1975). Where selection is made to obtain parents for recombination

GA can be used to solve the complicated problem such as discontinuous and multimodal objective functions because they can find global optimum without enquired any derivatives. The special characteristics of GA that differ from conventional optimization method are summarized in Table 1.

Table 4 The different characteristics between the conventional optimization and GA method

Item	Conventional Method	GA method
1. Derivative	Require	Not require
2. Noncontinuous function	Can handle	Cannot handle
3. Initial solution	Single	Many (equal to number of population size)
4. Calculation time	Faster	Slower
5. Nonlinear function (complex function)	More probably to get local optimum solution	More probably to get global optimum solution
6. Step length	Deterministic	Probabilistic
7. Search method	Serial search	Parallel search

Source: Goldberge (1989)

The basic algorithm of GA can be described as the following steps
(Wasanapradit, 2000)

1. Choose a randomly generated population (feasible candidate solution)
2. Calculate the fitness of each chromosome in the population.
3. Selection process with chose the population to evolve for new population by genetic operation.
4. Check new population by genetic operations; crossover and mutation.
5. Check termination condition
6. Go to step 2

The general structure of GA can be summarized as shown Figure 4.

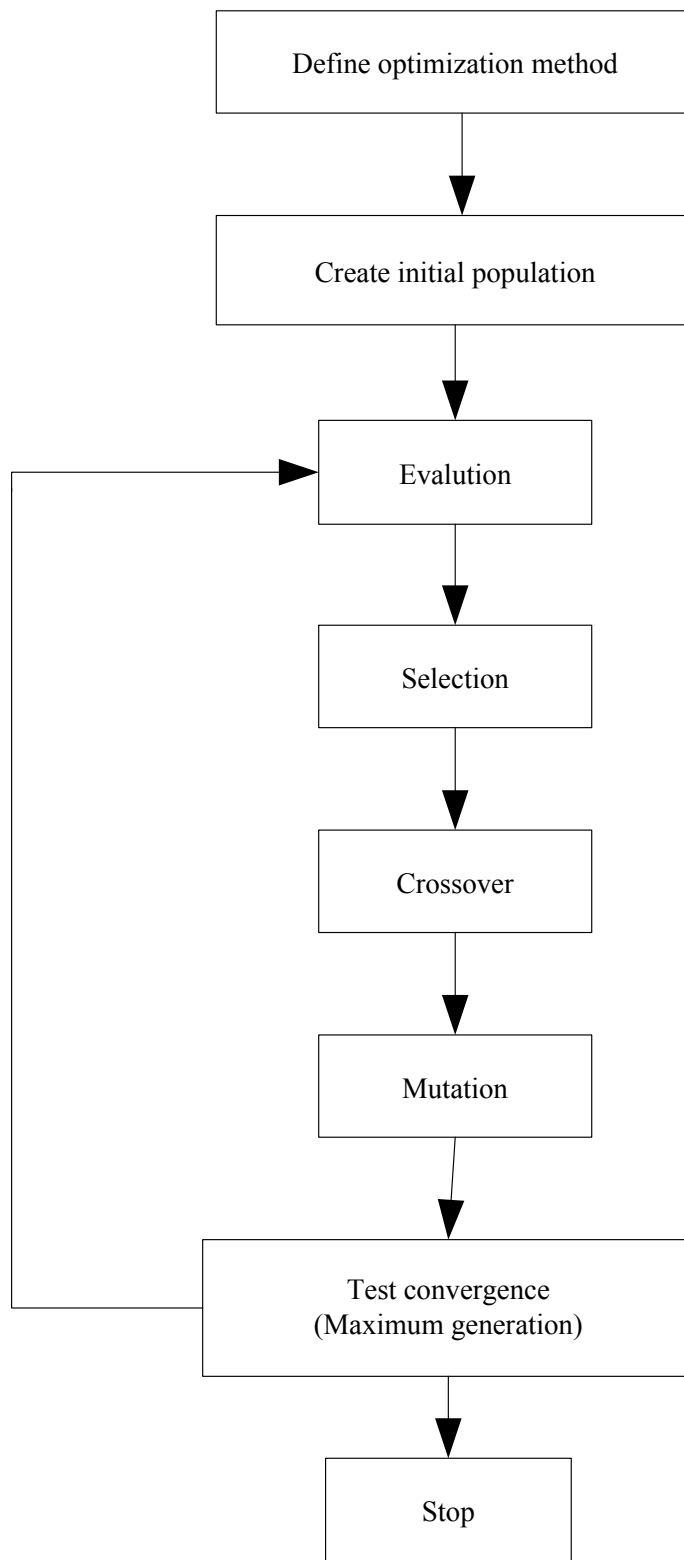


Figure 4 The standard GA

2. Simple GA for optimization problem

In this section we will explain in detail about how a simple GA is applied to optimization. (Mitsuo and Runwei, 1996)

Optimization problem

The numerical example of unconstrained optimization problem is given as follows:

$$\max f(x_1, x_2) = 21.5 + x_1 \sin(4\pi x_1) + x_2 \sin(20\pi x_2) \quad (1)$$

$$-3.0 \leq x_1 \leq 12.1$$

$$4.1 \leq x_2 \leq 5.8$$

Representation (Encoding)

Conventional GA, decision variables have to be encoded to binary string. The length of the string depends on the required precision. For example, the domain of variables x_i is $[a_j, b_j]$ and required precision is five places after the decimal point. The precision requirement implies that the range of domain of each variable should be divided into at least $(b_j - a_j) \times 10^4$ size ranges. The required bits (denoted with m_j) for a variable is calculated as follows;

$$2^{m_j-1} < (b_j - a_j) \times 10^4 \leq 2^{m_j} \quad (2)$$

The mapping from a binary string to a real number for variables x_i is straight forward and completed as follows:

$$x_j = a_j + decimal(substring_j) \times \frac{(b_j - a_j)}{2^{m_j} - 1} \quad (3)$$

Where decimal (substring) represents the decimal value of binary substring for decimal variables x_j

Suppose that the precision is set as five places after the decimal point. The required bits for variables x_1 and x_2 are calculated from equation (2) as follows:

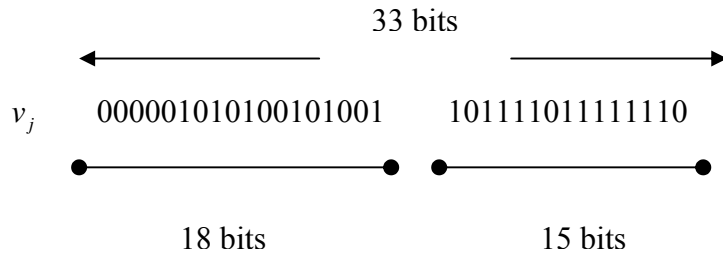
$$(12.1 - (-3.0)) \times 10^4 = 151,000$$

$$2^{17} < 151,000 \leq 2^{18}, \quad m_1 = 18$$

$$(5.8 - 4.1) \times 10^4 = 17,000$$

$$2^{14} < 17,000 \leq 2^{15}, \quad m_2 = 15$$

The total length of a chromosome 33 is bits, which can be represented as follows:



Decoding

The corresponding values for variables x_1 and x_2 are given below:

Table 5 The decimal number of the binary number

	Binary Number	Decimal number
x_1	0 0 0 0 0 1 0 1 0 1 0 0 1 0 1 0 0 1	5417
x_2	1 0 1 1 1 1 0 1 1 1 1 1 1 1 1 0	24318

Source: Mitsuo and Runwei (1996)

From equation (3),

The corresponding value for variables x_1 and x_2 are given below:

$$x_1 = -3.0 + 5417 \times \frac{12.1 - (-3.0)}{2^{18} - 1} = -2.687969$$

$$x_2 = 4.1 + 24318 \times \frac{5.8 - (4.1)}{2^{15} - 1} = 5.361653$$

Initial population

Initial population is randomly generated as follows:

$$v_1 = [00000101010010100110111101111110]$$

$$v_2 = [001110101110011000000010101001000]$$

$$v_3 = [111000111000001000010101001000110]$$

$$v_4 = [100110110100101101000000010111001]$$

$$v_5 = [000010111101100010001110001101000]$$

$$v_6 = [1111101010110110000000010110011001]$$

$$v_7 = [110100010011111000100110011101101]$$

$$v_8 = [001011010100001100010110011001100]$$

$$v_9 = [111110001011101100011101000111101]$$

$$v_{10} = [111101001110101010000010101101010]$$

The corresponding decimal values are:

$$v_1 = [x_1, x_2] = [-2.687969, 5.361653]$$

$$v_2 = [x_1, x_2] = [0.474101, 4.170144]$$

$$v_3 = [x_1, x_2] = [10.419457, 4.661461]$$

$$v_4 = [x_1, x_2] = [6.159951, 4.109598]$$

$$v_5 = [x_1, x_2] = [-2.301286, 4.477282]$$

$$v_6 = [x_1, x_2] = [11.788084, 4.174346]$$

$$v_7 = [x_1, x_2] = [9.342067, 5.121702]$$

$$v_8 = [x_1, x_2] = [-0.330256, 4.694977]$$

$$v_9 = [x_1, x_2] = [11.671267, 4.873501]$$

$$v_{10} = [x_1, x_2] = [11.446273, 4.171908]$$

Evaluation

The process of evaluating the fitness of a chromosome consists of the following three steps:

Step 1: Convert the chromosome's genotype to its phenotype. Here, this means converting binary string into relative real values $x^k = (x^k_1, x^k_2)$; $k = 1, 2, \dots, \text{pop_size}$.

Step 2: Evaluate the objective function $f(x^k)$.

Step 3: Convert the value of objective function into fitness. For the maximizing problem, the fitness is simply equal to the value of objective function $\text{eval}(v^k) = f(x^k)$, $k = 1, 2, \dots, \text{popsize}$.

The fitness function values of above chromosomes are as follows:

$$\text{eval}(v_1) = f(-2.687969, 5.361653) = 19.805119$$

$$\text{eval}(v_2) = f(0.474101, 4.170144) = 17.370896$$

$$\text{eval}(v_3) = f(10.419457, 4.661461) = 9.590546$$

$$\text{eval}(v_4) = f(6.159951, 4.109598) = 29.406122$$

$$\text{eval}(v_5) = f(2.301286, 4.477282) = 15.686091$$

$$\text{eval}(v_6) = f(11.788084, 4.174346) = 11.900541$$

$$\text{eval}(v_7) = f(9.342067, 5.121702) = 17.968717$$

$$\text{eval}(v_8) = f(0.330256, 4.694977) = 19.763190$$

$$\text{eval}(v_9) = f(11.671267, 4.873501) = 26.401669$$

$$\text{eval}(v_{10}) = f(11.446273, 4.171908) = 10.252480$$

It is clear that chromosome v_4 is the strongest one and that chromosome v_3 is the weakest one.

Selection

Selection process is used to select the some chromosome from parents and offspring to be new population. There are many selection methods such as tournament selection, roulette wheel selection and ranking selection. These methods use the fitness value of each chromosome to decide whether it will survive or not.

In most practices, a roulette wheel approach is adopted as the selection procedure; it belongs to the fitness-proportional selection and can select a new population with respect to the probability distribution based on the fitness values. The roulette wheel can be constructed as follows:

1. Calculate the fitness value $eval(v_k)$ for each chromosome v_k :

$$eval(v_k) = f(x), \quad k = 1, 2, \dots, pop_size$$

2. Calculate the total fitness for the population

$$F_{total} = \sum_{k=1}^{pop_size} eval(v_k)$$

3. Calculate selection probability p_k for each chromosome v_k :

$$P_k = \frac{eval(v_k)}{F_{total}}, \quad k = 1, 2, \dots, pop_size$$

4. Calculate cumulative probability q_k for each chromosome v_k :

$$q_k = \sum_{j=1}^{pop_size} P_j, \quad k = 1, 2, \dots, pop_size$$

The selection process begins by spinning the roulette wheel equal to population size times: each time, a single chromosome is selected for a new population in the following way:

Procedure: Selection

Step 1: Generate a random number r from the range $[0, 1]$.

Step 2: If $r \leq q_1$, then select the first chromosome v_1 ; otherwise, select the k^{th} chromosome v_k ($2 \leq k \leq pop_size$) such that $q_{k-1} \leq r \leq q_k$

The total fitness F_{total} of the population is:

$$F_{\text{total}} = \sum_{k=1}^{10} eval(v_k) = 178.135372$$

The probability of a selection p_k for each chromosome v_k ($j = 1, \dots, 10$) is as follows:

$$\begin{aligned}
 p_1 &= 0.111180, & p_2 &= 0.097515, & p_3 &= 0.053839 \\
 p_4 &= 0.165077, & p_5 &= 0.088057, & p_6 &= 0.066806 \\
 p_7 &= 0.100815, & p_8 &= 0.110945, & p_9 &= 0.148211 \\
 p_{10} &= 0.057554
 \end{aligned}$$

The cumulative probabilities q_k for each chromosome v_k ($j = 1, \dots, 10$) is as follows:

$$\begin{aligned}
 q_1 &= 0.111180, & q_2 &= 0.208695, & q_3 &= 0.262534 \\
 q_4 &= 0.427611, & q_5 &= 0.515668, & q_6 &= 0.582475 \\
 q_7 &= 0.683290, & q_8 &= 0.794234, & q_9 &= 0.942446 \\
 q_{10} &= 1.000000
 \end{aligned}$$

Now we are ready to spin the roulette wheel 10 times, and each time we select a single chromosome for a new population. Let us assume that a random sequence 10 numbers from the range $[0, 1]$ is as follows:

$$\begin{aligned}
 &0.301431 & 0.322062 & 0.766503 & 0.881893 \\
 &0.350871 & 0.583392 & 0.177618 & 0.343242 \\
 &0.032685 & 0.197577 & &
 \end{aligned}$$

The first number $r_1 = 0.301431$ is greater than q_3 and smaller than q_4 , meaning that the chromosome v_4 is selected for the new population; the second number $r_2 = 0.322062$ is greater than q_3 and smaller than q_4 , meaning that the chromosome v_4 is again selected for the new population; and so on. Finally, the new population consists of the following chromosomes:

$$v'_1 = [100110110100101101000000010111001] (v_4)$$

$$v'_2 = [100110110100101101000000010111001] (v_4)$$

$$v'_3 = [001011010100001100010110011001100] (v_8)$$

$$v'_4 = [111110001011101100011101000111101] (v_9)$$

$$v'_5 = [100110110100101101000000010111001] (v_4)$$

$$v'_6 = [110100010011111000100110011101101] (v_7)$$

$$v'_7 = [0011101011100110000000010101001000] (v_2)$$

$$v'_8 = [100110110100101101000000010111001] (v_4)$$

$$v'_9 = [00000101010010100110111101111110] (v_1)$$

$$v'_{10} = [0011101011100110000000010101001000] (v_2)$$

Crossover

Crossover is used to create two new chromosomes (offspring) from two existing chromosomes (parents) picked from the current population. Both one-point and two-point crossover techniques are used in the search processes. In one-point crossover, two chromosomes are randomly selected as parents from the pool of chromosomes and cut at a randomly selected point. The tails, which are parts after the cutting point, are swapped and two new chromosomes are formed.

The crossover rate (denoted by P_C) is defined as the ratio of the number of offspring produced in each to population size. A higher crossover rate allows exploration of the more solution space and reduces the changes of setting for a false optimum. But if this rate is too high, it results in the wastage of a lot of computation time in exploring unpromising regions of the solution space.

Crossover used here is one-cut-point method. If the probability of crossover is set as $P_C = 0.25$, so we expect that, on average, 25% of chromosome undergo crossover. Crossover is preformed in the following way:

Procedure: Crossover

```

Begin

    k = 0

    While (k ≤ 10) do
        rk = random number from [0,1];

        If (rk < 0.25) then
            Selection vk as one parent for crossover
        end

        k = k+1:
    end

end.

```

Figure 5 The general structure of crossover

Source: Gen and Cheng (1996)

Assume that the sequence of random numbers is

0.625721	0.266823	0.288644	0.295114
0.163274	0.567461	0.085940	0.392865
0.770714	0.548656		

This means that the chromosome v'_5 and v'_7 were selected for crossover. We generate random integer number *pos* from the range [1,32] (because 33 is the total length of a chromosome) as cutting point or in other words, the position of the crossover point. Assume that the generated number *pos* equals 1, the two chromosomes are cut after the first bit, and offspring are generated by exchanging the right parts of them as follows:

$$v'_5 = [100110110100101101000000010111001]$$

$$v'_7 = [0011101011100110000000010101001000]$$

Then, the selected chromosome will be replaced with their resulting offspring as follows:

$$v'_5 = [1011101011100110000000010101001000]$$

$$v'_7 = [000110110100101101000000010111001]$$

Mutation

Mutation operates on one individual (chromosome) at a time that makes the offspring very different from their parents by changing the value of some genes in chromosome randomly. For example in binary coding solution, some genes are randomly selected and flipped from 1 to 0 and vice versa. From this operation, population that is converging onto some optimum can jump is not a different optima that may be the global optimum.

The mutation rate (denoted by P_m) is defined as the percentage of the total numbers of genes in the population. The mutation rate controls the rate at which new genes are introduced into the population for trial. If it is too low, many genes that would have been useful are never tried out. But if it is too high, there will be much random perturbation. The offspring will start losing their resemblance to the parents, and the algorithm will lost the ability to learn from the history of the search.

Assume that the 18th gene of the chromosome v_1 is selected for a mutation. Since the gene is 1, it would be flipped into 0. Thus the chromosome after mutation would be

$$\begin{array}{c}
 v'_1 = [100110110100101101000000010111001] \\
 \downarrow \\
 v'_1 = [100110110100101100000000010111001]
 \end{array}$$

The probability of mutation is set as $P_m = 0.01$, so we expect that, on average, 1% of total bit of population would undergo mutation. There are $m \times \text{pop_size} = 33 \times 10 = 330$ bits in the whole population; we expect 33 mutation per generation. Every bit has an equal chance to be mutated. Thus we need to generate a sequence of random numbers r_m ($m = 1, \dots, 330$) from the range $[0,1]$. Mutation is performed in the following way:

Procedure: Mutation

Begin

$m = 0$;

While ($m \leq 330$) do

$r_m =$ random number from $[0,1]$;

if ($r_m < 0.01$) then

select position v_k as one parent for mutation;

end

$m = m+1$

end

end.

Figure 6 The general structure of mutation

Source: Gen and Cheng (1996)

Suppose that the following genes in Table 3 will go through mutation:

Table 6_ The position of mutated genes in mutated chromosomes

bit-pos	chrom_num	bit_num	random_num
105	4	6	0.009857
164	5	32	0.003113
129	7	1	0.000946
329	10	32	0.001282

Source: Mitsuo and Runwei (1996)

After replaced old chromosome with their mutated chromosome, we get the final population as follows:

$$v'_1 = [100110110100101101000000010111001]$$

$$v'_2 = [100110110100101101000000010111001]$$

$$v'_3 = [001011010100001100010110011001100]$$

$$v'_5 = [100110110100101101000000010111001]$$

$$v'_6 = [110100010011111000100110011101101]$$

$$v'_7 = [0011101011100110000000010101001000]$$

$$v'_8 = [100110110100101101000000010111001]$$

$$v'_9 = [00000101010010100110111101111110]$$

$$v'_{10} = [0011101011100110000000010101001000]$$

The corresponding decimal values of variables $[x_1, x_2]$ and fitness are as follows:

$$f(6.159951, 4.109598) = 29.406122$$

$$f(6.159951, 4.109598) = 29.406122$$

$$f(0.330256, 4.694977) = 19.763190$$

$$f(11.907206, 4.873501) = 5.70281$$

$$f(8.024130, 4.170248) = 19.91025$$

$$f(9.342067, 5.121702) = 17.958717$$

$$f(6.159951, 4.109598) = 29.406122$$

$$f(6.159951, 4.109598) = 29.406122$$

$$f(-2.687969, 5.361653) = 19.805119$$

$$f(0.474101, 4.170248) = 17.370896$$

This is completed the one iteration of GA. The test run is terminated after 1000 generations. We have obtained the best chromosome, v^* , in the 419th generation as follows:

$$v^* = (111110000000111000111101001010110)$$

$$\text{eval}(v^*) = f(11.631407, 5.724824) = 38.818208$$

$$x^*_1 = 11.631407$$

$$x^*_2 = 5.724824$$

$$f(x^*_1, x^*_2) = 38.81820$$

Formulation of the estimation parameter

1. Structure of the mathematic model

The majority of mathematical models for estimation chemical kinetic rate constant can be classified in one of these two categories; algebraic and differential equation (Englezoos and Kalogerakis, 2001). The models are employed throughout this thesis

1.1 Algebraic equation models

In mathematical terms, these models are of the form

$$y = f(x, k) \quad (13)$$

where

$k = [k_1, k_2, \dots, k_p]^T$ is a p-dimensional vector of parameters whose numerical values are unknown.

$x = [x_1, x_2, \dots, x_n]^T$ is a n-dimensional vector of independent variables (also called regressor or input variables) which are either fixed for each experiment by the experimentalist or which are measured.

$y = [y_1, y_2, \dots, y_m]^T$ is a m-dimensional vector of dependent variables (also often described as response variables or the output vector) there are the model variables which are actually measure in the experiments.

$f = [f_1, f_2, \dots, f_m]^T$ is a m-dimensional vector of dependent variables (also often described as response variables or the output vector) there are the model variables which are actually measure in the experiments.

Equation (13), the mathematical model of the process, is very general and it covers many cases, namely,

- (i) The single response with a single independent variable model (i.e., $m=1, n=1$)

$$y = f(x; k_1, k_2, \dots, k_p)$$

- (ii) The single response with several independent variable model (i.e., $m=1, n>1$)

$$y = f(x_1, x_2, \dots, x_n; k_1, k_2, \dots, k_p)$$

- (iii) The multi-response with several independent variables model ((i.e., $m>1, n>1$))

$$\begin{bmatrix} y_1 \\ y_2 \\ \cdot \\ \cdot \\ \cdot \\ y_m \end{bmatrix} = \begin{bmatrix} f_1(x_1, x_2, \dots, x_n; k_1, k_2, \dots, k_p) \\ f_2(x_1, x_2, \dots, x_n; k_1, k_2, \dots, k_p) \\ \cdot \\ \cdot \\ \cdot \\ f_m(x_1, x_2, \dots, x_n; k_1, k_2, \dots, k_p) \end{bmatrix}$$

1.2 Differential equation models

Let us first concentrate on dynamic systems described by a set of ordinary differential equation (ODEs). In certain occasions the governing ordinary differential equations can be solved analytically and as far as parameters estimation is concentrated, the problem is described by a set of algebraic equations. If however, the ODEs cannot be solved analytically, the mathematical model is more complex. In general, the model equations can be written in the form

$$\frac{dx(t)}{dt} = f(x(t), u, k); \quad x(t) = x_0$$

$$y(t) = Cx(t)$$

or

$$y(t) = h(x(t), k)$$

where

$k = [k_1, k_2, \dots, k_p]^T$ is a p -dimensional vector of parameters whose numerical values are unknown.

$x = [x_1, x_2, \dots, x_n]^T$ is a n -dimensional vector of state variables.

$x_0 = [x_{10}, x_{20}, \dots, x_{n0}]^T$ is a n -dimensional vector of initial conditions for the state variables and they are assumed to be known precisely.

$u = [u_1, u_2, \dots, u_r]^T$ is a r -dimensional vector of manipulated variables which are either set by the experimentalist and their numerical values are precisely known or they have been measured

$f = [f_1, f_2, \dots, f_n]^T$ is a n -dimensional vector function of known form (the differential equations)

$y = [y_1, y_2, \dots, y_m]^T$ is a m -dimensional output vector i.e., the set of variables that are measured experimentally.

C = the $m \times n$ observation matrix which indicates the state variables (or linear combinations of state variables) that are measured experimentally.

$h = [h_1, h_2, \dots, h_m]^T$ is a m -dimensional vector function of known form that relates in a nonlinear fashion the state vector to the output vector.

2. The objective function

In general, the unknown parameter vector k is found by minimizing a scalar function often referred to as the objective function. We shall denote this function as $S(k)$ to indicate the dependence on the chosen parameters.

The objective function is a suitable measure of the overall departure of the model calculated values from the measurements. For an individual measurement the departure from the model calculated values is represented by the residual e_i . For example, the i^{th} residual of an explicit algebraic model is

$$e_i = [\hat{y}_i - f(x_i, k)]$$

Where the model based value $f(x_i, k)$ is calculation using the estimated parameter values.

In this thesis, we minimize the sum of squares of error (SSE) without any weighting factor, i.e.

$$S_{LS}(k) = \sum_{i=1}^N e_i^T e_i$$

Numerical method

In the present research, high-order Runge-Kutta method was used to solve differential equation, its schemes are more practical to use because of their higher accuracy, and the derivation of the constants is similar, but more complicated. We consider a four order Runge-Kutta scheme, we can write it in the form

$$y_{i+1} = y_i + w_1 k_1 + w_2 k_2 + w_3 k_3 + w_4 k_4$$

Whereas the w_1, \dots are the weight $(1/6, 2/6, 2/6, 1/6)$, and then k_1, \dots are h times various approximations to the slopes at points in the step, and are given by:

$$k_1 = hf(x_i, y_i)$$

$$k_2 = hf(x_i + a_1 h, y_i + b_1 k_1)$$

$$k_3 = hf(x_i + a_2 h, y_i + b_2 k_1 + b_3 k_2)$$

$$k_4 = hf(x_i + a_3 h, y_i + b_4 k_1 + b_5 k_2 + b_6 k_3)$$

Where the a_1, \dots and b_1, \dots are constants to be determined. Using techniques similar to those used in the second order Runge-Kutta method, the most frequently used choice of the constants lead to the iteration scheme:

$$y_{i+1} = y_i + h(f_1 + 2f_2 + 2f_3 + f_4)/6$$

Where:

$$f_1 = f(x_i, y_i)$$

$$f_2 = f(x_i + h/2, y_i + hf_1/2)$$

$$f_3 = f(x_i + h/2, y_i + hf_2/2)$$

$$f_4 = f(x_i + h, y_i + f_3)$$

MATERIALS AND METHODS

Materials

1. Material

- 1.1 A 1000 ml of three necked glass flask reactor
- 1.2 Hot plate magnetic stirrer(SCHOTT model series GmbH D-55122)
- 1.3 Cooler
- 1.4 Centrifuge
- 1.5 Stopwatch
- 1.6 Analytical balance (2 and 4 digits)
- 1.7 Digital thermometer control
- 1.8 Gas chromatography (SHIMADZU series 2010 gas)
- 1.9 DB5-HT column (0.32mm x 0.1um x 15 m) from Agilent technology, Inc

2. Chemicals

- 2.1 Vegetable oils (refined, bleached and deodorized palm oil) from super market.
- 2.2 Methanol with A.R. grade of purity from Lab-Scan (Ireland).
- 2.3 Strontium oxide with 99.9 % of purity from Aldrich. It was shown in Figure 1.
- 2.4 MSTFA with > 97 % of purity from Fluka (Switzerland).
- 2.5 N-heptane with A.R. grade of purity from Lab-Scan (Ireland).
- 2.6 Pyridine with A.R. grade of purity from Sigma (Japan).
- 2.7 Glycerol standard for GC standard from Sigma (Japan).
- 2.8 1-Monolauroyl-rac-glycerol (C12:0) for GC standard from Sigma (Japan).
- 2.9 1-Monomyristoyl-rac-glycerol (C14:0) for GC standard from Sigma (Japan).
- 2.10 DL- α -palmitin (C16:0) for GC standard from Sigma (Japan).

- 2.11 1-Stearoyl-rac-glycerol (C18:0) for GC standard from Sigma (Japan).
- 2.12 Dilaurin (C12:0) for GC standard from Supelco (Japan).
- 2.13 Dimyristin (C14:0) for GC standard from Supelco (Japan).
- 2.14 Dipalmitin (C16:0) for GC standard from Supelco (Japan).
- 2.15 Distearin (C18:0) for GC standard from Supelco (Japan).
- 2.16 Trilaurin (C12:0) for GC standard from Supelco (Japan).
- 2.17 Trimyristin (C14:0) for GC standard from Supelco (Japan).
- 2.18 Tripalmitin (C16:0) for GC standard from Supelco (Japan).
- 2.19 Tristearin (C18:0) for GC standard from Supelco (Japan).
- 2.20 Tricaprin (C10:0) for GC standard from Supelco (Japan).

3. Gases

- 3.1 Hydrogen (99.999%), for flame ionization detector (FID).
- 3.2 Helium (99.999%), as a carrier gas.
- 3.3 Nitrogen (99.99%), as mixer gas.
- 3.4 Oxygen, supplied by air pump.



Figure 7 Strontium oxide powder with 99.9 of purity

Methods

1. Transesterification of vegetable oils using heterogeneous catalyst

Transesterification reaction of vegetable oils was performed in three-necked flask. The glass reflux condenser was used to condense methanol vapor back to the reaction mixture. The reaction heat was supplied by using the hotplate magnetic stirrer equipped with a temperature controller that was capable of maintaining the temperature within $\pm 0.5^{\circ}\text{C}$ as shown in the Figure 1

1.1) 500 grams of palm olein was weighed and filled to the reactor.

1.2) The desired amount of methanol was weighed and mixed with oil in the reactor and heated to the desired temperature.

1.3) The mixture was carried out until it reached the desired temperature.

1.4) 15 grams of strontium oxide was weighed and filled to a mixture then a speed of magnetic stirrer was changed to a desired speed throughout the experiment.

1.5) The sample was withdrawn quickly from the reactor at 2, 4, 6, 8, 10, 15, 20, 30, 60, 120 and 180 min. with micropipette, about 3ml of mixture per sample.

1.6) A sample was centrifuged to separate solid catalyst. The speed of centrifugal was 1000 rpm during 120 seconds.

1.7) The liquid phase mixture was evaporated a residual methanol out of the mixture.

1.8) The mixture was collected and 0.5 g of mixture was taken to analyze for tri-, di-, monoglycerides and free glycerin using GC.

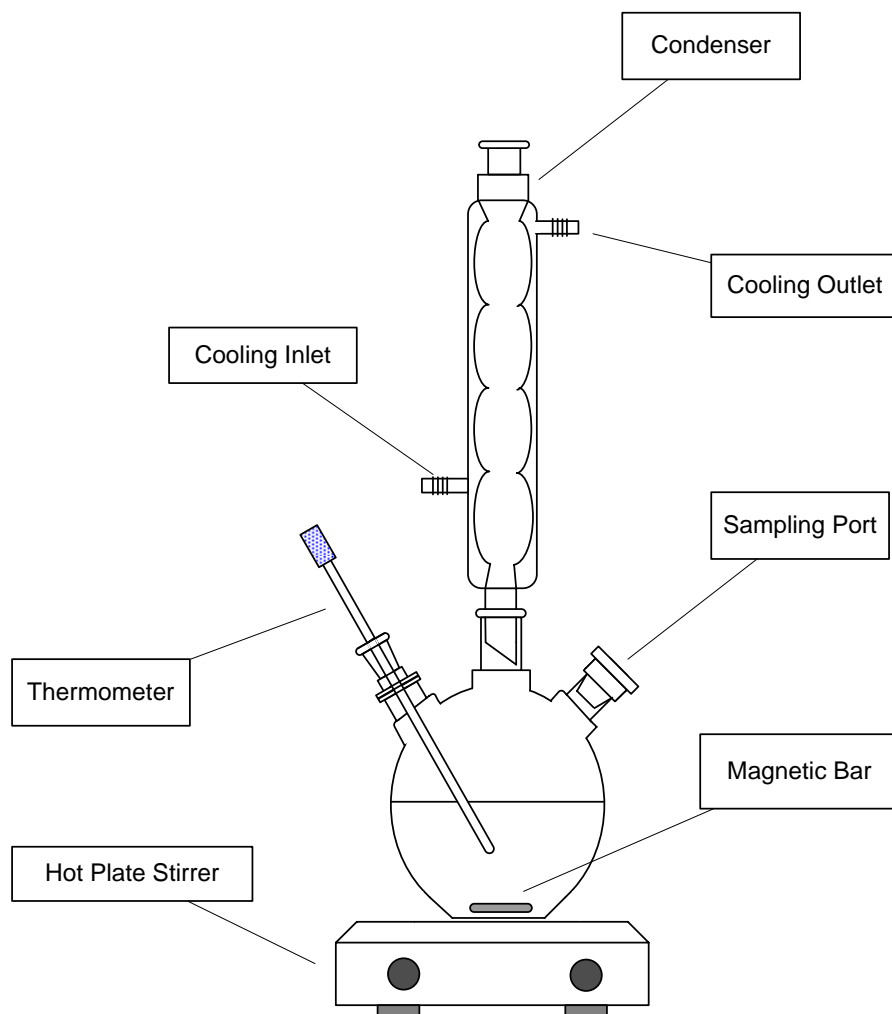


Figure 8 Three neck-glass flask as a slurry reactor.

2. Analysis methods

The samples were collected from the transesterification reaction that was analyzed to find the concentration of TG, DG, MG and GL by gas chromatography. The analysis procedure is as follow:

2.1) 50 mg of sample was weighted and filled to 5 ml of vial by the analytical balance (4 digits).

2.2) 100 uL of both MSTFA and Internal standard (0.8 g of tricaprin in 10 mL of pyridine) were weighted by micropipette and filled into a sample vial.

2.3) Waiting during 15 min. for the derivative reaction of MSTFA.

2.4) Added 8 mL of n-heptane to a sample vial then mixed throughout a vial.

2.5) Take 1 uL of this mixture to analysts by gas chromatography that the result was presented using a peak area. The standard curve that was a peak area versus concentration, it was used to convert the peak area to the concentration of sample in TG, DG, MG and G form. The standard curve of TG, DG, MG and G is as follows:

Glycerol concentration:

$$G \text{ (\%w/w)} = \left[a_g \left(\frac{A_g}{A_{IS}} \right) + b_g \right] \cdot W_{IS} \cdot \frac{100}{W} \quad (1.)$$

Monoglyceride concentration:

$$G_M \text{ (\%w/w)} = \left[a_m \left(\frac{A_m}{A_{IS}} \right) + b_m \right] \cdot W_{IS} \cdot \frac{100}{W} \quad (2.)$$

Diglyceride concentration:

$$G_D \text{ (\%w/w)} = \left[a_d \left(\frac{A_d}{A_{IS}} \right) + b_d \right] \cdot W_{IS} \cdot \frac{100}{W} \quad (3.)$$

Triglyceride concentration:

$$G_T \text{ (\%w/w)} = \left[a_t \left(\frac{A_t}{A_{IS}} \right) + b_t \right] \cdot W_{IS} \cdot \frac{100}{W} \quad (4.)$$

Where

G_i = Concentration of component i (%w/w) within a sample

A_i = Peak area of glycerol within a sample

A_{IS} = Peak area of internal standard within a sample

W_{IS} = Weight of internal standard within a sample

W = Weight of sample

a_i = The slope of standard curve of component i

b_i = The interception of standard curve of component i

i = Triglycetide, diglyceride, monoglyceride and glyceride component

3. Mass transfer resistance

In this section, the triglycerides, diglycerides, monoglycerids concentration were detected and analyzed at 65 °C throughout the experiment while the agitator speed was vary at 500, 700 and 1000 rpm.

4. Appropriate GA parameter

In this section we will find appropriate GA parameters for estimation of kinetic rate constants of palm olein oil transesterification reaction. We have selected the GA parameters to study performance in six cases as follow:

Case 1 number of population size of GA

The selected value of population size for study in this case is 100, 250, 500, 1000 and 2000. The other parameters of genetic algorithm were used by the default value.

Case 2 maximum generation number

In this case, we intend to find the maximum number of generation that should be used in this research. The chosen value for study is equal to 100, 300, 500, and 1000.

Case 3 crossover fraction

In this case, the approximate crossover fraction will be investigated. The chosen crossover fraction for this study is equal to 0.3, 0.5 and 0.8.

Case 4 mutation rate

The mutation rate value at 0.01, 0.05, 0.10, 0.20, 0.30, 0.40 and 0.50 were chosen to find the suitable value for parameter estimation of kinetic rate constant.

Case 5 migration rate

In this case, we investigated the suitable values of migration rate. It was chosen at 0.01, 0.1, 0.2, 0.4, 0.6 and 0.8.

Case 6 hybrid function

In this case, the hybrid function was intersected as the helping search tool for GA. It consisted of none, fminsearch, patternsearch and fminunc.

5. Estimation of kinetic parameters

In this work, two kinetic models, pseudo-homogeneous and Langmuir-Hinshewood models were selected to used for description of kinetic experiment of palm olein oil transesterification. Both models were classified to two case that consist of FAME concentration with or without in the model.

5.1 Pseudo-Homogeneous model

Case 1: Reversible reaction in all steps

The general form of the governing set of differential equation characterizing the reversible reaction in all steps showed in Equations 5 – 9.

Triglycerides:

$$\frac{dC_{TG}}{dt} = -k_1 C_{TG} + k_2 C_{DG} \quad (5.)$$

Diglycerides:

$$\frac{dC_{DG}}{dt} = k_1 C_{TG} - k_2 C_{DG} C_{FAME} - k_3 C_{DG} - k_4 C_{MG} C_{FAME} \quad (6.)$$

Monoglycerides:

$$\frac{dC_{MG}}{dt} = k_3 C_{DG} - k_4 C_{MG} C_{FAME} + k_5 C_{MG} + k_6 C_G C_{FAME} \quad (7.)$$

Glycerides:

$$\frac{dC_{MG}}{dt} = k_5 C_{MG} - k_6 C_{GL} C_{FAME} \quad (8.)$$

Fatty acid methyl ester:

$$\begin{aligned} \frac{dC_{FAME}}{dt} = & k_1 C_{TG} - k_2 C_{DG} C_{FAME} + k_3 C_{DG} - k_4 C_{MG} C_{FAME} \\ & + k_5 C_{MG} - k_6 C_G C_{FAME} \end{aligned} \quad (9.)$$

Case 2: Irreversible reaction

In case of PH model with irreversible reaction, the governing set of differential equation characterizing the irreversible reaction is separated into with or without FAME concentration that showed in Equations 10 – 18.

Without FAME concentration

Triglycerides:

$$\frac{dC_{TG}}{dt} = -k_1 C_{TG} \quad (10.)$$

Diglycerides:

$$\frac{dC_{DG}}{dt} = k_1 C_{TG} - k_2 C_{DG} \quad (11.)$$

Monoglycerides:

$$\frac{dC_{MG}}{dt} = k_2 C_{DG} - k_3 C_{MG} \quad (12.)$$

Glycerol:

$$\frac{dC_G}{dt} = k_3 C_{MG} \quad (13.)$$

With FAME concentration

Triglycerides:

$$\frac{dC_{TG}}{dt} = -k_1 C_{TG} \quad (14.)$$

Diglycerides:

$$\frac{dC_{DG}}{dt} = k_1 C_{TG} - k_2 C_{DG} \quad (15.)$$

Monoglycerides:

$$\frac{dC_{MG}}{dt} = k_2 C_{DG} - k_3 C_{MG} \quad (16.)$$

Glycerol:

$$\frac{dC_G}{dt} = k_3 C_{MG} \quad (17.)$$

Fatty acid methyl ester:

$$\frac{dC_{FAME}}{dt} = k_1 C_{TG} + k_2 C_{DG} + k_3 C_{MG} \quad (18.)$$

where k_1 , k_2 and k_3 are the reaction rate constants.

Case 3: Reversible reaction in step 3 (monoglyceride step)

In case of reversible reaction in step 3, the governing set of differential equation characterizing the irreversible reaction is showed in Equations 19 – 23.

Triglycerides:

$$\frac{dC_{TG}}{dt} = -k_1 C_{TG} \quad (19.)$$

Diglycerides:

$$\frac{dC_{DG}}{dt} = k_1 C_{TG} - k_2 C_{DG} \quad (20.)$$

Monoglycerides:

$$\frac{dC_{MG}}{dt} = k_2 C_{DG} - k_3 C_{MG} + k_4 C_{GL} C_{FAME} \quad (21.)$$

Glycerol:

$$\frac{dC_G}{dt} = k_3 C_{MG} - k_4 C_{GL} C_{FAME} \quad (22.)$$

Fatty acid methyl ester:

$$\frac{dC_{FAME}}{dt} = k_1 C_{TG} + k_2 C_{DG} C_{FAME} + k_3 C_{MG} - k_4 C_{GL} C_{FAME} \quad (23.)$$

5.2 Langmuir-Hinshelwood model

In case of Langmuir-Hinshelwood (PH) model, it was classified into two types of model. Firstly, the power number in the adsorption term is equal to two. The second one is one in power number.

Case 1: Irreversible reaction

Without FAME concentration

There is the rate of reaction of transesterification that based on the Langmuir-Hinshelwood model, the set of differential equations characterizing as follows:

Triglycerides:

$$\frac{dC_{TG}}{dt} = -r_1$$

Diglycerides:

$$\frac{dC_{DG}}{dt} = r_1 - r_2$$

Monoglycerides:

$$\frac{dC_{MG}}{dt} = r_2 - r_3$$

Glycerides:

$$\frac{dC_{GL}}{dt} = r_3$$

Fatty acid methyl ester:

$$\frac{dC_G}{dt} = r_1 + r_2 + r_3$$

In case of LH type 1, the resulting rate equations are as follows

$$r_1 = \frac{k_1 \cdot K_t \cdot C_{TG}}{\left(1 + K_t \cdot C_{TG} + K_d \cdot C_{DG} + K_m \cdot C_{MG} + K_g \cdot C_{GL}\right)^2} \quad (24.)$$

$$r_2 = \frac{k_2 \cdot K_d \cdot C_{DG}}{\left(1 + K_t \cdot C_{TG} + K_d \cdot C_{DG} + K_m \cdot C_{MG} + K_g \cdot C_{GL}\right)^2} \quad (25.)$$

$$r_3 = \frac{k_3 \cdot K_m \cdot C_{MG}}{\left(1 + K_t \cdot C_{TG} + K_d \cdot C_{DG} + K_m \cdot C_{MG} + K_g \cdot C_{GL}\right)^2} \quad (26.)$$

In case of LH type 2, the resulting rate equations are as follows

$$r_1 = \frac{k_1 \cdot K_t \cdot C_{TG}}{\left(1 + K_t \cdot C_{TG} + K_d \cdot C_{DG} + K_m \cdot C_{MG} + K_g \cdot C_{GL}\right)} \quad (27.)$$

$$r_2 = \frac{k_2 \cdot K_d \cdot C_{DG}}{\left(1 + K_t \cdot C_{TG} + K_d \cdot C_{DG} + K_m \cdot C_{MG} + K_g \cdot C_{GL}\right)} \quad (28.)$$

$$r_3 = \frac{k_3 \cdot K_m \cdot C_{MG}}{\left(1 + K_t \cdot C_{TG} + K_d \cdot C_{DG} + K_m \cdot C_{MG} + K_g \cdot C_{GL}\right)} \quad (29.)$$

With FAME concentration

The differential equation characterizing the irreversible reaction is showed in Equations 13 – 19.

Triglycerides:

$$\frac{dC_{TG}}{dt} = -r_1$$

Diglycerides:

$$\frac{dC_{DG}}{dt} = r_1 - r_2$$

Monoglycerides:

$$\frac{dC_{MG}}{dt} = r_2 - r_3$$

Glycerol:

$$\frac{dC_G}{dt} = r_3$$

Fatty acid methyl ester:

$$\frac{dC_{FAME}}{dt} = r_1 + r_2 + r_3$$

In case of LH type 1, the resulting rate equations are as follows

$$r_1 = \frac{k_1 \cdot K_t \cdot C_{TG}}{\left(1 + K_t \cdot C_{TG} + K_d \cdot C_{DG} + K_m \cdot C_{MG} + K_g \cdot C_{GL} + K_f C_{FAME}\right)^2} \quad (30.)$$

$$r_2 = \frac{k_2 \cdot K_d \cdot C_{DG}}{\left(1 + K_t \cdot C_{TG} + K_d \cdot C_{DG} + K_m \cdot C_{MG} + K_g \cdot C_{GL} + K_f C_{FAME}\right)^2} \quad (31.)$$

$$r_3 = \frac{k_3 \cdot K_m \cdot C_{MG}}{\left(1 + K_t \cdot C_{TG} + K_d \cdot C_{DG} + K_m \cdot C_{MG} + K_g \cdot C_{GL} + K_f C_{FAME}\right)^2} \quad (32.)$$

In case of LH type 2, the resulting rate equations are as follows

$$r_1 = \frac{k_1 \cdot K_t \cdot C_{TG}}{\left(1 + K_t \cdot C_{TG} + K_d \cdot C_{DG} + K_m \cdot C_{MG} + K_g \cdot C_{GL} + K_f C_{FAME}\right)} \quad (33.)$$

$$r_2 = \frac{k_2 \cdot K_d \cdot C_{DG}}{\left(1 + K_t \cdot C_{TG} + K_d \cdot C_{DG} + K_m \cdot C_{MG} + K_g \cdot C_{GL} + K_f C_{FAME}\right)} \quad (34.)$$

$$r_3 = \frac{k_3 \cdot K_m \cdot C_{MG}}{\left(1 + K_t \cdot C_{TG} + K_d \cdot C_{DG} + K_m \cdot C_{MG} + K_g \cdot C_{GL} + K_f C_{FAME}\right)} \quad (35.)$$

Case 2: Reversible reaction in step 3 (monoglyceride step)

The differential equation characterizing the irreversible reaction is showed in Equations 36 – 43.

Triglycerides:

$$\frac{dC_{TG}}{dt} = -r_1$$

Diglycerides:

$$\frac{dC_{DG}}{dt} = r_1 - r_2$$

Monoglycerides:

$$\frac{dC_{MG}}{dt} = r_2 - r_3 + r_4$$

Glycerol:

$$\frac{dC_G}{dt} = r_3 - r_4$$

Fatty acid methyl ester:

$$\frac{dC_{FAME}}{dt} = r_1 + r_2 + r_3 - r_4$$

In case of LH type 1, the resulting rate equations are as follows

$$r_1 = \frac{k_1 \cdot K_t \cdot C_{TG}}{\left(1 + K_t \cdot C_{TG} + K_d \cdot C_{DG} + K_m \cdot C_{MG} + K_g \cdot C_{GL} + K_f C_{FAME}\right)^2} \quad (36.)$$

$$r_2 = \frac{k_2 \cdot K_d \cdot C_{DG}}{\left(1 + K_t \cdot C_{TG} + K_d \cdot C_{DG} + K_m \cdot C_{MG} + K_g \cdot C_{GL} + K_f C_{FAME}\right)^2} \quad (37.)$$

$$r_3 = \frac{k_3 \cdot K_m \cdot C_{MG}}{\left(1 + K_t \cdot C_{TG} + K_d \cdot C_{DG} + K_m \cdot C_{MG} + K_g \cdot C_{GL} + K_f C_{FAME}\right)^2} \quad (38.)$$

$$r_4 = \frac{k_4 \cdot K_g \cdot C_{GL}}{\left(1 + K_t \cdot C_{TG} + K_d \cdot C_{DG} + K_m \cdot C_{MG} + K_g \cdot C_{GL} + K_f C_{FAME}\right)^2} \quad (39.)$$

In case of LH type 2, the resulting rate equations are as follows

$$r_1 = \frac{k_1 \cdot K_t \cdot C_{TG}}{\left(1 + K_t \cdot C_{TG} + K_d \cdot C_{DG} + K_m \cdot C_{MG} + K_g \cdot C_{GL} + K_f C_{FAME}\right)} \quad (40.)$$

$$r_2 = \frac{k_2 \cdot K_d \cdot C_{DG}}{\left(1 + K_t \cdot C_{TG} + K_d \cdot C_{DG} + K_m \cdot C_{MG} + K_g \cdot C_{GL} + K_f C_{FAME}\right)} \quad (41.)$$

$$r_3 = \frac{k_3 \cdot K_m \cdot C_{MG}}{\left(1 + K_t \cdot C_{TG} + K_d \cdot C_{DG} + K_m \cdot C_{MG} + K_g \cdot C_{GL} + K_f C_{FAME}\right)} \quad (42.)$$

$$r_4 = \frac{k_4 \cdot K_g \cdot C_{GL}}{\left(1 + K_t \cdot C_{TG} + K_d \cdot C_{DG} + K_m \cdot C_{MG} + K_g \cdot C_{GL} + K_f C_{FAME}\right)} \quad (43.)$$

Where k_1 , k_2 , k_3 and k_4 are the reaction rate constants and K_t is the adsorption equilibrium constant of TG, K_d is the adsorption equilibrium constant of DG, K_m is the adsorption equilibrium constant of MG, K_g is the adsorption equilibrium constant of GL and K_f is the adsorption equilibrium constant of FAME.

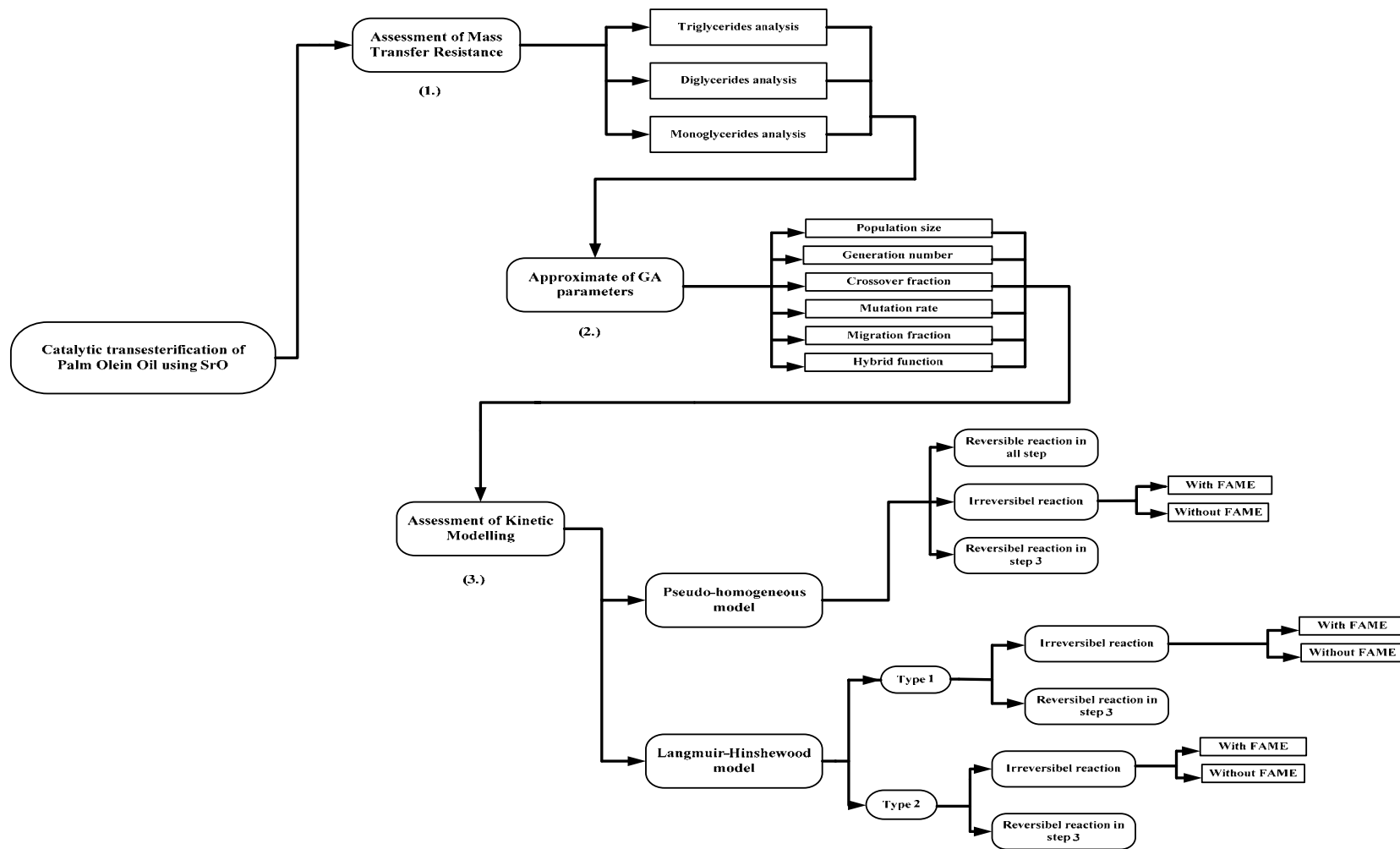


Figure 9 The procedure flowchart of kinetic study of catalytic transesterification of palm olein oil over SrO

RESULTS AND DISCUSSIONS

In this chapter, there were divided into three main parts for the palm olein oil transesterification with methanol over strontium oxide. Firstly, the mass transfer resistance was analyzed to verify that the overall rate of reaction is not limited by the rate of mass transfer. Before the kinetic modelings begin, the best values of genetic algorithm operators were investigated for given to the best solution of the kinetic parameter estimation. Finally, the kinetic results were study and used to choose the suitable kinetic model that showed the good correlation between the calculated and experimental values.

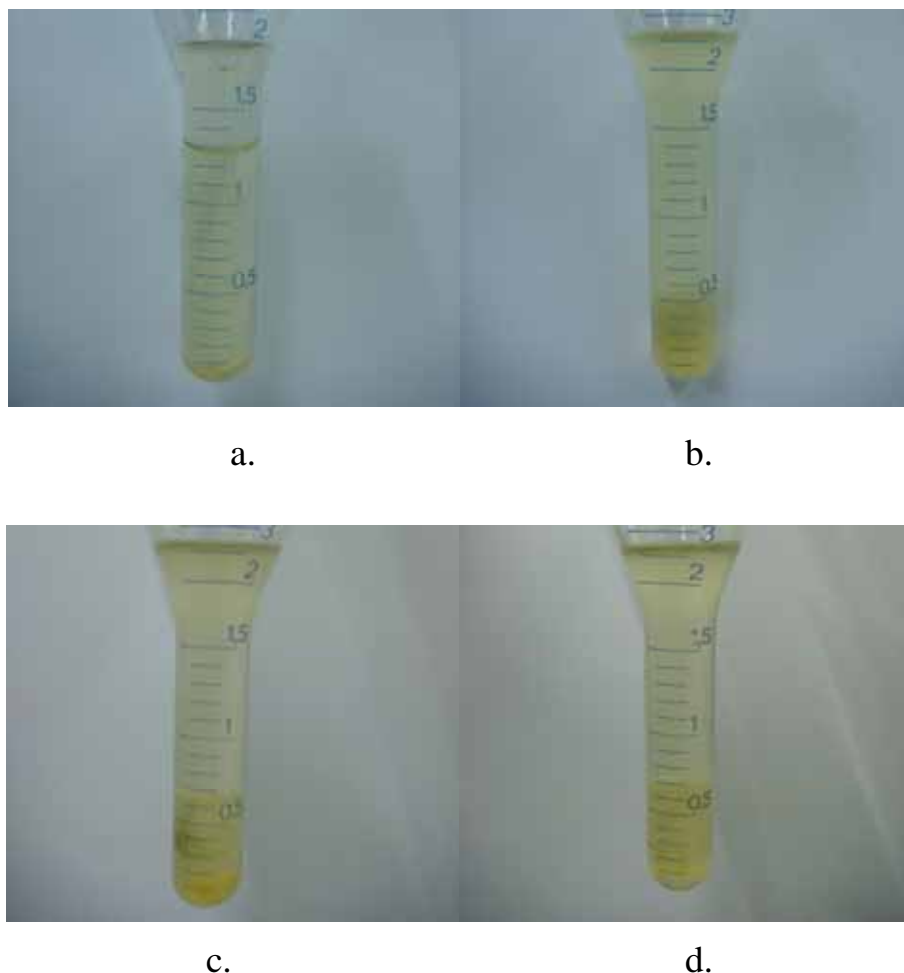


Figure 10 The sampling mixture at various reaction time from transesterification reaction at 65 °C of reaction temperature, 1000 rpm of agitator speed that was centrifuged ; a. 5 min, b. 10 min, c. 15 min, d. 20 min

In Figure 10, it shows the sampling mixture from transesterification reaction under 65 °C of temperature and 1000 rpm of agitator speed. It was collected at the desired reaction time throughout the experiment. As seen in Figure 10(a.), after the centrifuge the sample could be separated into three layers of liquid phase. The upper layer was the methanol. Comparison of the density of all chemicals in the reaction except strontium oxide, the methanol was the lowest one and the highest density was glycerol. In the earlier step of reaction, the solubility between the palm olein oil and methanol had a small value so that after the sample was centrifuged the methanol appeared on the top of the centrifuge tube. The middle layer, it is a mixture that consisted of triglycerides, diglycerides, monoglycerides and fatty acid methyl ester or biodiesel because their similar chemical structure made them mixed together. The lower one is mostly glycerol that was produced from the reaction. The strontium oxide was settled at the bottom of the centrifuged tube.

For longer reacted time, the high glycerol was produced as seen in Figure 10(b) and only two layers appear. Due to the fatty acid methyl ester appear the chemical property as a mixing solvent between methanol and oil that enables to mix them to one layer of liquid phase. The similar phenomena was shown in Figures 10(c.) -10(d.), the upper phase on the centrifuged tube was the mixing of triglycerides, diglycerides, monoglycerides and fatty acid methyl ester, the lower one is the glycerol and strontium oxide at the bottom.

In addition, the samples at the reaction time during 30 -120 min with the same reaction condition, it was not showed because the physical layer was similar to the sample at 20 min.

1. Assessment of mass transfer resistance

In the transesterification reaction of palm olein oil over strontium oxide, it is a solid-liquid system that had the diffusion effect of chemical species moved from the bulk fluid to a catalyst surface before reacted to the product chemical, so that we must to investigate the effect of diffusion of chemical species or mass transfer resistance on the overall rate of chemical reaction.

In this study, the effect of mass transfer resistance will be investigated and analyzed. The mass transfer resistance was studied to confirm that the overall rate is not limited by mass transfer rate and thus could be neglected.

Table 7 The experimental data of transesterification that showed the effect of agitator speeds and reaction times on the diglyceride and triglyceride concentration.

Time (min)	Triglyceride concentration (mol/g-catalyst)			Diglyceride concentration (mol/g-catalyst)		
	500	700	1000	500	700	1000
	(rpm)	(rpm)	(rpm)	(rpm)	(rpm)	(rpm)
0	0.026322	0.026322	0.026322	0.014373	0.014373	0.014373
2	0.012657	0.012873	0.011441	0.007401	0.008254	0.006821
4	0.005975	0.005953	0.005715	0.003729	0.004106	0.003306
6	0.003506	0.003546	0.003616	0.001543	0.001627	0.001308
8	0.001872	0.001865	0.001997	0.000936	0.000989	0.000743
10	0.000868	0.000846	0.000718	0.000298	0.000298	0.000298
15	0.000245	0.000176	0.000176	0.000141	0.000141	0.000141
20	0.000044	0.000044	0.000044	0.000141	0.000141	0.000141
30	0.000044	0.000044	0.000044	0.000141	0.000141	0.000141
60	0.000044	0.000044	0.000044	0.000141	0.000141	0.000141

Table 8 The experimental data of transesterification that showed the effect of agitator speeds and reaction times on the glyceride and monoglycerides concentration.

Time (min)	Glyceride concentration (mol/g-catalyst)			Monoglyceride concentration (mol/g-catalyst)		
	500	700	1000	500	700	1000
	(rpm)	(rpm)	(rpm)	(rpm)	(rpm)	(rpm)
0	0.001050	0.001050	0.001050	0.002203	0.002157	0.002157
2	0.016649	0.016830	0.017083	0.003062	0.003117	0.003208
4	0.026891	0.026746	0.027434	0.005256	0.005182	0.004917
6	0.031813	0.032139	0.032284	0.005667	0.005576	0.006078
8	0.034564	0.034709	0.034998	0.005941	0.005667	0.005466
10	0.038690	0.038871	0.038726	0.005895	0.005841	0.005064
15	0.040138	0.039848	0.040536	0.005859	0.004991	0.004808
20	0.040355	0.040717	0.041115	0.005749	0.005000	0.004625
30	0.041006	0.041079	0.040898	0.005658	0.005109	0.004753
60	0.041115	0.041042	0.041260	0.005585	0.005009	0.004652

As showed in Tables 7 and 8, the concentration of glycerol, monoglycerides, diglycerides and triglycerides were sampled at the designed agitator speed and designed time. All samples were collected with three repeats that marked to reduce the error from an experiment. In case of agitator speed effect, it showed the slightly difference in the concentration of the interesting chemicals when the agitator speed was increased. For the effect of time during 0-30 min period of the reaction time, the concentration of all chemicals showed the more difference. Analysis of variance (ANOVA) was used to analyst there data. This method based on variance ratios to determine whereas or not significant differences exist among the means of several speed of agitator.

In this section, the results are divided into three parts, the effect of time and agitator speed on the triglyceride concentration, on diglyceride concentration and finally on the monoglycerides concentration.

Triglyceride analysis

Two-way analysis of variances was selected for the investigation of the effect of speed agitator on the chemical reaction rate that is a conversion of triglyceride. As show in Table 9, the result of two-way analysis of variances, they have three speeds (columns) and ten times (rows).

Table 9 The two-way analysis of variance of triglyceride concentration by MATLAB statistic toolbox at the agitator speed of 500, 700 and 1000 rpm

Source of variation	df	SS	MS	F	Prob>F
Columns	2	0.00000	0.00000	1.27	0.3051
Rows	9	0.00190	0.00021	3429.9	0.0000
Error	18	0.00000	0.00000	-	-
Total	29	0.00191	-	-	-

The *p-value* for the effect of agitator speed at 0.3051 means that there does not appear to be any effect of agitator speed on the reaction. This indicates that the mass transfer resistance of the transesterification reaction of palm olein oil over strontium oxide had a negligible effect on the reaction.

The *p-value* for the time effect is zero to four decimal places. This is a strong indication that the triglyceride conversion varies from one time to another.

Diglyceride analysis

In case of diglyceride concentration, the data from Table 1 was analyzed by two-way ANOVA and the result was showed in Table 10. It consists of three speeds (columns) and ten times (rows) like a triglyceride concentration.

Table 10 The two-way analysis of variance of diglyceride concentration by MATLAB statistic toolbox at the speed of 500, 700 and 1000 rpm

Source of variation	df	SS	MS	F	Prob>F
Columns	2	0.00000	1.957e-07	3.34	0.0586
Rows	9	0.00059	6.553e-05	1116.92	0.0000
Error	18	0.00000	5.868e-08	-	-
Total	29	0.00059	-	-	-

From Table 10, it shows that the *p-value* of columns is equal to 0.0586. If we consider the *p-value* between Tables 3 and 4, the results of time effect on both cases are the same. However, the *p-value* of mass transfer resistance in case of diglyceride analysis was lower than triglycerides. This indicates that the mass transfer resistance showed the more effect on diglyceride.

Monoglyceride analysis

Table 11 The two-way analysis of variance of monoglycerides concentration by MATLAB statistic toolbox at the speed of 500, 700 and 1000 rpm

Source of variation	df	SS	MS	F	Prob>F
Columns	2	1.353e-06	6.765e-07	7.82	0.0036
Rows	9	3.804e-05	4.226e-06	48.88	0.0000
Error	18	1.556e-06	8.647e-08	-	-
Total	29	4.095e-06	-	-	-

As it was shown in Table 11, the hypothesis of effect of the column variable that is the agitator speed was rejected, but the time has an effect on the reaction. The *p-value* for the effect of agitator speed is 0.0036; this indicated that the speed of agitator had an effect on the monoglycerides. This result is similar to the case of diglyceride concentration

From the previous results, it received from the agitator speed at 500, 700 and 1000 rpm. In case of diglycerides and monoglycerides, if the speed was only considered at 700 and 1000 rpm, the result that was analyzed by two-way ANOVA showed the opposite direction.

According to *p-value* is 0.1067 (Table 12) the increment of in the agitator speed would not influence to the effect on the concentration of monoglycerides. However, the reaction time is the main effect on the reaction in all chemicals condition. Considering both results from Tables 11 and 12, the agitator speed of 500 showed the unsuitable condition for the transesterification over strontium oxide and the mass transfer resistance of monoglycerides reaction step was noticed at this speed.

Table 12 The two-way analysis of variance of monoglyceride concentration by MATLAB statistic toolbox at the speed of 700 and 1000 rpm

Source of variation	df	SS	MS	F	Prob>F
Columns	1	1.845e-06	1.845e-06	3.21	0.1067
Rows	9	2.331e-06	2.589e-06	45.03	0.0000
Error	9	5.169e-06	5.744e-06	-	-
Total	19	2.401e-06	-	-	-

2. Estimation parameters with GA

In this section, GA toolbox by MATLABTM was used to investigate the parameter estimation, the kinetic reaction rate constants, and the appropriate GA parameters will be investigate and tested with the kinetic data of transesterification for the best GA parameters.

Case 1 Approximate population size for estimation of chemical kinetic rate constants.

Population type has been set as double vector. The results of the estimation of chemical kinetic rate constants with Pseudo-homogeneous (PH) and Langmuir-Hinshelwood (LH) model at $T = 65\text{ }^{\circ}\text{C}$ are shown in Tables 13 and 14. The fitness values of PH and LH model at 100, 250, 500, 1000 and 2000 were 2.75103e-04, 2.7459e-04, 2.7410e-04, 2.7383e-04, 2.7294e-04, 1.24e-03, 1.15e-03, 1.11e-03, 1.02e-03 and 1.0190e-03, respectively. If we only consider the effect of population size on the fitness values that slightly decreased with increasing the population size, it means the increment of population size enables the genetic algorithm to search more points and thereby obtain a better result. Both models, PH and LH, showed the results in the same direction. However, the larger of population size used the longer of calculated time while the fitness values slightly increased. For this reason, the suitable population size of GA is 100 in both models.

Table 13 GA parameters and results of population size value for the kinetic rate constant of PH model at $T = 65^{\circ}\text{C}$

GA parameters	Population size				
	100	250	500	1000	2000
Maximum generation	100	100	100	100	100
Crossover fraction	0.8	0.8	0.8	0.8	0.8
Mutation rate	0.01	0.01	0.01	0.01	0.01
Migration fraction	0.2	0.2	0.2	0.2	0.2
Hybrid function	None	None	None	None	None
Total time (h)	0.69	1.71	3.35	6.54	13.08
Fitness value($\times 10^4$)	2.7510	2.7459	2.7410	2.7383	2.7294

Table 14 GA parameters and results of population size value for the kinetic rate constant of LH model at $T = 65^{\circ}\text{C}$

GA parameters	Population size				
	100	250	500	1000	2000
Maximum generation	100	100	100	100	100
Crossover fraction	0.8	0.8	0.8	0.8	0.8
Mutation rate	0.01	0.01	0.01	0.01	0.01
Migration fraction	0.2	0.2	0.2	0.2	0.2
Hybrid function	None	None	None	None	None
Total time (h)	0.69	1.69	3.40	6.51	13.08
Fitness value($\times 10^3$)	1.2459	1.1534	1.1198	1.0214	1.0190

Case 2 Approximate generation number for estimation of chemical kinetic rate constants

The results of case 2 for the estimation of chemical kinetic rate constants with PH and LH model at $T = 65^{\circ}\text{C}$ are shown in Tables 15 and 16. The increment of the maximum generation will give the better result and increase the analyzing time. However, it slightly increased when comparing with the generation. Therefore, the maximum generation equal to 100 is chosen because of slightly difference of the result and the shorter computation time in both models.

Table 15 GA parameters and results of generation number for the kinetic rate constant of PH model at $T = 65^{\circ}\text{C}$

GA parameters	Maximum generation			
	100	300	500	1000
Population size	100	100	100	100
Crossover fraction	0.8	0.8	0.8	0.8
Mutation rate	0.01	0.01	0.01	0.01
Migration fraction	0.2	0.2	0.2	0.2
Hybrid function	None	None	None	None
Total time (h)	0.70	1.70	3.47	6.71
Fitness value($\times 10^4$)	2.7510	2.7389	2.7373	2.7372

Table 16 GA parameters and results of generation number for the kinetic rate constant of LH model at $T = 65^{\circ}\text{C}$

GA parameters	Maximum generation			
	100	300	500	1000
Population size	100	100	100	100
Crossover fraction	0.8	0.8	0.8	0.8
Mutation rate	0.01	0.01	0.01	0.01
Migration fraction	0.2	0.2	0.2	0.2
Hybrid function	None	None	None	None
Total time (h)	0.75	1.75	3.42	6.53
Fitness value($\times 10^3$)	1.2459	1.2390	1.2298	1.2201

Case3 Approximate crossover fraction for estimation of chemical kinetic rate constants

The suitable crossover fraction determined with GA by MATLABTM. The scattered type was selected as a crossover function. As seen in Tables 17 and 18, the results of PH and LH models at $T = 65^{\circ}\text{C}$ get the similar trend, the analyzing times have not a significant different when the crossover fraction was increased while the fitness value decreased with increasing the crossover fraction. The suitable crossover fraction for both models is selected at 0.8.

Table 17 GA parameters and results of crossover fraction value for the kinetic rate constant of PH model at T = 65 °C

GA parameters	Crossover fraction		
	0.3	0.5	0.8
Population size	100	100	100
Maximum generation	100	100	100
Mutation rate	0.01	0.01	0.01
Migration fraction	0.2	0.2	0.2
Hybrid function	None	None	None
Total time (h)	0.64	0.64	0.64
Fitness value(*10 ⁴)	2.8123	2.7459	2.7410

Table 18 GA parameters and results of crossover fraction value for the kinetic rate constant of LH model at T = 65 °C

GA parameters	Crossover fraction		
	0.3	0.5	0.8
Population size	100	100	100
Maximum generation	100	100	100
Mutation rate	0.01	0.01	0.01
Migration fraction	0.2	0.2	0.2
Hybrid function	None	None	None
Total time (h)	0.64	0.64	0.64
Fitness value(*10 ³)	1.3550	1.2982	1.2150

Case 4: Approximate mutation rate for estimation of chemical kinetic rate constants.

In case 4, uniform type was chosen as a mutation rate. The suitable mutation rates are determined and the results are showed in the tables 19 and 20, which found that the increment of this value will give the high fitness value that mean the answer far away from objective values. Due to the mutation rate may lead the solution searching out off the feasible region. The mutation rate at 0.01 was chosen.

Table 19 GA parameters and results of mutation fraction value for the kinetic rate constant of PH model at $T = 65^{\circ}\text{C}$

GA parameters	Mutation rate						
	0.01	0.05	0.10	0.20	0.30	0.40	0.50
Population size	100	100	100	100	100	100	100
Maximum generation	100	100	100	100	100	100	100
Crossover fraction	0.8	0.8	0.8	0.8	0.8	0.8	0.8
Migration fraction	0.2	0.2	0.2	0.2	0.2	0.2	0.2
Hybrid function	None	None	None	None	None	None	None
Total time (h)	0.64	0.64	0.64	0.64	0.64	0.64	0.64
Fitness value($\times 10^4$)	2.7410	2.9571	2.9673	2.9790	2.8930	2.9567	2.9901

Table 20 GA parameters and results of mutation fraction value for the kinetic rate constant of LH model at $T = 65^{\circ}\text{C}$

GA parameters	Mutation rate						
	0.01	0.05	0.10	0.20	0.30	0.40	0.50
Population size	100	100	100	100	100	100	100
Maximum generation	100	100	100	100	100	100	100
Crossover fraction	0.8	0.8	0.8	0.8	0.8	0.8	0.8
Migration fraction	0.2	0.2	0.2	0.2	0.2	0.2	0.2
Hybrid function	None	None	None	None	None	None	None
Total time (h)	0.64	0.64	0.64	0.64	0.64	0.64	0.64
Fitness value($\times 10^3$)	1.2150	1.410	1.392	1.437	1.4489	1.3456	1.4595

Case 5: Approximate migration fraction for estimation of chemical kinetic rate constants.

The suitable migration fraction can be determined for the optimum condition. The forward direction and the interval at 20 were chosen throughout the estimation. The results of migration fraction on PH and LH model at 65°C are showed in Tables 21 and 22. The results of both models showed that the migration fraction play the litter effect on the fitness value. Due to the migration is the operator of genetic algorithm that makes a few chance of the individual. Thus, migration fraction of 0.2 is chosen because of the default value.

Table 21 GA parameters and results of migration fraction value for the kinetic rate constant of PH model at T = 65 °C

GA parameters	Migration fraction					
	0.01	0.1	0.2	0.4	0.6	0.8
Population size	100	100	100	100	100	100
Maximum generation	100	100	100	100	100	100
Crossover fraction	0.8	0.8	0.8	0.8	0.8	0.8
Mutation rate	0.01	0.01	0.01	0.01	0.01	0.01
Hybrid function	None	None	None	None	None	None
Total time (h)	0.64	0.64	0.64	0.64	0.64	0.64
Fitness value(*10 ⁴)	2.7209	2.7381	2.7500	2.749	2.7900	2.744

Table 22 GA parameters and results of migration fraction value for the kinetic rate constant of LH model at T = 65 °C

GA parameters	Migration fraction					
	0.01	0.1	0.2	0.4	0.6	0.8
Population size	100	100	100	100	100	100
Maximum generation	100	100	100	100	100	100
Crossover fraction	0.8	0.8	0.8	0.8	0.8	0.8
Mutation rate	0.01	0.01	0.01	0.01	0.01	0.01
Hybrid function	None	None	None	None	None	None
Total time (h)	0.64	0.64	0.64	0.64	0.64	0.64
Fitness value(*10 ³)	1.217	1.1177	1.2079	1.1889	1.1889	1.2080

Case 6: Hybrid function for estimation of chemical kinetic rate constants.

In case 6, another minimization functions such as fminsearch, patternsearch, fminunc that was selected to use and run after the genetic algorithm terminates in order to improve the fitness value. The effects of hybrid function on the fitness values are determined and the results are shown in Tables 23 and 24 for PH and LH models at 65 °C, respectively. It showed the better solution when the hybrid function was used because the hybrid function used the final point from the genetic algorithm as an initial point.

However, the results of PH model showed a litter difference of fitness value from GA operator including the hybrid function when it was compared with LH model. Due to the LH model is more complex than PH model. For this reason, none and fminunc were chosen in PH and LH model as hybrid function.

Table 23 GA parameters and results of migration fraction value for the kinetic rate constant of PH model at T = 65 °C

GA parameters	Hybrid function			
	fminsearch	patternsearch	fminunc	none
Population size	100	100	100	100
Maximum generation	100	100	100	100
Crossover fraction	0.8	0.8	0.8	0.8
Mutation rate	0.01	0.01	0.01	0.01
Migration fraction	0.2	0.2	0.2	0.2
Total time (h)	>0.64	>0.64	>0.64	0.64
Fitness value(*10 ⁴)	2.7270	2.7490	2.7386	2.7500

Table 24 GA parameters and results of migration fraction value for the kinetic rate constant of LH model at $T = 65^{\circ}\text{C}$

GA parameters	Hybrid function			
	fminsearch	patternsearch	fminunc	none
Population size	100	100	100	100
Maximum generation	100	100	100	100
Crossover fraction	0.8	0.8	0.8	0.8
Mutation rate	0.01	0.01	0.01	0.01
Migration fraction	0.2	0.2	0.2	0.2
Total time (h)	>0.64	>0.64	>0.64	0.64
Fitness value(*10 ³)	1.1481	1.0947	0.9807	1.2150

3. Assessment of kinetic investigation

For the kinetic investigation that studied the effect of temperature on the overall reaction rate, the conversion of triglycerides, diglycerides, monoglycerides and glycerol at 65 , 60 and 55 °C were shown in Figures 11 , 12 and 13, respectively. As it can be seen in Figure 11, triglycerides was very rapid consumed within 30 min of reaction time. The first intermediate of reaction, diglyceride, was also rapid decreased. In case of monoglycerides that was the second intermediate, it was slight increased in the earlier step of reaction and decreased in the following time of reaction. Therefore, the reaction temperature was shown the more effect on the monoglycerides conversion as seen in Figures 12 and 13.

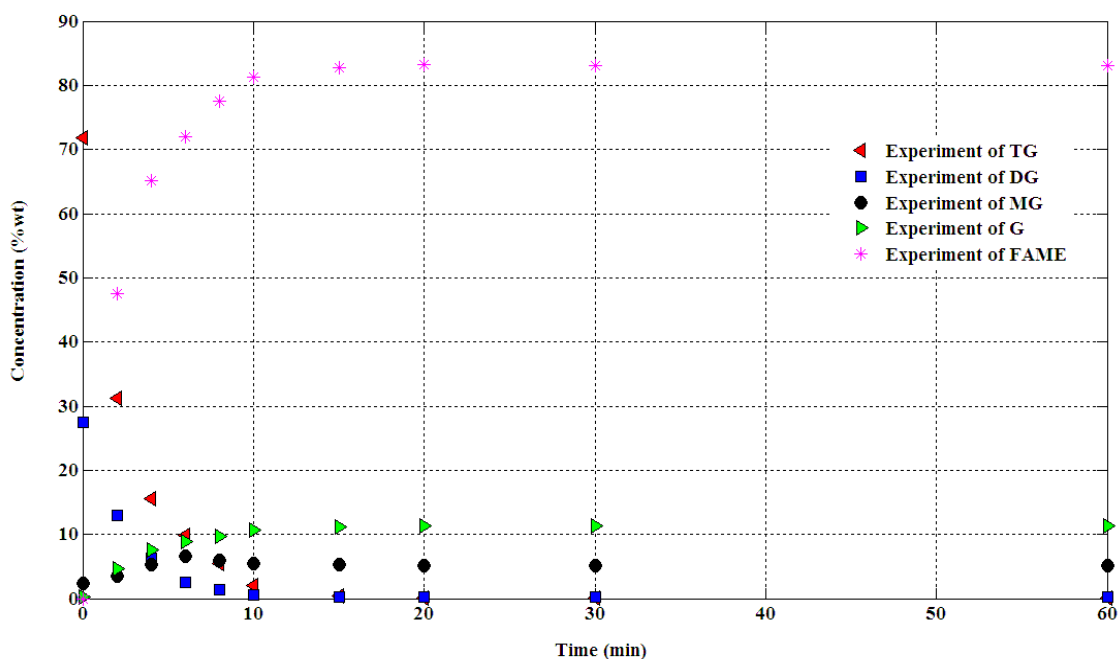


Figure 11 Experimental results at 65 °C of reaction temperature, 1000 rpm of agitator speed (wt%).

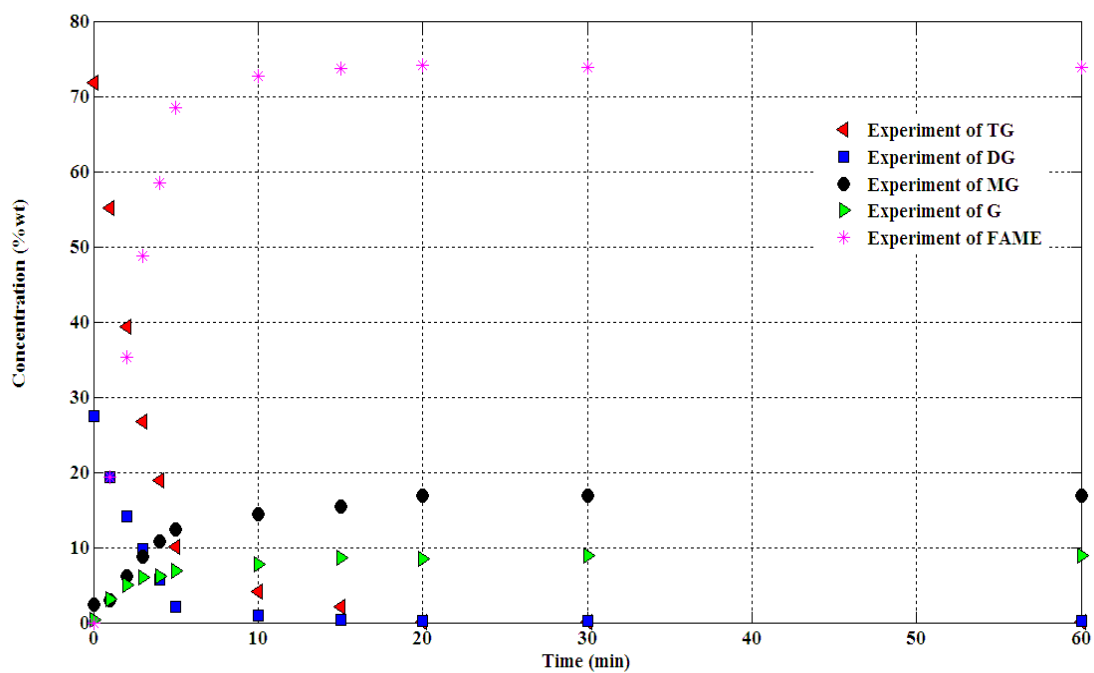


Figure 12 Experimental results at 60 °C of reaction temperature, 1000 rpm of agitator speed (wt%).

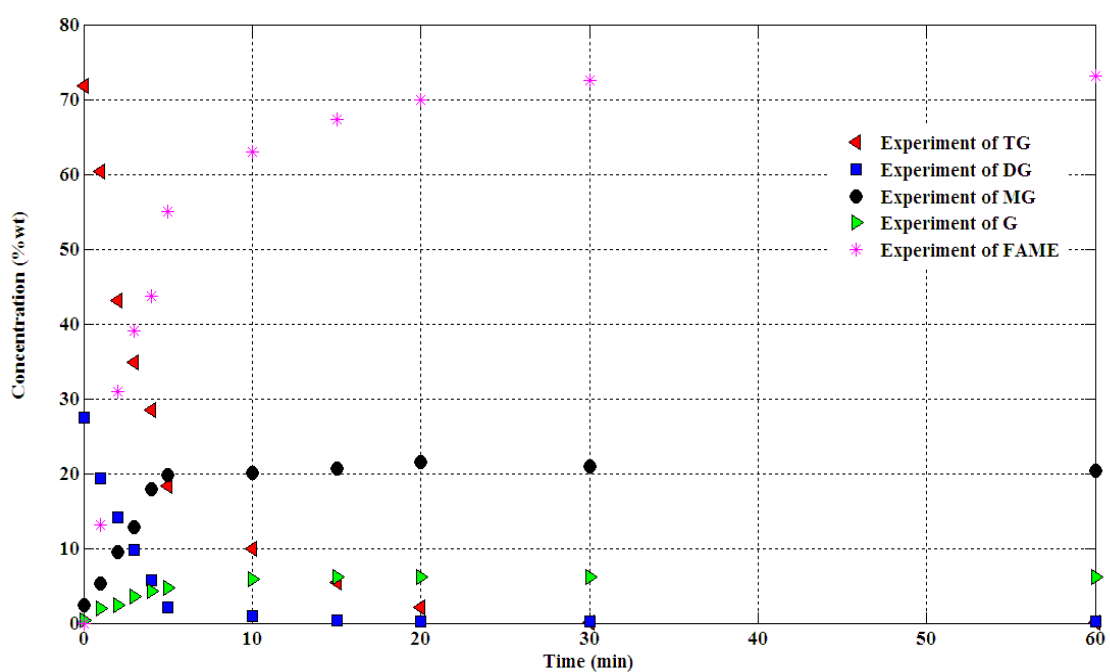


Figure 13 Experimental results at 55 °C of reaction temperature, 1000 rpm of agitator speed (wt%).

In the kinetic investigation, the liquid sample of the transesterification reaction was analyzed by using GC method only. The GC results consist of the amount of triglycerides, diglycerides, monoglycerides and glyceride that was shown in wt% (g/100 g of sample). In case of fatty acid methyl ester, it was obtained by the summation of all glyceride components minus the weight of sample.

Before kinetic modelings begin, the kinetic data must be converted from mass unit to mole unit. The fatty acid composition of palm olein oil used in this experiment consist of 34.98 % of palmitic acid, 13.78% of steric acid, 41.23% of oleic acid and 10.01% of linoleic acid. Based on the fatty acid composition, the average molecular weight of TG, DG, MG and FAME from the palm oil was approximated to be 909.88, 637.29, 364.69 and 287.59, respectively. For the estimation method of molecular weights of these components was shown in Appendix C. Change of component mole versus reaction time of the reaction in the reactor at 65, 60 and 55 °C is given in Figures 14, 15 and 16, respectively.

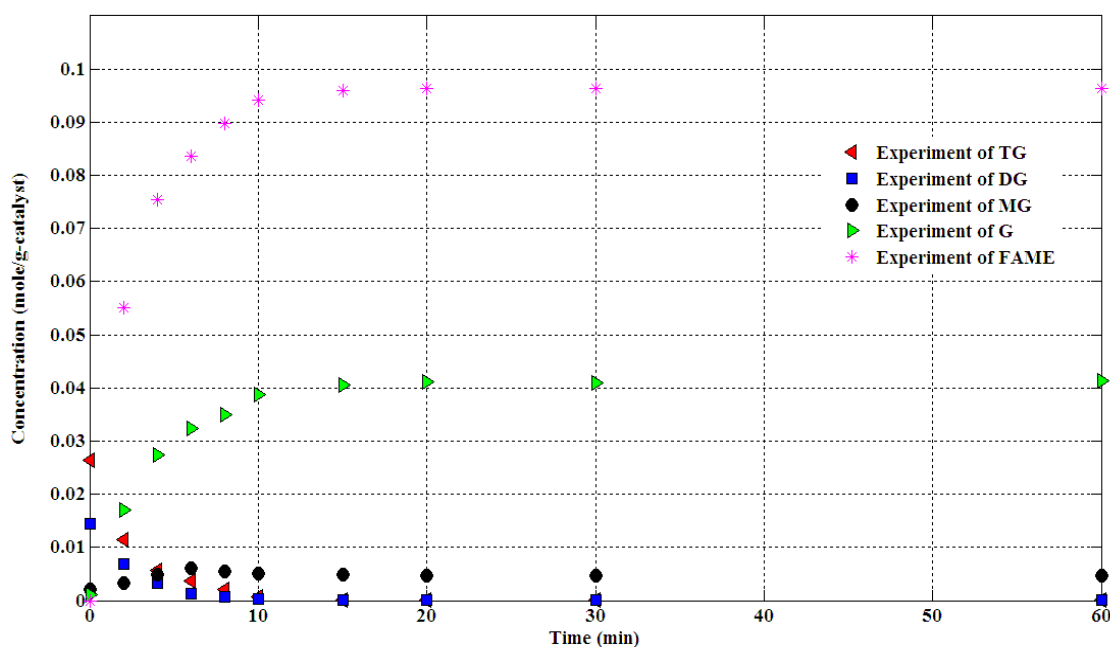


Figure 14 Experimental results at 65 °C of reaction temperature, 1000 rpm of agitator speed (mole/g-catalyst).

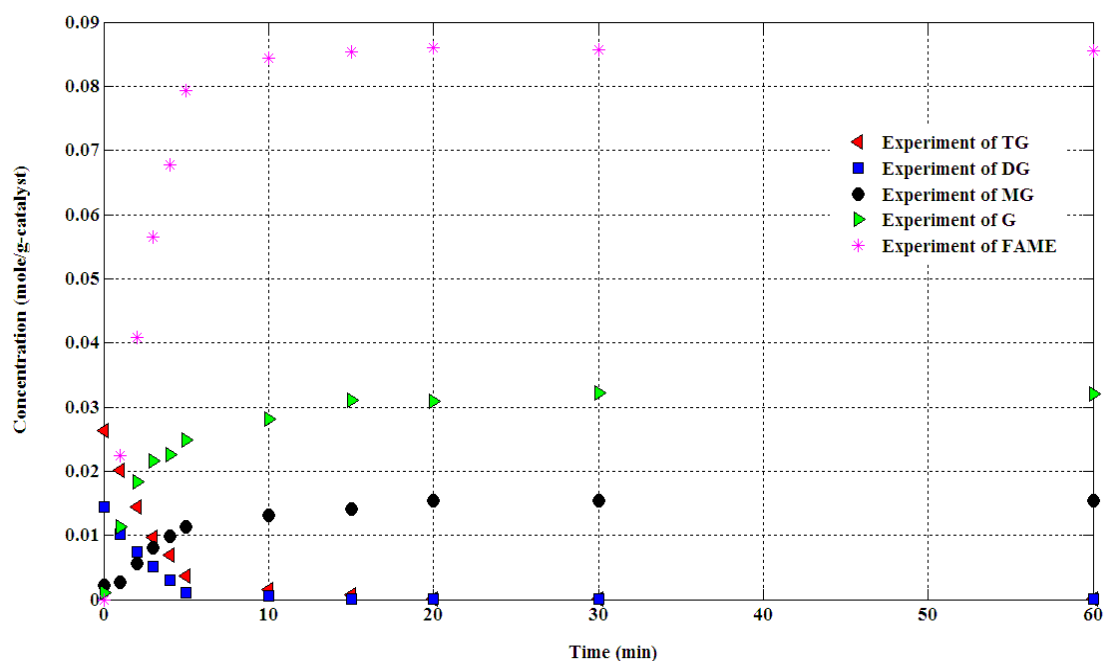


Figure 15 Experimental results at 60 °C of reaction temperature, 1000 rpm of agitator speed (mole/g-catalyst).

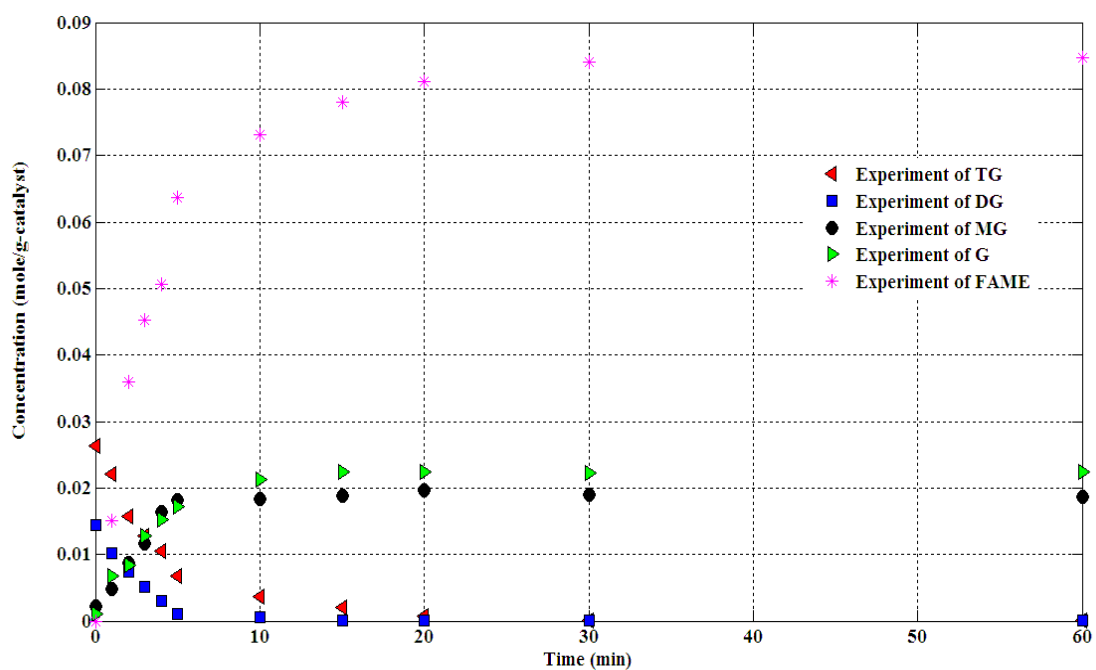


Figure 16 Experimental results at 55 °C of reaction temperature, 1000 rpm of agitator speed (mole/g-catalyst).

In this section, it must be noted that the purpose of this exercise is not to prove rigorously the surface reaction mechanism; rather, the aim is to develop a kinetic model that yields a suitable level of accuracy, relative to experimental results. Both models were estimated by two cases, first one was estimated without FAME concentration in the model and the second was included FAME.

In case of pseudo homogeneous model, it was investigated by comparing the kinetic results at 65 °C of reaction temperature with kinetic model that based on the elementary of reversible reaction from three steps of transesterification of palm olein oil. As seen in Figure 17, the three step of reversible reaction of transesterification could not be described the kinetic result from strontium oxide as solid catalyst.

The irreversible reaction step was performed and tested as shown in Figure 18. The result showed that it gave the higher possible kinetic model when compared with Figure 17, but not suitable to describe the reaction.

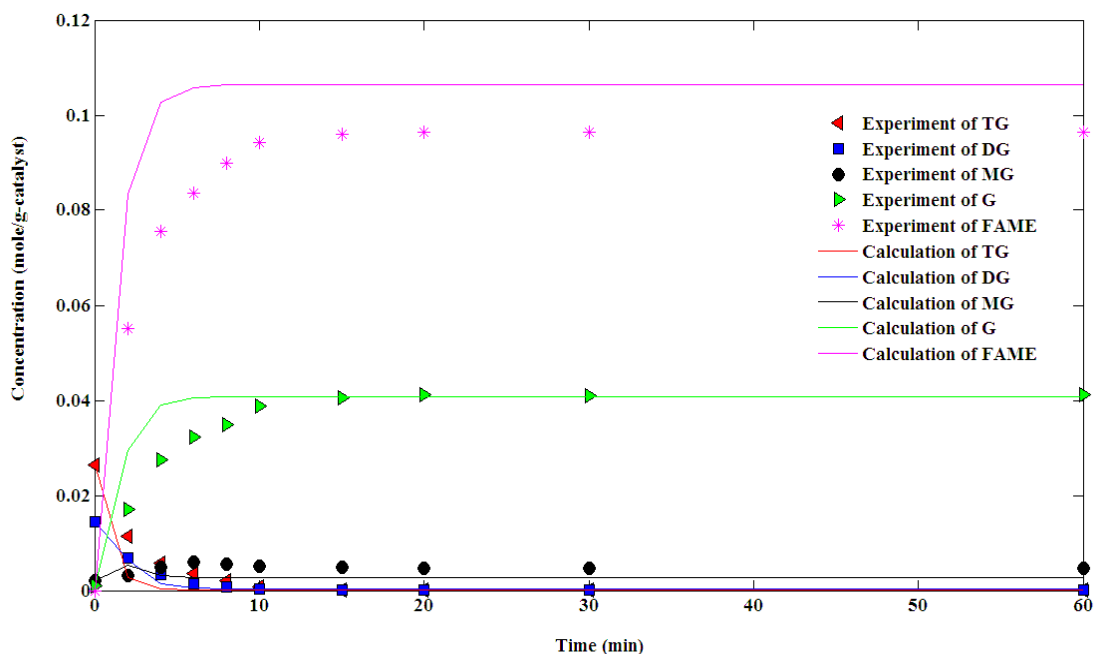


Figure 17 Transesterification at $T = 65\text{ }^{\circ}\text{C}$; Experimental data and calculated of PH model (reversible reaction in all step)

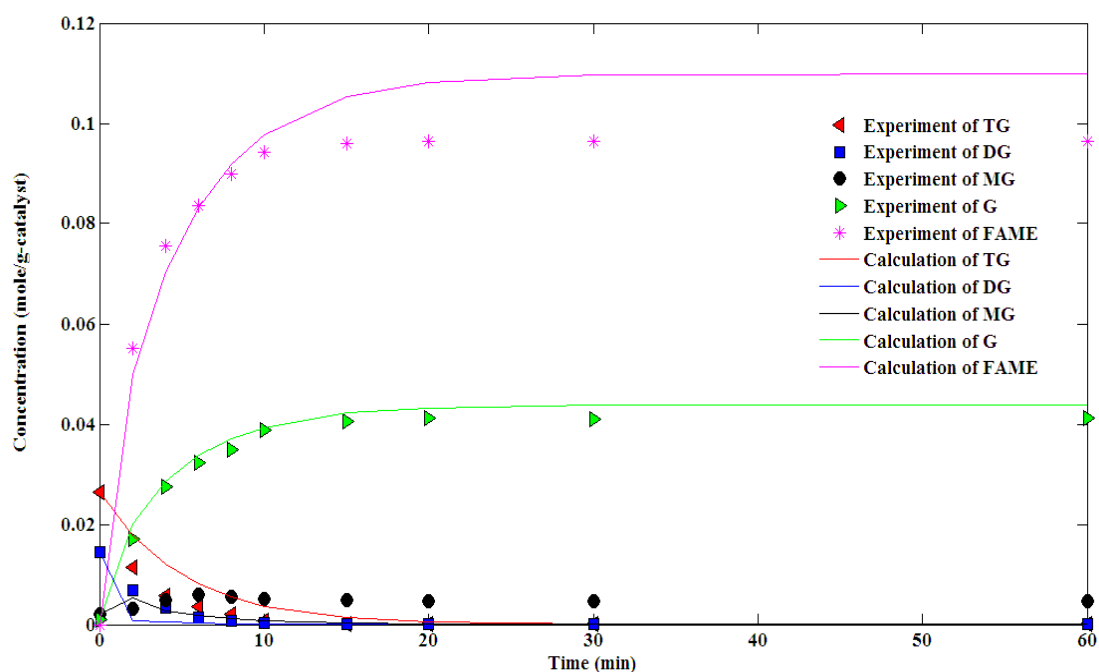


Figure 18 Transesterification at $T = 65^{\circ}\text{C}$; Experimental data and calculated of PH model (irreversible reaction) with FAME concentration

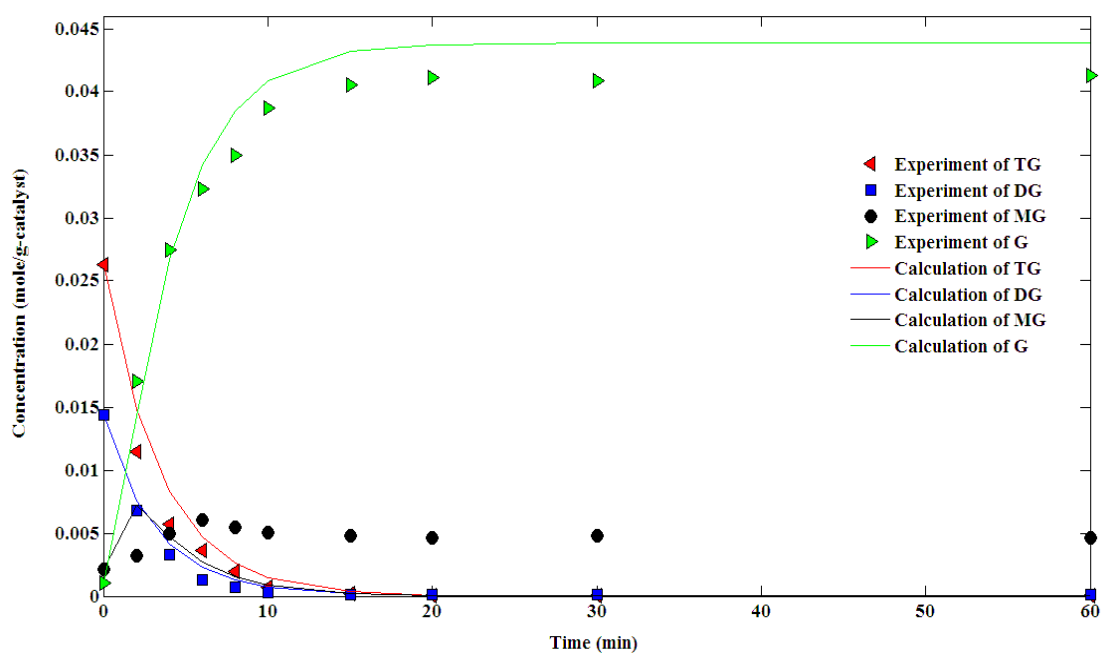


Figure 19 Transesterification at $T = 65^{\circ}\text{C}$; Experimental data and calculated of PH model (irreversible reaction) without FAME concentration

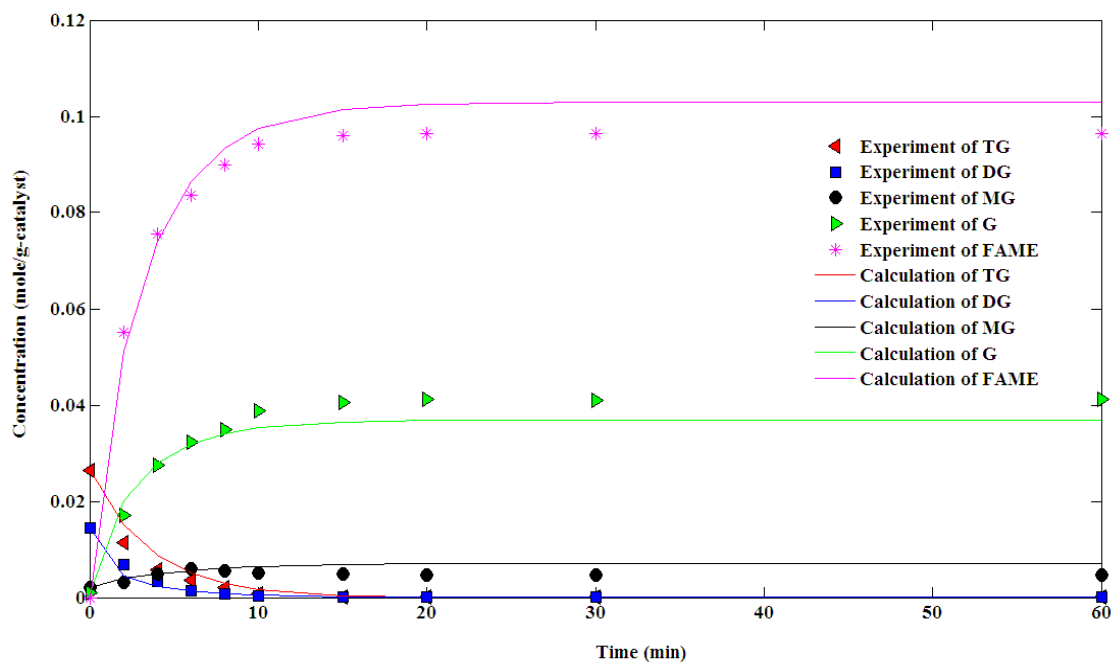


Figure 20 Transesterification at $T = 65\text{ }^{\circ}\text{C}$; Experimental data and calculated of PH model (reversible reaction in step 3)

Based on the Figure 18, the irreversible reaction step was used without the concentration of FAME. The result of this model was showed in Figure 19. It showed the better description of transesterification reaction except the concentration of monoglycerides. The calculation results of monoglycerides concentration that increased in the earlier step of reaction time and then it was consumed to disappear in the last one. This result contrasted with the experimental result.

According to Figure 20, the reversible reaction in third step, monoglycerides reaction step, was added into the kinetic model without FAME concentration. It showed the good correlation with kinetic result, and could be used to describe the monoglycerides concentration throughout the experiment.

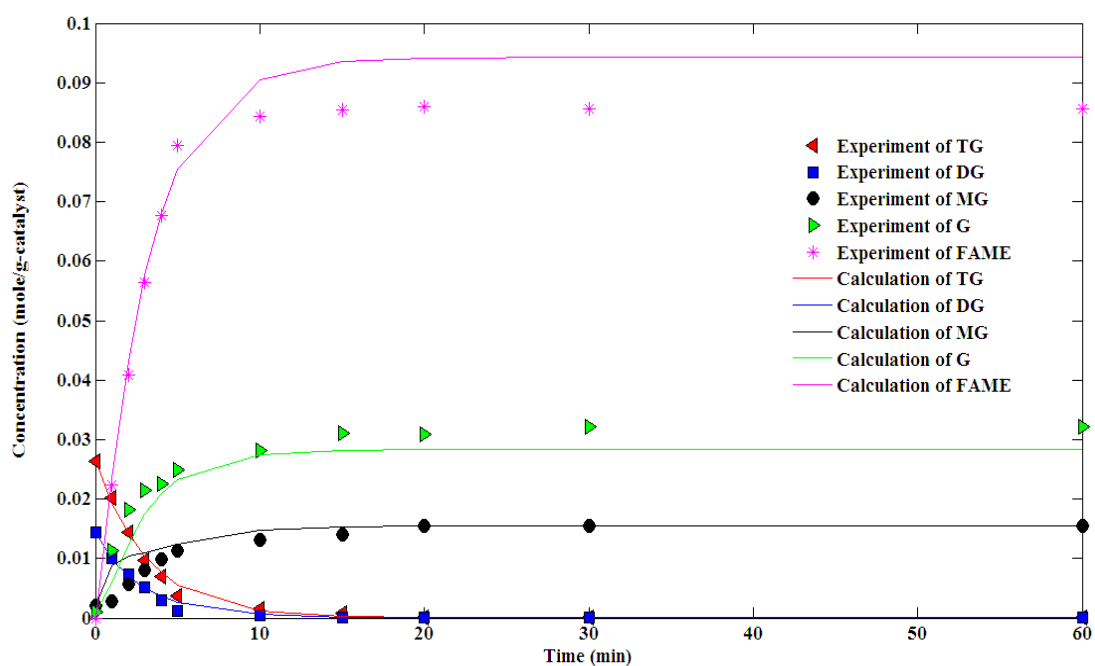


Figure 21 Transesterification at $T = 60\text{ }^{\circ}\text{C}$; Experimental data and calculated of PH model (reversible reaction in step 3)

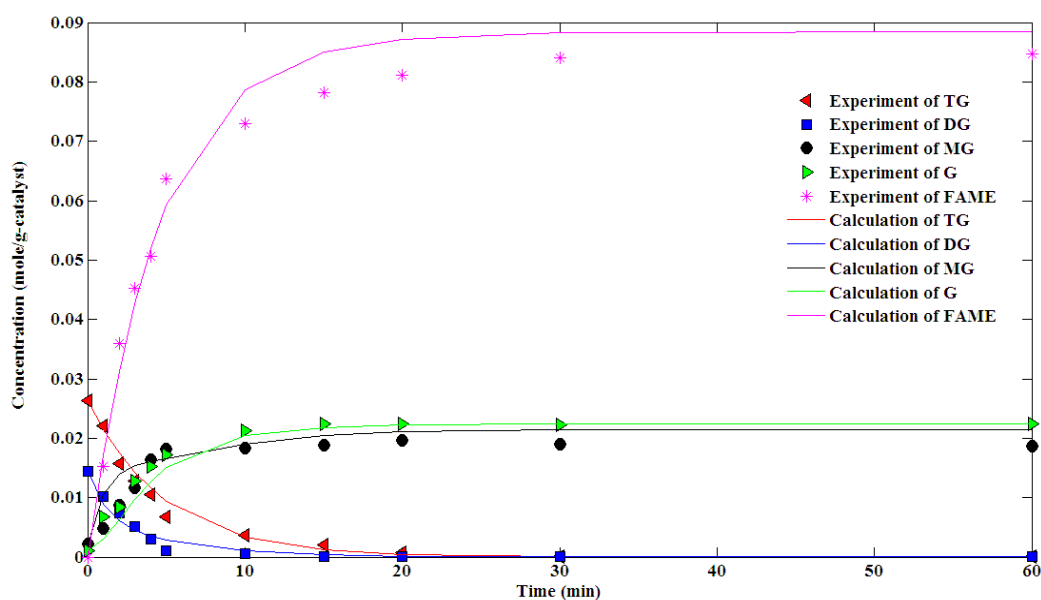


Figure 22 Transesterification at $T = 55\text{ }^{\circ}\text{C}$; Experimental data and calculated of PH model (reversible reaction in step 3)

However, both of these models have slightly difference between experiment and calculation result. For pseudo homogeneous model, it could be used in case of with or without FAME concentration that included in the kinetic model.

Figures 21 and 22 compare the experimentally observed values to the simulated values versus time using the PH model that based on the elementary reaction of transesterification of palm olein oil, and only reversible reaction on third step at 60 °C and 55 °C of reaction temperature, respectively.

In case of Langmuir-Hinshewood model, it could be separated by the power of adsorption term into two models that consisted of LH model (type 1) and LH model (type2). For LH model (type 1), the power number is equal to one and it is two in LH model (type 2).

The results of kinetic investigation at 65 °C of reaction temperature with LH model (type 1) were showed in Figures 23 – 26. As showed in Figure 23, type 1 of LH model based on irreversible reaction without FAME concentration that was used to validate the experimental results. The result was similar to the case of PH model irreversible reaction without FAME concentration. It could not be used to calculate the concentration of monoglycerides. However, LH model (type 1) showed the lower fitness value when it was compared with PH model in the same condition, that it means the calculated values of this one was nearly the experimentally values.

For the irreversible reaction with FAME concentration of LH model (type 1), the result was showed in Figure 24. As comparing with Figure 18, it was showed the higher accuracy of calculated values. Although the better of calculated value was received from this model, they had an error in FAME concentration.

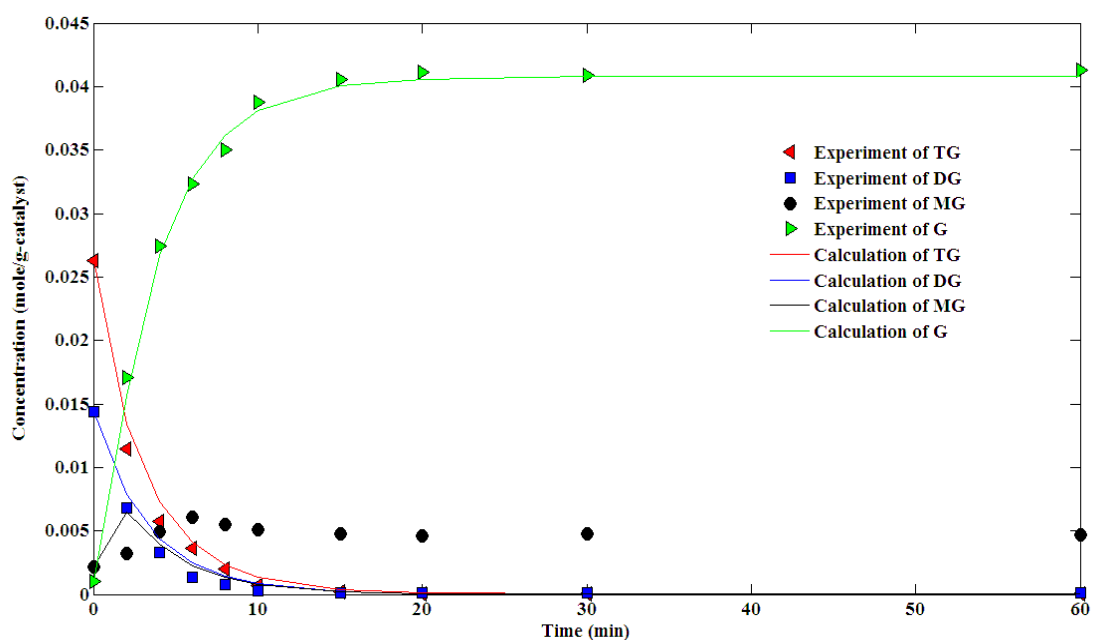


Figure 23 Transesterification at $T = 65\text{ }^{\circ}\text{C}$: Experimental data and calculated of LH model, type 1 (irreversible reaction) without FAME concentration.

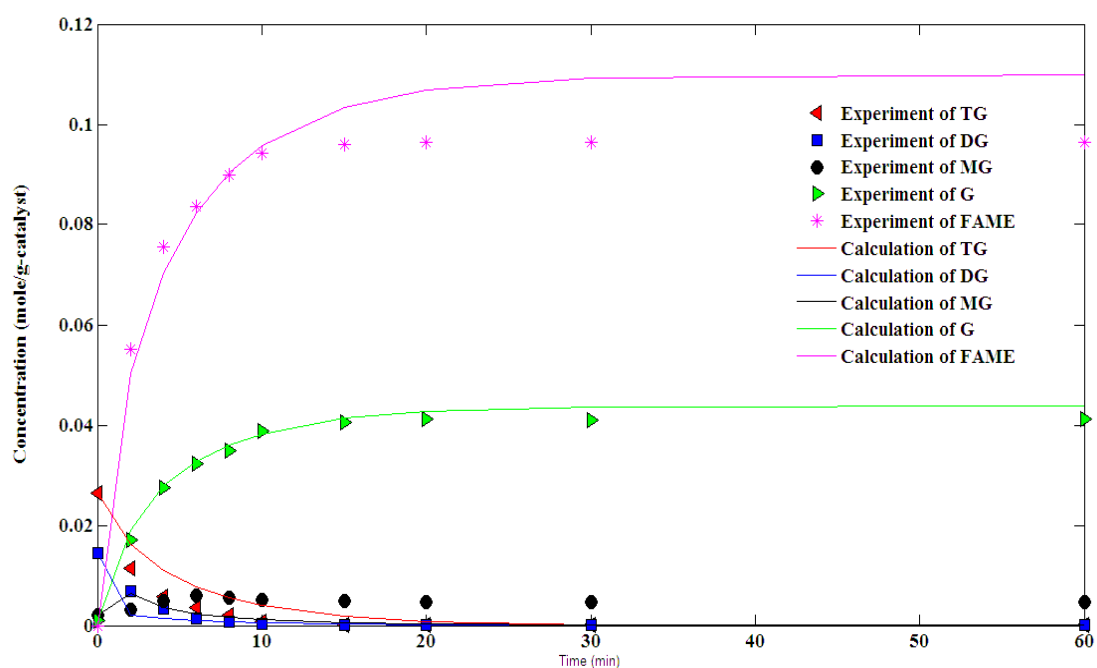


Figure 24 Transesterification at $T = 65\text{ }^{\circ}\text{C}$; Experimental data and calculated of LH model, type 1 (irreversible reaction) with FAME concentration.

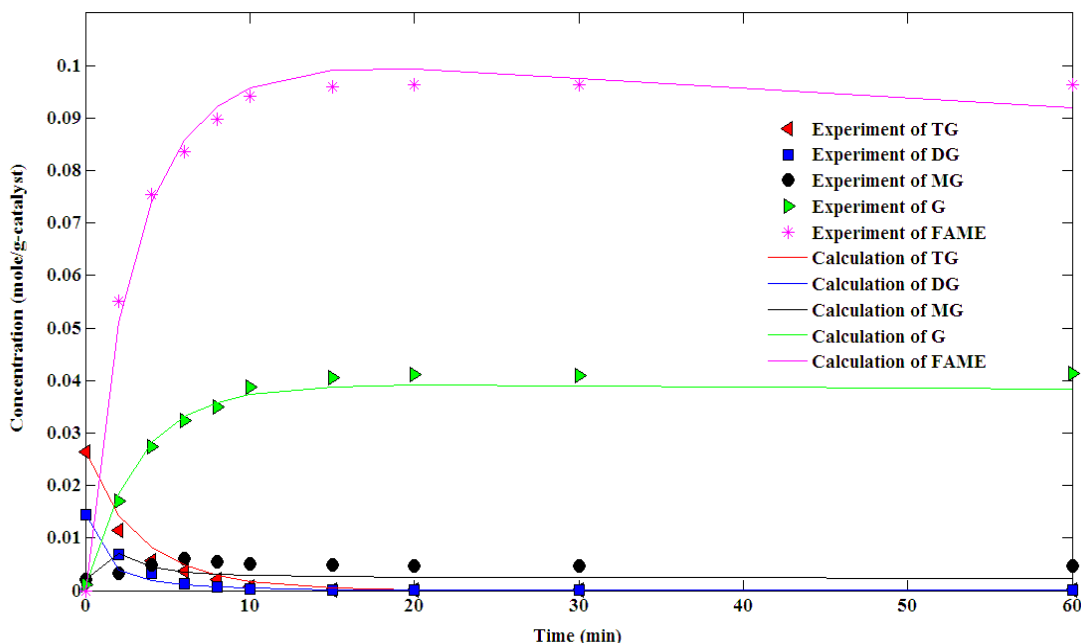


Figure 25 Transesterification at $T = 65\text{ C}$: Experimental data and calculated of LH model, type 1 (reversible reaction in step 3)

As can be seen in the Figure 25, LH model (type 1) without FAME concentration that was considered the reversible reaction only appeared in step 3. It showed the similar trend of results as the previous result from LH model except the concentration of triglycerides. The calculate values of triglycerides concentration showed an impossible value for the kinetic reaction that was the negative.

Figure 25 was the LH model (type 1), reversible reaction in step 3. It showed the best calculated value for the reaction by LH model type 1. It could be used to predict all chemical species of transesterification with high correlation.

In case of LH model type 2, the validation results were showed in Figures 26 - 28. The result of irreversible reaction without FAME concentration was showed in Figure 26. It showed the good calculated results except monoglycerides concentration that is similar to case of LH type 1, irreversible reaction without FAME concentration.

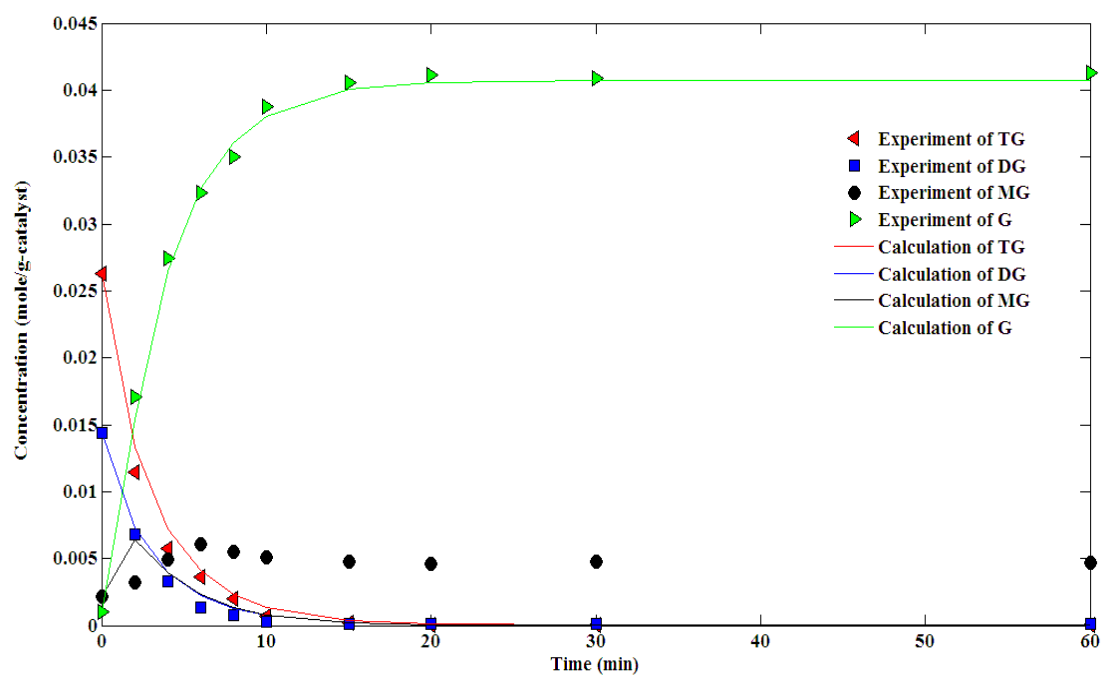


Figure 26 Transesterification at $T = 65\text{ }^{\circ}\text{C}$: Experimental data and calculated of LH model, type 2 (irreversible reaction) without FAME concentration.

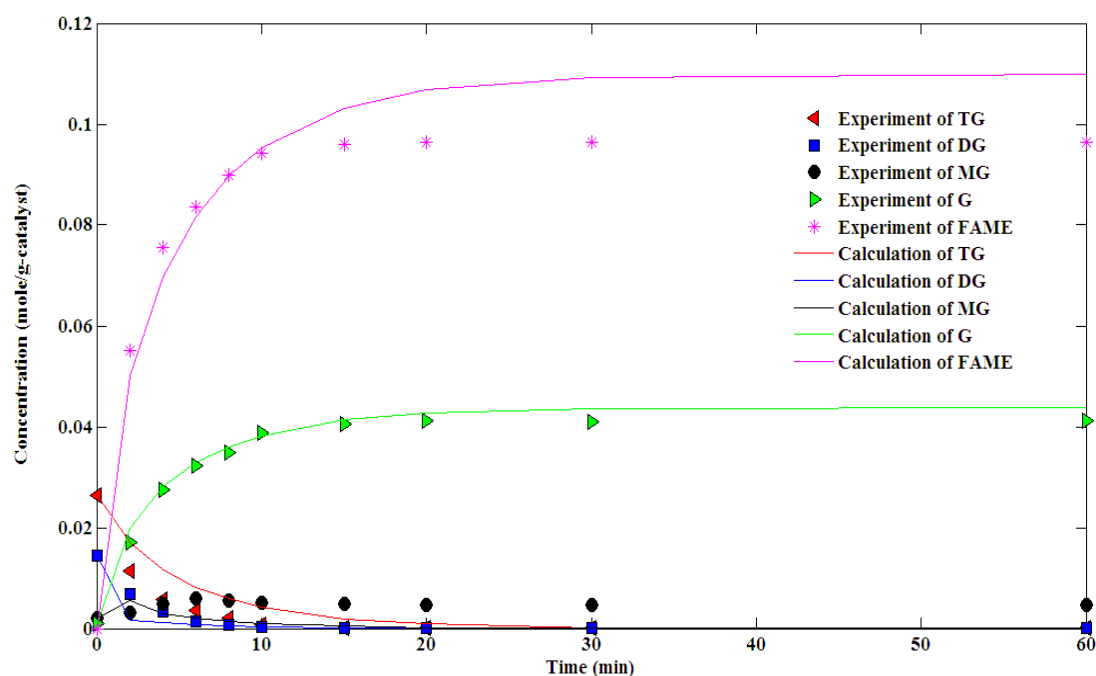


Figure 27 Transesterification at $T = 65\text{ }^{\circ}\text{C}$; Experimental data and calculated of LH model, type 2 (irreversible reaction) with FAME concentration.

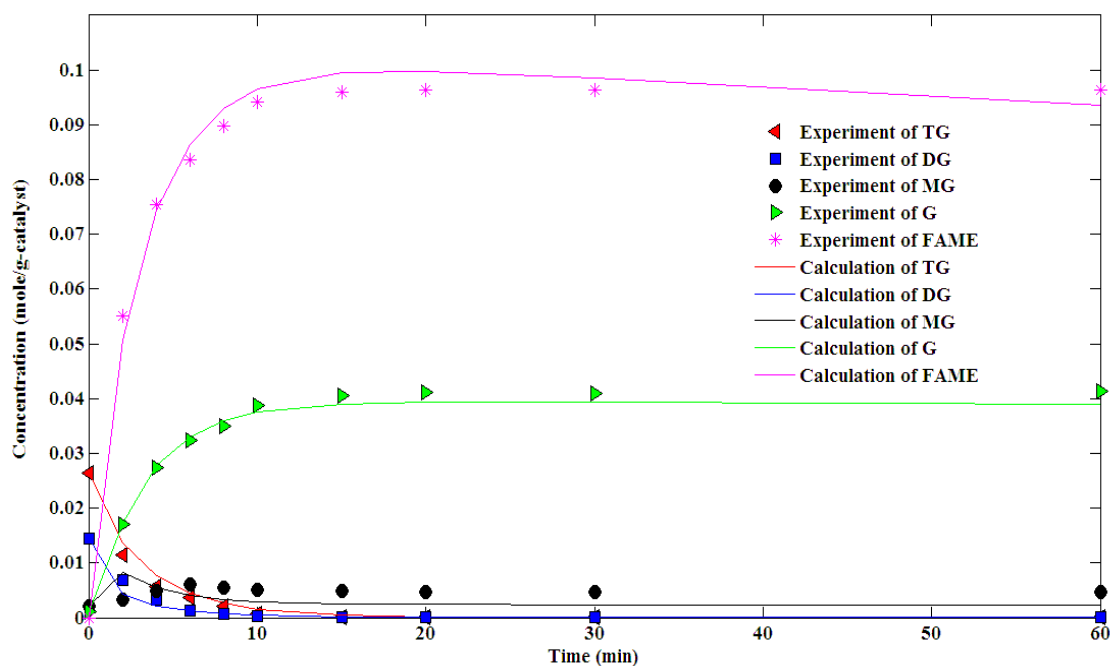


Figure 28 Transesterification at $T = 65\text{ }^{\circ}\text{C}$: Experimental data and calculated of LH model, type 2 (reversible reaction in step 3)

According to the Figures 27 - 28, the calculated results of LH model type 2 were similar to type 1 except the case of LH model, type 2 that based on the reversible reaction in step 3 without FAME concentration

Table 25 The fitness value ($\times 10^4$) of LH model of type 1 and 2 that based on the irreversible reaction and reversible reaction in step 3 at $65\text{ }^{\circ}\text{C}$ of reaction temperature

Component in model	LH model type 1		LH model type 2	
	Irreversible reaction	Reversible reaction in step 3	Irreversible reaction	Reversible reaction in step 3
Without FAME	2.05	1.91	2.29	2.13
With FAME	5.60	1.74	6.76	1.89

Finally, the LH model between type 1 and 2 were compared to found the better kinetic model. As can be seen in Table 25, the fitness value of these models was used to select the better one. Both type of LH model could be classified to two cases, with or without FAME concentration. The fitness value of all case in type 1 showed better solution than to type 2.

The LH type1 model was used to estimate the kinetic result of transesterification at 60 and 55°C of reaction temperature, as shows in Figures 29 and 30, respectively.

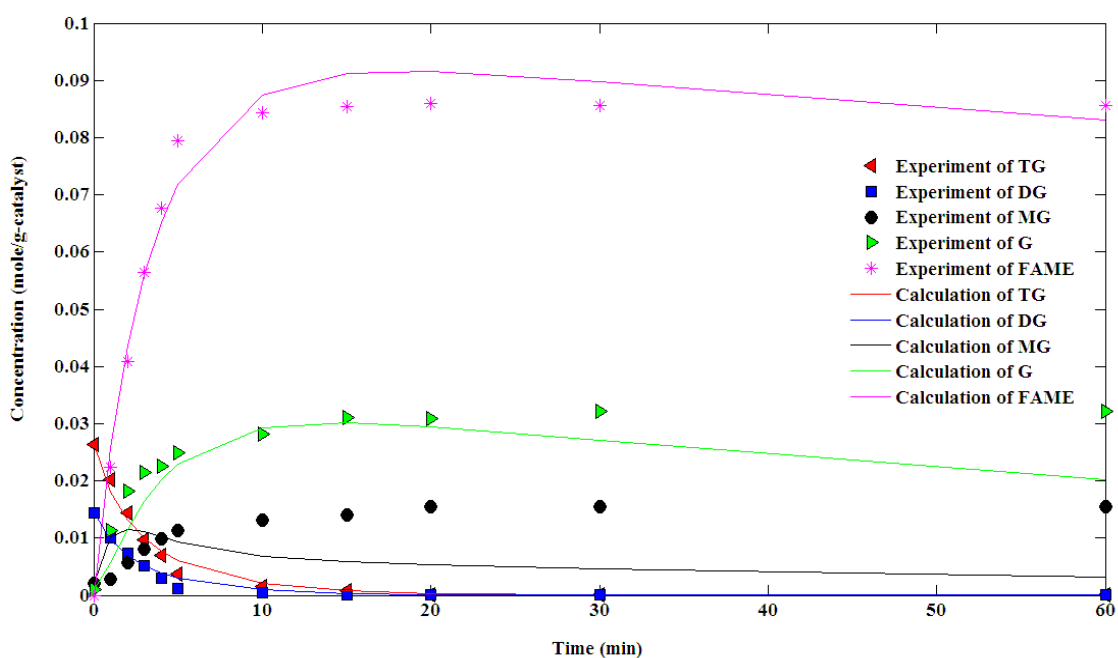


Figure 29 Transesterification at $T = 60\text{ }^{\circ}\text{C}$: Experimental data and calculated of LH model, type 1 (reversible reaction in step 3)

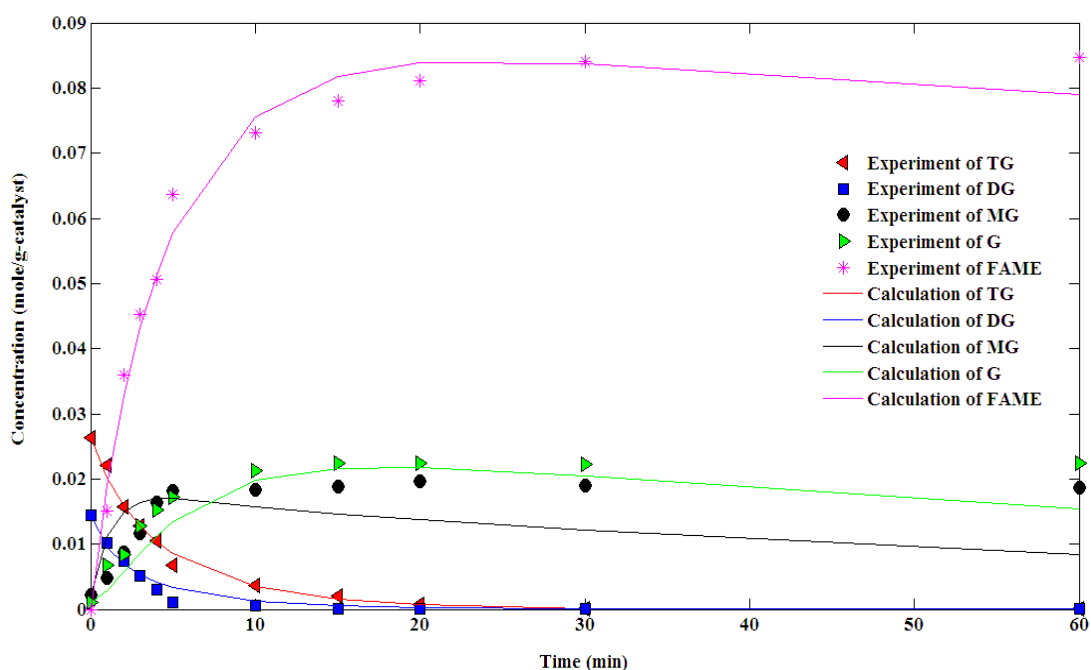


Figure 30 Transesterification at $T = 55\text{ }^{\circ}\text{C}$: Experimental data and calculated of LH model, type 1 (reversible reaction in step 3)

Table 26 The fitness value ($\times 10^4$) of PH and LH type 1 model that based on the irreversible reaction and reversible reaction in step 3 at $65\text{ }^{\circ}\text{C}$ of reaction temperature

Component in model	PH model		LH type 1 model	
	Irreversible reaction	Reversible reaction in step 3	Irreversible reaction	Reversible reaction in step 3
Without FAME	2.28	2.74	2.05	1.91
With FAME	10.00	3.52	5.60	1.74

For the results of comparisons between PH and LH type 1 model, it was showed in Table 26. Both models were classified similar to the previous comparison, LH type 1 and LH type 2. As can be seen in the table, LH type 1 model showed more suitable than PH one in all case except reversible reaction in step 3 and model without FAME concentration. However, PH model could be used to explain the kinetic result as well as LH type 1 model.

As see in the previous result, the reversible reaction in step 3 with or without FAME concentration showed the lower of error from the difference between the calculated and experimental result.

Table 27 The kinetic reaction rate constants of PH model with FAME concentration at various temperatures

Kinetic rate constant	Temperature (K)		
	328	333	338
k_1	0.1450	0.2780	0.3100
k_2	0.9140	0.9680	1.3140
k_3	0.1460	0.8210	2.1950
k_4	0.9150	0.7300	0.3620

The kinetic rate constant of PH model with FAME concentration were showed in Table 27. The kinetic reaction rates almost always increase with temperature. As can be seen in Table 27, k_1 value from TG \rightarrow DD reaction showed the lowest value that means the TG \rightarrow DG step is the rate-limiting step in this reaction.

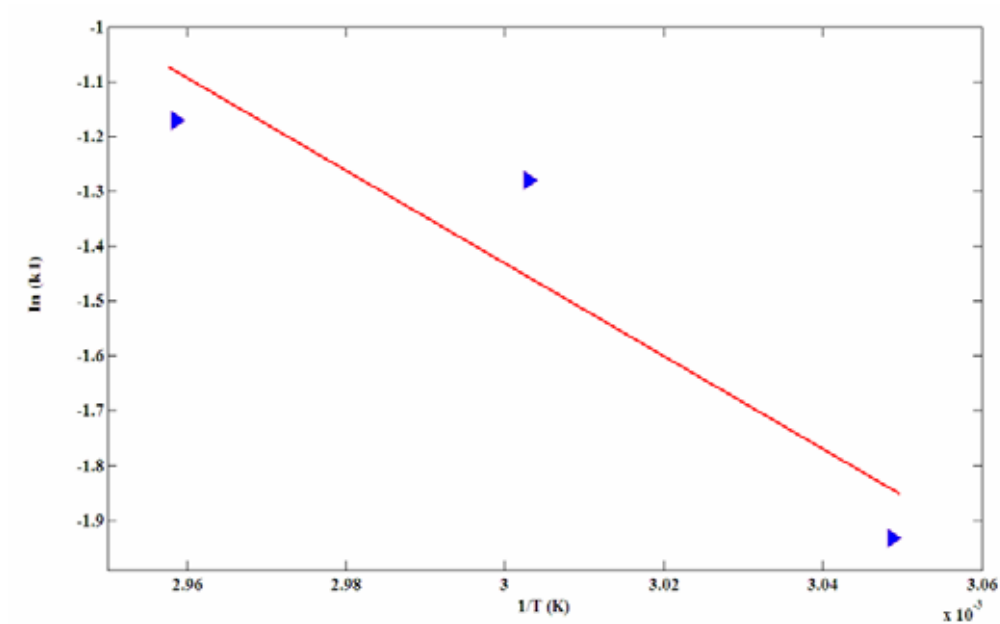


Figure 31 Arrhenius plot for transesterification reaction rate constants between $\ln(k_1)$ and $1/T$ (K^{-1}), $R^2 = 0.8611$

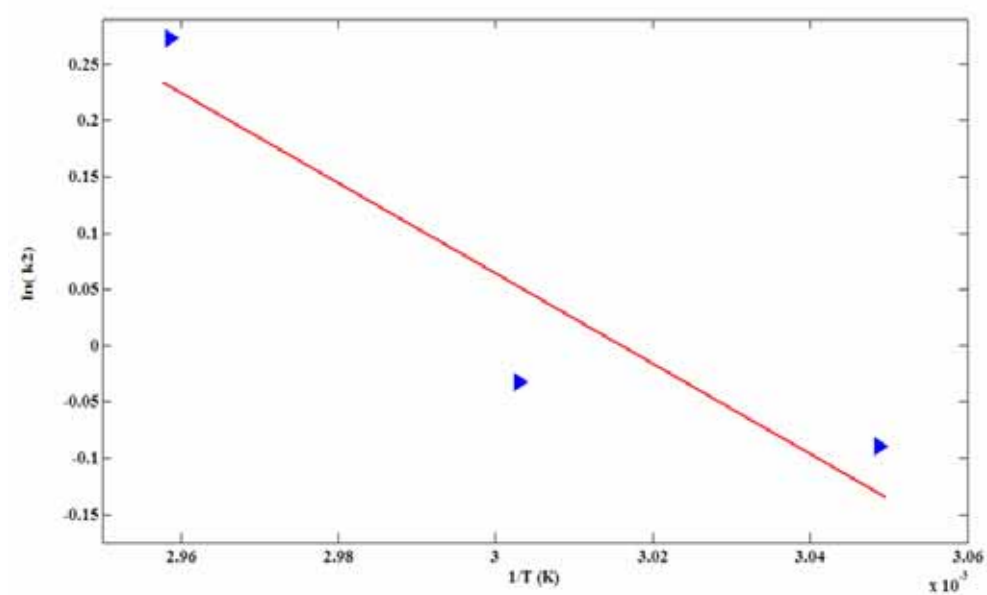


Figure 32 Arrhenius plot for transesterification reaction rate constants between $\ln(k_2)$ and $1/T$ (K^{-1}), $R^2 = 0.8592$

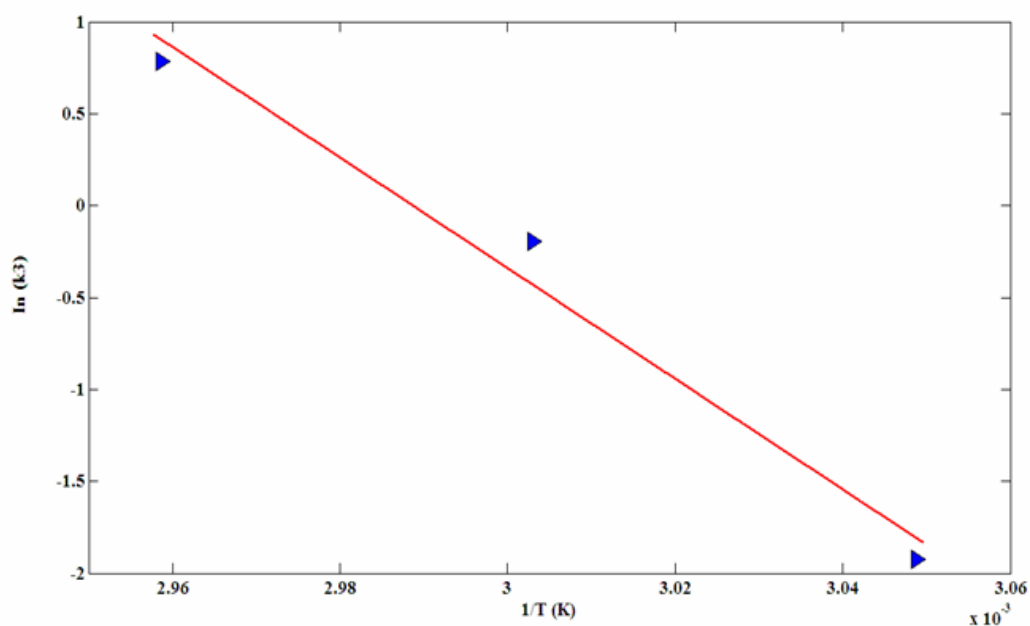


Figure 33 Arrhenius plot for transesterification reaction rate constants between $\ln(k_3)$ and $1/T \text{ (K}^{-1}\text{)}$, $R^2 = 0.9781$

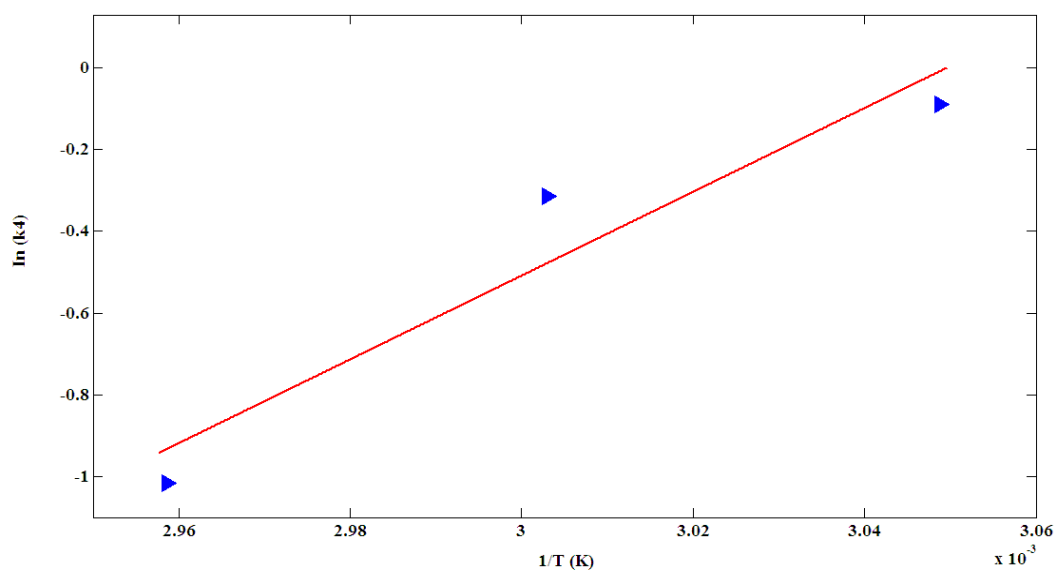


Figure 34 Arrhenius plot for transesterification reaction rate constants between $\ln(k_4)$ and $1/T \text{ (K}^{-1}\text{)}$, $R^2 = 0.9146$

As showed in Figures 31 – 34, the arrhenius' equation was plotted to investigate the activation energy of the transesterification. The activation energy of each step was showed in Table 28

Table 28 Energy of activation (J/mol) of transesterification reaction

Reaction	Rate constant	Ea (J/mol)	ko (min ⁻¹)
TG → DG	k ₁	7.0281E+04	2.4649E+10
DG → MG	k ₂	3.3342E+04	1.7897E+05
MG → G	k ₃	2.5014E+05	1.1254E+39
G → MG	k ₄	-8.5243E+04	2.6332E-14

Table 29 The kinetic reaction rate constants of LH model type 1 with FAME concentration at various temperatures

Kinetic rate constant	Temperature (K)		
	328	333	338
k ₁	0.6920	1.5640	0.7063
k ₂	1.3970	1.7110	0.5993
k ₃	0.3750	0.5993	0.9967
k ₄	0.9050	0.5170	2.5830
K _{TG}	0.4470	0.2940	0.5171
K _{DG}	0.7550	0.7500	2.0684
K _{MG}	0.8000	1.3790	1.4591
K _G	0.5800	0.6590	0.2189
K _{FAME}	4.4040	5.2330	2.0043

In case of LH type 1 model, the parameter of with FAME concentration were showed in Tables 29.

CONCLUSION AND RECOMMENDATIONS

Conclusion

In this work, the kinetics of the catalytic transesterification of palm olein oil using strontium oxide was studied. Nowadays, the transesterification of vegetable oil by solid catalyst was very attractive to substitute the conventional process that used homogeneous base catalysts such as sodium or potassium hydroxide. Many researchers have proposed the kinetic model of these catalysts. However, the kinetic of heterogeneous catalyzed transesterification of vegetable oil had a little information.

The mass transfer resistance was investigated and showed the minor effect on the reaction. ANOVA analysis was used and analyzed the data at 500, 700 and 1000 rpm of agitator speed. In case of triglyceride analysis, all desired speed of agitator did not show the effect on the reaction. However, at the speed of 500 rpm the effect on the diglycerides and monoglycerides conversion was determined while 700 and 1000 rpm of agitator speed showed nothing. As the previous mention, the recommendation of desired agitator speed for the reaction should be selected upper 700 rpm to reduce the mass transfer resistance in this reaction.

For the parameters estimation, genetic algorithm (GA) was used to estimate the model parameters. GA is generally able to find good solutions in reasonable amounts of time. But as it is applied to larger and harder problems, there are an increment in the time required to find adequate solutions. As consequences of this, there have been multiple efforts to make GA faster and one of most promising choices is to find the best GA parameters. The approximate of GA parameters were studied to find the best values of these one. The best value of population size, generation number, crossover fraction, mutation rate, migration fraction and hybrid function, were 100, 100, 0.8, 0.01, 0.2 and none, respectively.

Pseudo-homogeneous (PH) and Langmiur-Hinshewood (LH) models were selected as kinetic modeling of transesterification of palm olein oil. LH model consisted of type 1 and type 2. As comparing the LH type 1 and type 2 had a litter difference of the calculated and experiment results while PH model had more error than LH model. The reversible reaction on step 3 only, monoglycerides step, showed the suitable mechanism to derive the model that based on the elementary reaction.

Both of these models were classified to the case of with or without FAME concentration that included into the model. Due to FAME concentration was received by an approximate method. Therefore, the results showed the good correlation between the calculated and experiment values in both case.

Finally, these kinetic models could be used in the process simulation such as size of reactor, reaction condition and cost of operation or construction in the future work.

Recommendations

1. In this work, the gas chromatography was used as an analysis method of kinetic study of palm olein transesterification. These chemicals of the reaction consisted of triglycerides, diglycerides, monoglycerides and glycerol that were detected and calculated. However, it was not the best method of analysis for kinetic study of vegetable oil transesterification. For more accuracy of analysis method, the other method such as gel permutation or high performance liquid chromatography should be used to analyze these components.

2. In analysis method, fatty acid methyl ester should be detected and analyzed from the experiment directly that showed the more accuracy of value than the estimated value.

3. In case of mass transfer resistance, Reynolds number should be used to substitute the speed of agitator for higher accuracy of scale up of process design.

4. The continuous reactor should be used to investigate the kinetic behavior of vegetable oil tranesterification for use in the scale up of reactor to the commercial scale.

5. In the kinetic modeling, the deactivation of catalyst should be considered in the model in order to know the life time of catalyst for the regeneration or replacement.

LITERATURE CITED

- Ayen, R.J. and M.S. Peter 1962. Catalytic Reduction of Nitric oxide. **Ind Eng Chem Proc Des Dev.**, 1: 204 - 207.
- Bellman, R., J. Jacquez, R. Kalaba and S. Schwimmer. 1967. Quasilinearization and the estimation of chemical rate constant from raw kinetic data. **Math Biosc.**, 1: 71-76.
- Booker, L.B. 1993. Recombination distributions for genetic algorithm. **Foundation of Genetic Algorithm 2**. Conference proceeding. 29 – 44.
- Chai-Hung, S., F. Chun-Chong, G. James, C. I-Ming. and W. Wen-Teng. 2008. A heterogeneous acid-catalyzed process for biodiesel production from enzyme hydrolyzed fatty acids. **AIChE Journal**. 54(1); 327 – 336.
- Choudary, B.M., M. Lakshmi Kantam, Ch. Venkat Reddy, S. Aranganathan, P. Lakshmi Santhi and F. Figueras. 2000. Mg-Al-O-t-Bu hydrotalcite: a new and efficient heterogeneous catalyst for transesterification. **Journal of molecular Catalysis**. 159: 411-416.
- Eftaxias, A., J. Front, A. Fortuny, A. Fabregat and F. Stuber 2002. Nonlinear kinetic parameter estimation using simulated annealing. **Computer & Chemical Engineering**, 26: 1725 – 1733.
- Furuta, S., H. Matsushashi and K. Arata. 2006. Biodiesel fuel production with solid amorphous-zirconia catalysis in fixed bed reactor. **Journal of Biomass and bioenergy** .30: 870-873.
- Furuta, S., H. Matsushashi and K. Arata. 2004. Biodiesel fuel production with solid super acid catalysis in fixed bed reactor under atmospheric pressure. **Journal of Catalysis Communication**, 5: 721-723.

- Gorzawski, H. and W.F. Hoelderich. 1998. Transesterification of methyl benzoate and dimethyl terephthalaate with ethylene glycol over super bases. **Journal of Applied catalysis**. 179: 131-137.
- Hibbert, B.D. 1992. A hybrid genetic algorithm for the estimation of kinetic parameters. **Chemometrics and Intelligent Laboratory System**, 19: 319 – 329.
- Hitoshi, M., Joelianingsih, Shoji H., N. Hiroshi, S. Yasuyuki, H.S.Tatang, H.T. Armansyah, and A. Kamaruddin. 2008. Biodiesel fuels from palm oil via the non-catalytic transesterification in a bubble column reactor at atmospheric pressure: a kinetic study. **Renewable Energy Journal** 33: 1629-1636.
- Huayang H., S. Shiyao, W. Tao and Z. Shenlin. 2007. Transesterification kinetics of soybean oil for production of biodiesel in supercritical methanol. **J. Amer. Oil. Chem. Soc.** 84: 399 – 404.
- Lee, K.W., X.Y. Jin, H.M. Jin, Y. Li, K. Young-Wun, and C. Keun-Woo. 2007. A kinetic study on the transesterification of glyceryl monooleate and soybean used frying oil to biodiesel. **J. Ind. Eng. Chem.**, 13(5). 799 - 807.
- Lui, X., H. Huayang, W. Yujun and Z. Shenlin 2007. Transesterification of soybean oil to biodiesel using SrO as a solid base catalyst. **Catalysis Communication** 8; 1107-1111.
- Marchetti, J. M., V.U. Miguel and A. F. Errazu. 2006. Heterogeneous esterification of oil with high amount of free fatty acids. **Journal of Fuel**.
- Mayer, U. and W.F. Hoelderich. 1998. Transesterification of methyl benzoate and dimethyl terephthalaate with ethylene glycol over basic zeolites. **Journal of Applied catalysis**. 178: 159-166.

- Miki, M., T. Hiroyasu, M. Kaneko and K. Hatanaka. 1999. A parallel genetic algorithm with distributed environment scheme. International Conference on Parallel and Distributed Processing Techniques and Applications.
- Moon, C., J. Kim, G. Choi, and Y. Seo. 2002. An efficient genetic algorithm for the traveling salesman problem with precedence constraints. **European journal of Operation Research**, 140: 606-617.
- Moradi, A.R., J. Ahmadpour and F. Yaripour. 2008. Intrinsic kinetics study of LPDME process from syngas over bi-functional catalyst. **Chemical Engineering Journal**.
- Moros, R., H. Kalies, G. Rex and St. Schaffarczyk. 1996. A genetic algorithm for generating initial parameter estimations for kinetic models of catalytic processes. **Comp. Chem. Eng.**, 20(10); 1257-1270
- Noureddini, H. and D. Zhu. 1997. Kinetics of transesterification of soybean oil. **JAACS** 74: 1457 – 1463.
- Peter, S., R. Granswindt, H.P. Neuner and E. Weidner. 2002. Alcoholysis of triacylglycerols by heterogeneous catalysis. **European Journal of Lipid Science and Technology**. 104: 324-330.
- Royaei, S.J., F. Cavus, S. Morteza, S. Sayed and T. Ashraf. 2008. A new Langmuir-Hinshelwood mechanism for the methanol to dimethylether dehydration reaction over clinoptilolite-zeolite catalyst. **Applied Catalysis A: General** 338: 114-120.
- Sankar, M., C.M. Nair, K.V.G.K. Murty and P. Manikandan. 2006. Transesterification of cyclic carbonates with methanol at ambient condition over tungstate-based solid catalysts. **Journal of Applied catalysis**. 108-114.

- Satterfield, C. N. 1991. **Heterogeneous Catalysis in Industrial Practice**, McGraw-Hill, Inc., USA.
- Serio, M.D., R. Tesser, A. Ferrara and E. Santacesaria. 2004. Heterogonous basic catalyst for the transesterification and the polycondensation reactions in PET production from DMT. **Journal of molecular Catalysis**. 212: 251-257.
- Suppes, G.J., M.A. Darari, J. Doskocil, P.J. Mankidy. and M. J. Goff. 2003. Transesterification of soy bean oil with metal catalysts. **Journal of Applied catalysis**.
- Sercheli, R.R.M. Vargas and U. Schuchardf. 1999. Alkylguanigine-catalyzed heterogeneous transesterification of soybean oil. **Journal of the American Oil chemists' Society**. 79:1208-1210.
- Yu, H., H. Feng, P. Yao and Y. Yuan. 2000. A combined genetic algorithm/ simulated annealing algorithm for large scale system energy integration. **Computer and Chemical Engineering**, 24: 2023-2035.
- Zajdlewicz, D.J. 2001. Development of a continuous biodiesel process by investigation into possible heterogeneous catalysts.

APPENDICES

Appendix A

Experimental results from gas chromatograph

Appendix Table A1 Results from gas chromatography

Peak#	RT	RRT	Area	Height	Compound Name
8	3.4900	0.17	23,627.90	2489.6	
9	3.7070	0.18	5,176.40	1326.7	
10	3.8230	0.19	1,429.50	458	
11	3.9030	0.19	1,971.50	462.4	
12	4.0050	0.20	1,693.00	560.4	
13	4.1410	0.20	100,461.50	49703.1	
14	4.3890	0.21	14,079.00	5276.5	
15	4.6370	0.23	12,069.20	6052.4	
16	5.2320	0.26	128,708.90	74808.9	
17	5.3780	0.26	88,000.10	51783.5	
18	6.3890	0.31	319,934.00	72205.9	glycerol
19	6.4500	0.32	85,566.00	6642.8	glycerol
20	7.9800	0.39	1,057.80	551.7	
21	8.0920	0.40	218,035.70	122209	
22	8.3970	0.41	1,063.60	384.3	
23	9.5710	0.47	121,476.60	68271.6	
24	10.2850	0.50	2,194.20	1132.4	
25	10.8750	0.53	12,677.00	5165.2	Mono_C10:0
26	11.1110	0.54	2,382,531.40	774338.4	
27	11.3420	0.55	3,758.40	795.4	
28	11.6610	0.57	3,151.60	952.5	
29	11.8760	0.58	5,028.40	2232.6	
30	12.0940	0.59	1,033.70	347.4	
31	12.2990	0.60	1,306.80	377.5	
32	12.4800	0.61	700,530.20	198277.4	
33	12.6010	0.62	3,204,198.80	819743.3	
34	12.7830	0.62	244,837.30	105605.5	Mono_C12:0
35	12.8490	0.63	12,465.50	3018.1	
36	12.9810	0.63	3,080.70	798.4	
37	13.1350	0.64	3,198.50	465.1	
38	13.3030	0.65	2,260.90	658.6	
39	13.4140	0.66	1,605.80	354.6	
40	13.6240	0.67	1,994.60	760.7	
41	13.6850	0.67	1,415.80	430.4	
42	14.3810	0.70	11,776.10	4075.6	
43	14.5820	0.71	1,823.50	703.7	
44	14.6580	0.72	19,515.90	7988.6	Mono_C14:0
45	16.3400	0.80	6,852.20	1712.5	
46	16.6340	0.81	4,473.70	1690.4	
47	16.9820	0.83	4,734.60	1169	
48	17.1110	0.84	1,439.30	633.4	
49	17.3490	0.85	3,831.10	1896	
50	17.7790	0.87	9,272.10	3011.3	
51	18.0640	0.88	7,339.70	3597.2	

Appendix Table A1 (Continued)

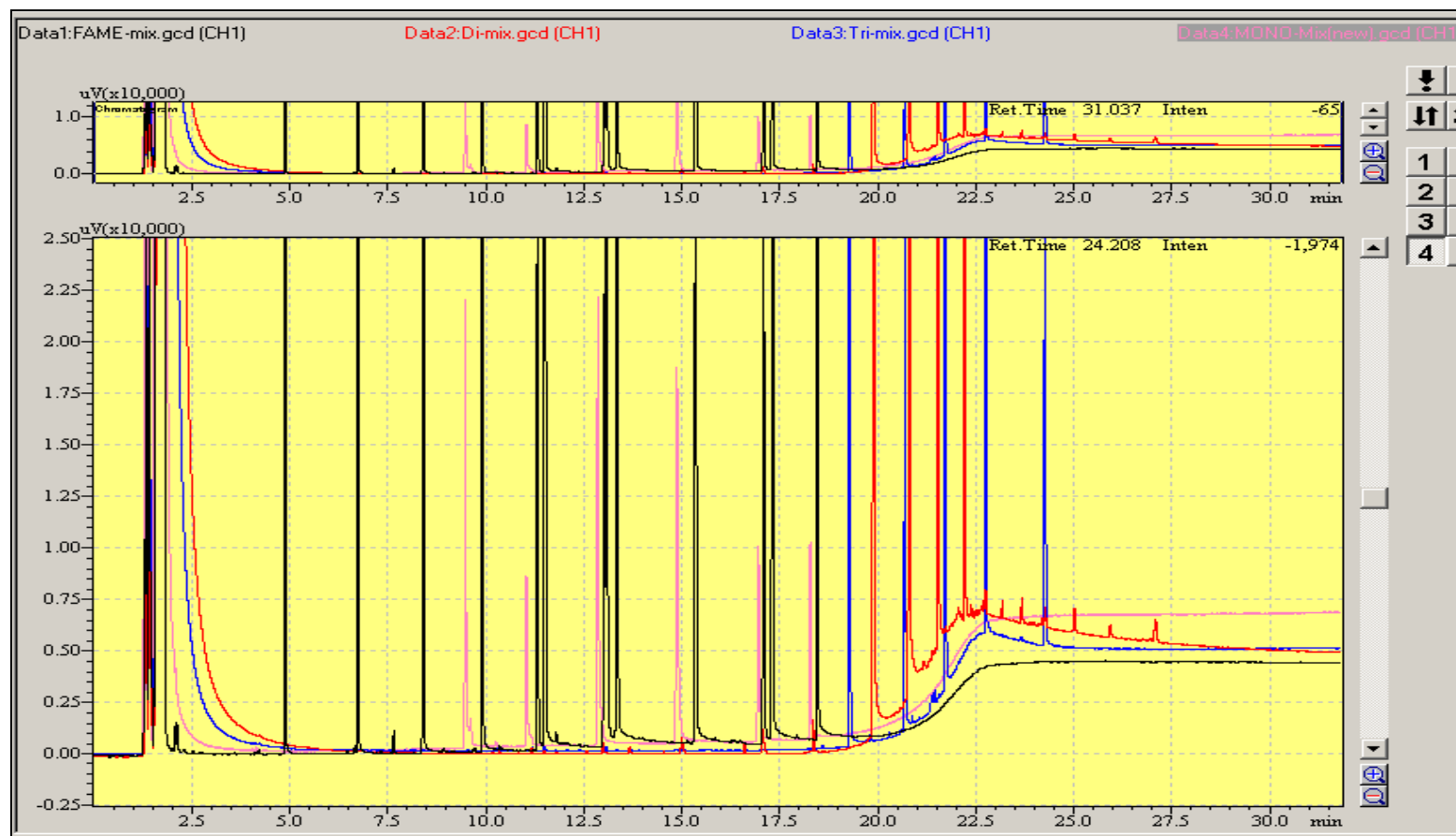
Peak#	RT	RRT	Area	Height	Compound Name
52	18.0990	0.88	11,287.40	2683	
53	18.2970	0.89	9,998.10	3569.3	Mono_C18:0
54	18.5000	0.90	62,586.00	515.4	Mono_C18:1
55	19.6120	0.96	1,058.50	535.8	Di_C12:0
56	19.9480	0.98	1,032.30	397.6	
57	20.0200	0.98	1,647.50	973.8	
58	20.4590	1.00	42,990.50	31,280.00	Internal Standard
59	20.7700	1.02	1,610.50	791.3	
43	20.5600	1.00	1,320.90	815.7	
44	20.7750	1.02	2,036.50	1000	Di_C14:0
45	20.8770	1.02	38,001.20	21355.9	
46	21.2180	1.04	64,829.60	32291.3	Di_C16:0
47	21.2810	1.04	21,908.90	14875.4	Di_C16:0
48	21.3350	1.04	1,871.80	1175.3	Di_C16:0
49	21.5380	1.05	248,835.90	101125.1	Tri_C12:0
50	21.5920	1.06	266,600.80	171366.3	Tri_C12:0
51	21.6480	1.06	13,178.20	7666.5	
52	21.8100	1.07	61,883.00	39267.2	
53	21.8460	1.07	105,042.90	66745.6	Di_C18:1
54	21.8820	1.07	184,367.50	94029.9	Di_C18:1
55	21.9510	1.07	8,559.80	3943.8	Di_C18:1
56	22.1550	1.08	64,481.10	35277.6	Di_C18:0
57	22.2200	1.09	6,274.20	2434.9	Di_C18:0
58	22.4810	1.10	91,558.90	23752.6	Tri_C14:0
59	22.8330	1.12	145,296.40	20614	
64	24.0180	1.17	5,830.10	1935.3	
65	24.4170	1.19	1,682,640.30	353120.5	Tri_C16:0
66	24.6820	1.21	10,435.00	2630.3	
67	25.1660	1.23	2,330,184.90	296927.4	
68	25.4690	1.24	3,516.80	785.3	
69	25.9900	1.27	554,609.70	71698.5	Tri_C18:0
70	27.0670	1.32	20,799.60	2531.1	Tri_c18:1
71	28.5090	1.39	1,556.10	264.7	
72	28.5930	1.40	1,761.80	357.7	

Appendix B

Standard solution of gas chromatography

Appendix Table B1 Standard solution of gas chromatography

Component	RT	RRT
Glycerol	6.386	0.31
Mono - C 8:0	9.481	0.46
Mono - C 10:0	11.040	0.53
Mono - C 12:0	12.862	0.62
Mono - C 14:0	14.880	0.72
Mono - C 16:0	16.959	0.82
Mono - C 18:0	18.283	0.89
Mono - C 18:1	18.590	0.90
Di - C 12:0	19.896	0.96
Di - C 14:0	20.801	1.01
Di - C 16:0	21.539	1.04
Di - C 18:0	22.219	1.08
Di - C 18:1	22.035	1.07
Tri - C 8:0	19.285	0.93
Tri - C 10:0	20.695	1.00
Tri - C 12:0	21.729	1.05
Tri - C 14:0	22.753	1.10
Tri - C 16:0	24.269	1.18
Tri - C 18:0	26.934	1.30
Tri - C 18:1	26.841	1.30
Internal Standard	20.647	1.00



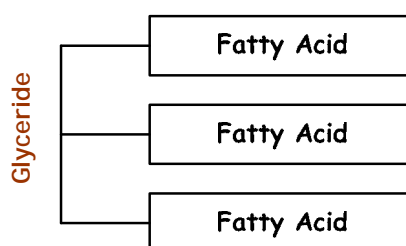
Appendix Figure B1 Standard solution graph of gas chromatography

Appendix C

Estimation of TG, DG and MG molecular weight
in palm olein oil

Estimation of TG, DG, MG and G molecular weight in palm olein oil:

The estimation of molecular weight of TG, DG, MD and G in palm olein oil, based on the chemical structure of TG that consist of three fatty acid and one glyceride, DG contained 2 fatty acid and one glyceride and MG is one fatty acid and one glyceride. The chemical structure of TG was shown in Appendix Figure C1.



Appendix Figure C1 Chemical structure of triglyceride

According to Appendix Figure C1 and the molecular of each fatty acid as show in Appendix Table C1, the molecular weights are estimated as follows;

Triglyceride:

$$MW(as\ palmitic) = 92.1 + (3 \times 256.43) = 861.39$$

$$MW(as\ stearic) = 92.1 + (3 \times 284.48) = 945.54$$

$$MW(as\ oleic) = 92.1 + (3 \times 282.47) = 939.51$$

$$MW(as\ Linoleic\ acid) = 92.1 + (3 \times 280.00) = 932.10$$

Based on the percentage of fatty acid composition in palm olein oil, multiplied the estimate molecular weight of TG with fatty acid composition. The average of TG molecular weight is as follows;

$$\begin{aligned}
 \text{Average of MW} &= (0.37 \times 861.39) + (0.04 \times 945.54) + (0.46 \times 939.51) \\
 &\quad + (0.13 \times 932.10) \\
 &= 909.88 \#
 \end{aligned}$$

Appendix Table C1 Fatty acid molecular weight

Fatty acid	Molecular weight
C16:0 (Palmitic acid)	256.43
C18:0 (Stearic acid)	284.48
C18:1 (Oleic acid)	282.47
C18:2 (Linoleic acid)	280.00
Glycerol	92.1

Diglyceride:

$$MW(\text{as palmitic}) = 92.1 + (2 \times 256.43) = 604.96$$

$$MW(\text{as stearic}) = 92.1 + (2 \times 284.48) = 661.06$$

$$MW(\text{as oleic}) = 92.1 + (2 \times 282.47) = 657.04$$

$$MW(\text{as Linoleic acid}) = 92.1 + (2 \times 280.00) = 637.29$$

$$\begin{aligned}
 \text{Average of MW} &= (0.37 \times 604.96) + (0.04 \times 661.06) + (0.46 \times 657.04) \\
 &\quad + (0.13 \times 637.29) \\
 &= 637.29 \#
 \end{aligned}$$

Monoglyceride:

$$MW(as\ palmitic) = 92.1 + (1 \times 256.43) = 348.53$$

$$MW(as\ stearic) = 92.1 + (1 \times 284.48) = 376.58$$

$$MW(as\ oleic) = 92.1 + (1 \times 282.47) = 374.57$$

$$MW(as\ Linoleic\ acid) = 92.1 + (1 \times 280.00) = 372.10$$

$$\begin{aligned} \text{Average of } MW &= (0.37 \times 348.43) + (0.04 \times 376.58) + (0.46 \times 374.57) \\ &\quad + (0.13 \times 364.69) \end{aligned}$$

$$= 364.69 \#$$

Appendix Table C2 Summary of the estimated molecular weight of TG, DG and MG in palm olein oil.

Fatty acid	% Composition	TG	DG	MG
C16:0 (Palmitic acid)	0.37	861.39	604.96	348.53
C18:0 (Stearic acid)	0.04	945.54	661.06	376.58
C18:1 (Oleic acid)	0.46	939.51	657.04	374.57
C18:2 (linoleic acid)	0.13	932.10	652.10	372.10
Palm olein (average)		<u>909.88</u>	<u>637.29</u>	<u>364.69</u>
total	1.00			

The validation of TG, DG and MG molecular weight that shown in Appendix Table C2, the estimated molecular weight of TG, DG and MG were used to calculate the molecular weight of palm olein oil by multiplied by weight fraction of TG,DG and MG in palm olein oil. The result was shown in Appendix Table C3

Appendix Table C3 The estimated molecular weight of palm olein oil.

	weight fraction	weight
TG	0.7200	655.12
DG	0.2740	174.62
MG	0.0236	8.61
G	0.0029	0.27
Estimate value	1.0205	<u>838.61</u>
Real value		<u>855.00</u>
SSE (%)		1.92

According to Appendix Table C3, the estimated molecular weight of palm olein oil was compared with the real one. The results show that the estimation value was suitable for use.

Appendix D

Analysis method for biodiesel sample

Analysis method for biodiesel sample:

1. When biodiesel sample was completely analyzed by gas chromatography as shown in Appendix table A1, following by identified graph using the standard solution as shown in Appendix B1., it was shown on the table below;

Appendix Table D1 Total area of fatty acid component

	C14:0	C16:0	C18:0	C18:1	Total Area	A_i/A_{IS}
G	-	-	-	-	217,000.00	5.11
MG	18,956.10		24,652.90	2,891.00	46,500.00	1.10
DG	-	53,379.80	21,018.40	98,601.80	173,000.00	4.08
TG	-	604,690.70	215,009.70	10,799.60	830,500.00	19.57
IS	-	-	-	-	42,437.60	1.00

2. To calculate the concentration of TG, DG, MD and G using the standard curve.

Glycerol Concentration:

$$\begin{aligned}
 G \text{ (\% w/w)} &= \left[a_g \left(\frac{A_g}{A_{IS}} \right) + b_g \right] \cdot W_{IS} \cdot \frac{100}{W} \\
 &= \left[0.5849 \left(\frac{A_g}{A_{IS}} \right) + 0.0036 \right] \cdot W_{IS} \cdot \frac{100}{W} \\
 &= \left[0.5849(5.1134) + 0.0036 \right] \times 0.808 \times \frac{100}{50} \\
 &= 4.84 \text{ (\%w/w)}
 \end{aligned}$$

Monoglyceride Concentration:

$$\begin{aligned}
 G_m \text{ (\% w / w)} &= \left[a_m \left(\frac{A_m}{A_{IS}} \right) + b_m \right] \cdot W_{IS} \cdot \frac{100}{W} \\
 &= \left[1.8091 \left(\frac{A_g}{A_{IS}} \right) + 0.2386 \right] \cdot W_{IS} \cdot \frac{100}{W} \\
 &= \left[1.8091(1.0957) + 0.2386 \right] \times 0.808 \times \frac{100}{50} \\
 &= 3.59 \text{ (\% w/w)}
 \end{aligned}$$

Diglyceride Concentration:

$$\begin{aligned}
 G_d \text{ (\% w / w)} &= \left[a_d \left(\frac{A_d}{A_{IS}} \right) + b_d \right] \cdot W_{IS} \cdot \frac{100}{W} \\
 &= \left[1.9801 \left(\frac{A_g}{A_{IS}} \right) + 0.1671 \right] \cdot W_{IS} \cdot \frac{100}{W} \\
 &= \left[1.9861(4.0766) + 0.1671 \right] \times 0.808 \times \frac{100}{50} \\
 &= 13.35 \text{ (\% w/w)}
 \end{aligned}$$

Triglyceride Concentration:

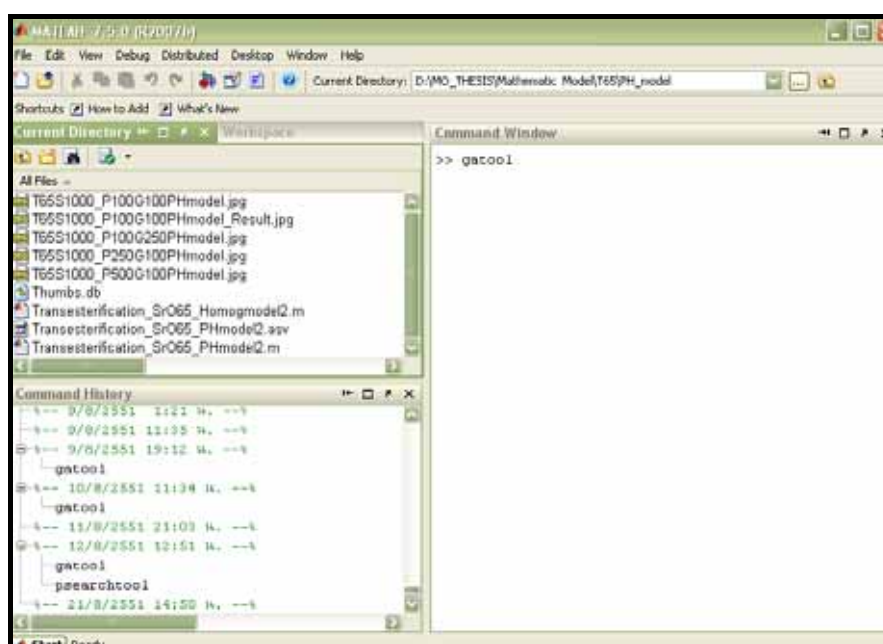
$$\begin{aligned}
 G_t \text{ (\% w/w)} &= \left[a_t \left(\frac{A_t}{A_{IS}} \right) + b_t \right] \cdot W_{IS} \cdot \frac{100}{W} \\
 &= \left[1.0237 \left(\frac{A_g}{A_{IS}} \right) + 0.0764 \right] \cdot W_{IS} \cdot \frac{100}{W} \\
 &= \left[1.0237(19.5699) + 0.0764 \right] \times 0.808 \times \frac{100}{50} \\
 &= 32.50 \text{ (\%w/w)}
 \end{aligned}$$

Appendix E
Genetic algorithm tool user manual

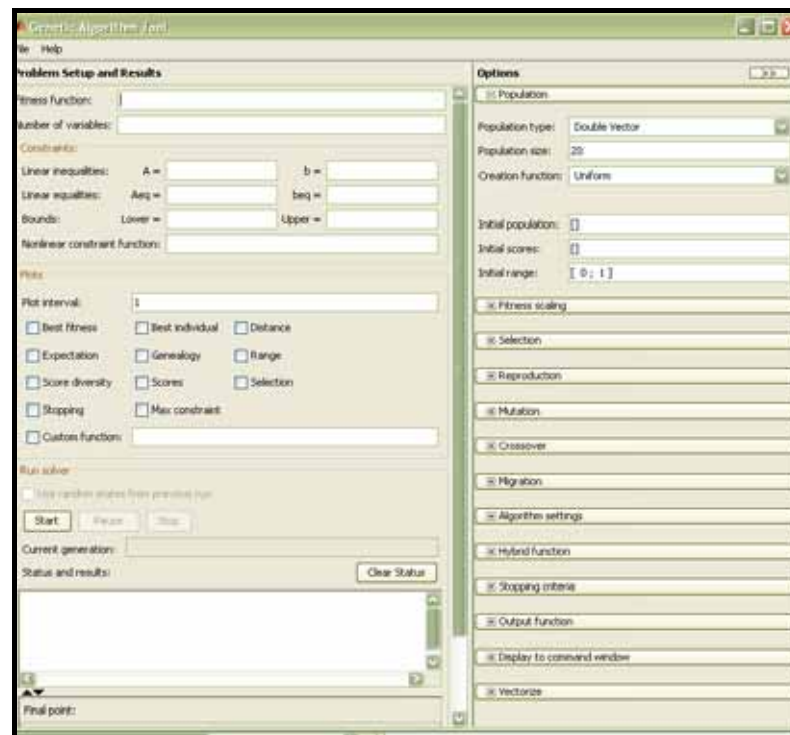
Genetic algorithm tool user manual:

In this research, GA tool was used to estimate chemical kinetic rate constants of transesterification reaction.

1. To open the tool, enter “gatool” at the MATLAB prompt.



2. This opens the Genetic Algorithm Tool, as shown in the following figure.

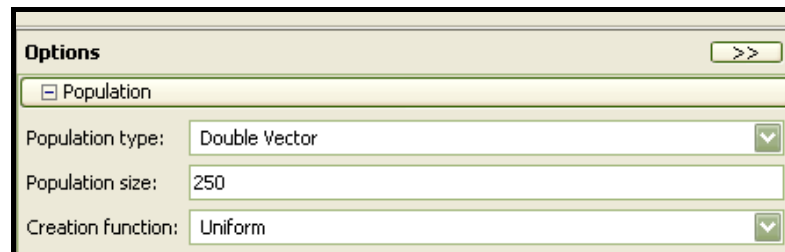


3. To enter the M-file that was the objective function and number of variable in GA Tool

- Fitness function — The function you want to minimize. Enter a handle to an M-file function that computes the fitness function.
- Number of variables — The number of independent variables for the fitness function.

Problem Setup and Results	
Fitness function:	@Transesterification_SrO65_PHmodel2
Number of variables:	4

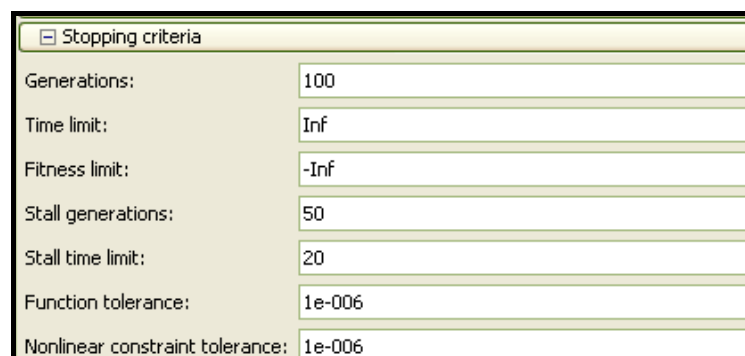
4. To enter the number of population



The image shows the 'Options' dialog box with the 'Population' tab selected. The 'Population type' is set to 'Double Vector', 'Population size' is 250, and 'Creation function' is 'Uniform'.

Options	
Population	
Population type:	Double Vector
Population size:	250
Creation function:	Uniform

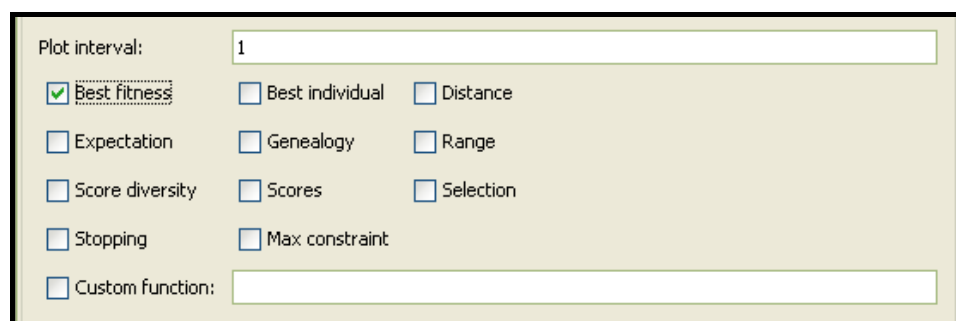
5. To enter the number of generation



The image shows the 'Stopping criteria' dialog box. The 'Generations' field is set to 100, 'Time limit' is 'Inf', 'Fitness limit' is '-Inf', 'Stall generations' is 50, 'Stall time limit' is 20, 'Function tolerance' is 1e-006, and 'Nonlinear constraint tolerance' is 1e-006.

Stopping criteria	
Generations:	100
Time limit:	Inf
Fitness limit:	-Inf
Stall generations:	50
Stall time limit:	20
Function tolerance:	1e-006
Nonlinear constraint tolerance:	1e-006

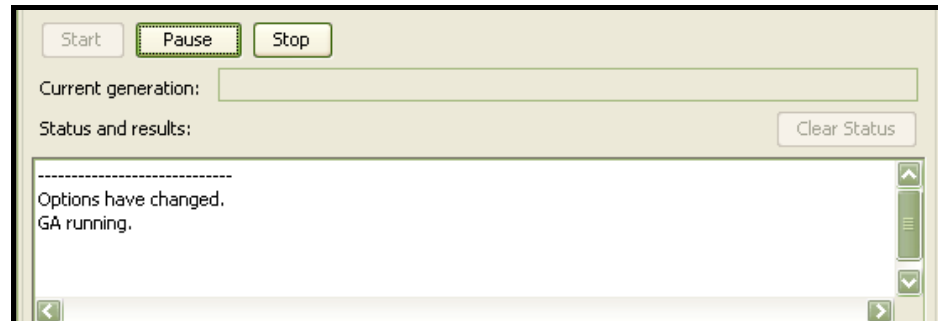
6. To click “ Best fitness ”



The image shows the 'Plotting options' dialog box. The 'Plot interval' is set to 1. The 'Best fitness' checkbox is checked. Other options include 'Best individual', 'Distance', 'Expectation', 'Genealogy', 'Range', 'Score diversity', 'Scores', 'Selection', 'Stopping', 'Max constraint', and 'Custom function'.

Plotting options	
Plot interval:	1
<input checked="" type="checkbox"/> Best fitness	<input type="checkbox"/> Best individual <input type="checkbox"/> Distance
<input type="checkbox"/> Expectation	<input type="checkbox"/> Genealogy <input type="checkbox"/> Range
<input type="checkbox"/> Score diversity	<input type="checkbox"/> Scores <input type="checkbox"/> Selection
<input type="checkbox"/> Stopping	<input type="checkbox"/> Max constraint
<input type="checkbox"/> Custom function:	

7. Finally, click “ start ” to run the GA tool



\

Appendix F

MATLAB™ code for pseudo-homogeneous model

[illegible]

Appendix G

MATLABTM code for Langmuir-Hinshelwood model

In this research, GA based program for solving chemical kinetic rate constants of transesterification reaction on GA tool were developed by Matlab™ program version 7.5.0 (R2007b). Langmuir-Hinshelwood model was selected.

File: Transesterification_SrO65_LHmodel2.m

Description : Find value of least square objective function

```

%%%%%%%%%%%%%%%%%%%%%%%%%%%%%%%%%%%%%%%%%%%%%%%%%%%%%%%%%%%%%%%%%%%%%%%%
%%%%%%%%
%Transesterification of Palm olein
%Irreversible reaction
%TG --r1--> DG + FAME
%DG --r2--> MG + FAME
%MG --r3--> G + FAME
%G + FAME --r4--> MG
%%%%%%%%%%%%%%%%%%%%%%%%%%%%%%%%%%%%%%%%%%%%%%%%%%%%%%%%%%%%%%%%%%%%%%%%
%%%%%%%%
%dTG/dt = -r1
%dDG/dt = r1 - r2
%dMG/dt = r2 - r3 + r4
%dG/dt = r3 - r4
%dFAME/dt = r1+r2+r3-r4
%%%%%%%%%%%%%%%%%%%%%%%%%%%%%%%%%%%%%%%%%%%%%%%%%%%%%%%%%%%%%%%%%%%%%%%%
%%%%%%%%
%Langmuir-Hinshelwood Model:
%r1 = k1*Kt*TG/(1+ Kt*TG+ Kd*DG+ Km*MG+ Kg*G)^2
%r2 = k2*Kd*DG/(1+ Kt*TG+ Kd*DG+ Km*MG+ Kg*G)^2
%r3 = k3*Km*MG/(1+ Kt*TG+ Kd*DG+ Km*MG+ Kg*G)^2
%r4 = k4*Kg*G/(1+ Kt*TG+ Kd*DG+ Km*MG+ Kg*G)^2
%k1 = k(1); k2 = k(2); k3 = k(3) k4 =k(4); kt = k(5); kd = k(6); km =
k(7); kg = k(8);
%%%%%%%%%%%%%%%%%%%%%%%%%%%%%%%%%%%%%%%%%%%%%%%%%%%%%%%%%%%%%%%%%%%%%%%%
%%%%%%%%
%The catalyst is SrO
%Temperature = 65 C
%Speed = 1000 RPM
function obj = Transesterification_SrO65_LHmodel2(k)
%%%%%%%%%%%%%%%%%%%%%%%%%%%%%%%%%%%%%%%%%%%%%%%%%%%%%%%%%%%%%%%%%%%%%%%%
%%%%%%%%
obj = 0;
rho = [];
%Initial Condition
h = 0.01;
t(1) = 0;
t0 = 0; % Initial time (min)
tf = 60; % final time (min)
n = (tf-t0)/h; %number of loops
%%%%%%%%%%%%%%%%%%%%%%%%%%%%%%%%%%%%%%%%%%%%%%%%%%%%%%%%%%%%%%%%%%%%%%%%
%%%%%%%%
%Initial Value
G(1) = 3.1488E-03; %0.29;
MG(1) = 6.4712E-03; %2.36;

```

```

DG(1) = 4.3120E-02; % 27.48;
TG(1) = 7.8966E-02; %71.85;
%FAME(1) = 0.00;
%%%%%%%%%%%%%%%%%%%%%%%%%%%%%%%%%%%%%%%%%%%%%%%%%%%%%%%%%%%%%%%%%%%%%%%%
%%%%%%%%
%%%%%%%%%%%%%%%%%%%%%%%%%%%%%%%%%%%%%%%%%%%%%%%%%%%%%%%%%%%%%%%%%%%%%%%%
%%%%%%%%
%Experiment Data in (Mole)
ti = [ 0 2 4 6 8 10 15 20 30 60 ];
Gi = [ 3.1488E-03 5.1249E-02 8.2302E-02 9.6851E-02 1.0499E-01
1.1618E-01 1.2161E-01 1.2334E-01 1.2269E-01 1.2378E-01 ];
MGi = [ 6.4712E-03 9.6246E-03 1.4752E-02 1.8235E-02 1.6397E-02
1.5191E-02 1.4423E-02 1.3875E-02 1.4259E-02 1.3847E-02 ];
DGi = [ 4.3120E-02 2.0462E-02 9.9170E-03 3.9229E-03 2.2282E-03
8.9441E-04 4.2367E-04 4.2367E-04 4.2367E-04 4.2367E-04 ];
TGi = [ 7.8966E-02 3.4323E-02 1.7145E-02 1.0848E-02 5.9898E-03
2.1541E-03 5.2754E-04 1.3189E-04 1.3189E-04 1.3189E-04 ];
%%%%%%%%%%%%%%%%%%%%%%%%%%%%%%%%%%%%%%%%%%%%%%%%%%%%%%%%%%%%%%%%%%%%%%%%
%%%%%%%%
%Numerical Method:Ruang_Kutta_4
tic
for i = 1:n
    RK1TG = -k(1)*k(5)*TG(1)/(1+ k(5)*TG(i)+ k(6)*DG(i)+ k(7)*MG(i)+
k(8)*G(i))^2;
    RK1DG = k(1)*k(5)*TG(1)/(1+ k(5)*TG(i)+ k(6)*DG(i)+ k(7)*MG(i)+
k(8)*G(i))^2 - k(2)*k(6)*DG(1)/(1+ k(5)*TG(i)+ k(6)*DG(i)+
k(7)*MG(i)+ k(8)*G(i))^2;
    RK1MG = k(2)*k(6)*DG(1)/(1+ k(5)*TG(i)+ k(6)*DG(i)+ k(7)*MG(i)+
k(8)*G(i))^2 - k(3)*k(7)*MG(1)/(1+ k(5)*TG(i)+ k(6)*DG(i)+
k(7)*MG(i)+ k(8)*G(i))^2 + k(4)*k(6)*MG(1)/(1+ k(5)*TG(i)+
k(6)*DG(i)+ k(7)*MG(i)+ k(8)*G(i))^2;
    RK1G = k(3)*k(7)*MG(1)/(1+ k(5)*TG(i)+ k(6)*DG(i)+ k(7)*MG(i)+
k(8)*G(i))^2 - k(4)*k(8)*MG(1)/(1+ k(5)*TG(i)+ k(6)*DG(i)+
k(7)*MG(i)+ k(8)*G(i))^2;
    %RK1FAME = k(1)*k(4)*TG(1)/(1+ k(4)*TG(i)+ k(5)*DG(i)+
k(6)*MG(i)+ k(7)*G(i)+ k(8)*FAME(i))^2 + k(2)*k(5)*DG(1)/(1+
k(4)*TG(i)+ k(5)*DG(i)+ k(6)*MG(i)+ k(7)*G(i)+ k(8)*FAME(i))^2 +
k(3)*k(6)*MG(1)/(1+ k(4)*TG(i)+ k(5)*DG(i)+ k(6)*MG(i)+ k(7)*G(i)+
k(8)*FAME(i))^2;
    %%%%%%%%%%%%%%%%%%%%%%%%%%%%%%%%%%%%%%%%%%%%%%%%%%%%%%%%%%%%%%%%%%%%%%%%%
    fTG1 = TG(i)+ RK1TG*h/2;
    fDG1 = DG(i)+ RK1DG*h/2;
    fMG1 = MG(i)+ RK1MG*h/2;
    fG1 = G(i)+ RK1G*h/2;
    %fFAME1 = FAME(i) + RK1FAME*h/2;
    %%%%%%%%%%%%%%%%%%%%%%%%%%%%%%%%%%%%%%%%%%%%%%%%%%%%%%%%%%%%%%%%%%%%%%%%%
    RK2TG = -k(1)*k(5)*fTG1/(1+ k(5)*fTG1+ k(6)*fDG1+ k(7)*fMG1+
k(8)*fG1)^2;
    RK2DG = k(1)*k(5)*fTG1/(1+ k(5)*fTG1+ k(6)*fDG1+ k(7)*fMG1+
k(8)*fG1)^2 - k(2)*k(6)*fDG1/(1+ k(5)*fTG1+ k(6)*fDG1+ k(7)*fMG1+
k(8)*fG1)^2;
    RK2MG = k(2)*k(6)*fDG1/(1+ k(5)*fTG1+ k(6)*fDG1+ k(7)*fMG1+
k(8)*fG1)^2 - k(3)*k(7)*fMG1/(1+ k(5)*fTG1+ k(6)*fDG1+ k(7)*fMG1+
k(8)*fG1)^2 + k(4)*k(6)*fG1/(1+ k(5)*fTG1+ k(6)*fDG1+ k(7)*fMG1+
k(8)*fG1)^2 ;
    RK2G = k(3)*k(7)*fMG1/(1+ k(5)*fTG1+ k(6)*fDG1+ k(7)*fMG1+
k(8)*fG1)^2 - k(4)*k(8)*fG1/(1+ k(5)*fTG1+ k(6)*fDG1+ k(7)*fMG1+
k(8)*fG1)^2;

```

```

%RK2FAME = k(1)*k(4)*fTG1/(1+ k(4)*fTG1+ k(5)*fDG1+ k(6)*fMG1+
k(7)*fG1+ k(8)*fFAME1)^2 + k(2)*k(5)*fDG1/(1+ k(4)*fTG1+ k(5)*fDG1+
k(6)*fMG1+ k(7)*fG1+ k(8)*fFAME1)^2 + k(3)*k(6)*fMG1/(1+ k(4)*fTG1+
k(5)*fDG1+ k(6)*fMG1+ k(7)*fG1+ k(8)*fFAME1)^2;
%%%%%%%%%%%%%%%%%%%%%%%%%%%%%%%%%%%%%%%%%%%%%%%%%%%%%%%%%%%%%%%%%%%%%%%%
fTG2 = TG(i)+ RK2TG*h/2;
fDG2 = DG(i)+ RK2DG*h/2;
fMG2 = MG(i)+ RK2MG*h/2;
fG2 = G(i)+ RK2G*h/2;
%fFAME2 = FAME(i) + RK2FAME*h/2;
%%%%%%%%%%%%%%%%%%%%%%%%%%%%%%%%%%%%%%%%%%%%%%%%%%%%%%%%%%%%%%%%%%%%%%%%
RK3TG = -k(1)*k(5)*fTG2/(1+ k(5)*fTG2+ k(6)*fDG2+ k(7)*fMG2+
k(8)*fG2)^2;
RK3DG = k(1)*k(5)*fTG2/(1+ k(5)*fTG2+ k(6)*fDG2+ k(7)*fMG2+
k(8)*fG2)^2- k(2)*k(6)*fDG2/(1+ k(5)*fTG2+ k(6)*fDG2+ k(7)*fMG2+
k(8)*fG2)^2;
RK3MG = k(2)*k(6)*fDG2/(1+ k(5)*fTG2+ k(6)*fDG2+ k(7)*fMG2+
k(8)*fG2)^2 - k(3)*k(7)*fMG2/(1+ k(5)*fTG2+ k(6)*fDG2+ k(7)*fMG2+
k(8)*fG2)^2 + k(4)*k(8)*fG2/(1+ k(5)*fTG2+ k(6)*fDG2+ k(7)*fMG2+
k(8)*fG2)^2;
RK3G = k(3)*k(7)*fMG2/(1+ k(5)*fTG2+ k(6)*fDG2+ k(7)*fMG2+
k(8)*fG2)^2 - k(4)*k(8)*fG2/(1+ k(5)*fTG2+ k(6)*fDG2+ k(7)*fMG2+
k(8)*fG2)^2;
%RK3FAME = k(1)*k(4)*fTG2/(1+ k(4)*fTG2+ k(5)*fDG2+ k(6)*fMG2+
k(7)*fG2+ k(8)*fFAME2)^2 + k(2)*k(5)*fDG2/(1+ k(4)*fTG2+ k(5)*fDG2+
k(6)*fMG2+ k(7)*fG2+ k(8)*fFAME2)^2 + k(3)*k(6)*fMG2/(1+ k(4)*fTG2+
k(5)*fDG2+ k(6)*fMG2+ k(7)*fG2+ k(8)*fFAME2)^2;
%%%%%%%%%%%%%%%%%%%%%%%%%%%%%%%%%%%%%%%%%%%%%%%%%%%%%%%%%%%%%%%%%%%%%%%%
fTG3 = TG(i)+ RK3TG*h;
fDG3 = DG(i)+ RK3DG*h;
fMG3 = MG(i)+ RK3MG*h;
fG3 = G(i)+ RK3G*h;
%fFAME3 = FAME(i) + RK3FAME*h/2;
%%%%%%%%%%%%%%%%%%%%%%%%%%%%%%%%%%%%%%%%%%%%%%%%%%%%%%%%%%%%%%%%%%%%%%%%
RK4TG = -k(1)*k(5)*fTG3/(1+ k(5)*fTG3+ k(6)*fDG3+ k(7)*fMG3+
k(8)*fG3)^2;
RK4DG = k(1)*k(5)*fTG3/(1+ k(5)*fTG3+ k(6)*fDG3+ k(7)*fMG3+
k(8)*fG3)^2 - k(2)*k(6)*fDG3/(1+ k(5)*fTG3+ k(6)*fDG3+ k(7)*fMG3+
k(8)*fG3)^2;
RK4MG = k(2)*k(6)*fDG3/(1+ k(5)*fTG3+ k(6)*fDG3+ k(7)*fMG3+
k(8)*fG3)^2 - k(3)*k(7)*fMG3/(1+ k(5)*fTG3+ k(6)*fDG3+ k(7)*fMG3+
k(8)*fG3)^2 + k(4)*k(8)*fG3/(1+ k(5)*fTG3+ k(6)*fDG3+ k(7)*fMG3+
k(8)*fG3)^2;
RK4G = k(3)*k(7)*fMG3/(1+ k(5)*fTG3+ k(6)*fDG3+ k(7)*fMG3+
k(8)*fG3)^2 - k(4)*k(8)*fG3/(1+ k(5)*fTG3+ k(6)*fDG3+ k(7)*fMG3+
k(8)*fG3)^2;
% RK4FAME = k(1)*k(4)*fTG3/(1+ k(4)*fTG3+ k(5)*fDG3+ k(6)*fMG3+
k(7)*fG3+ k(8)*fFAME3)^2 + k(2)*k(5)*fDG3/(1+ k(4)*fTG3+ k(5)*fDG3+
k(6)*fMG3+ k(7)*fG3+ k(8)*fFAME3)^2 + k(3)*k(6)*fMG3/(1+ k(4)*fTG3+
k(5)*fDG3+ k(6)*fMG3+ k(7)*fG3+ k(8)*fFAME3)^2;
%%%%%%%%%%%%%%%%%%%%%%%%%%%%%%%%%%%%%%%%%%%%%%%%%%%%%%%%%%%%%%%%%%%%%%%%
TG(i+1) = TG(i) + (RK1TG + 2*RK2TG + 2*RK3TG + RK4TG)*h/6;
DG(i+1) = DG(i) + (RK1DG + 2*RK2DG + 2*RK3DG + RK4DG)*h/6;
MG(i+1) = MG(i) + (RK1MG + 2*RK2MG + 2*RK3MG + RK4MG)*h/6;
G(i+1) = G(i) + (RK1G + 2*RK2G + 2*RK3G + RK4G)*h/6;
%FAME(i+1) = FAME(i) + (RK1FAME + 2*RK2FAME + 2*RK3FAME +
RK4FAME)*h/6;
t(i+1) = t(i) + h;

```


CURRICULUM VITAE

NAME : Mr. Kasamar PETCHTABTIM

BIRTH DATE : June 13, 1980

BIRTH PLACE : Trang, Thailand

EDUCATION	:	<u>YEAR</u>	<u>INSTITUTE</u>	<u>DEGREE/DIPLOMA</u>
		2003	King Mongkut's Institute of Technology Ladkrabang	B.Sci.. Environmental Chemistry
		2009	Kasetsart University	M.E. (Chemical Engineering)

WORK PLACE : Faculty of Engineering, Kasetsart University and Thailand
Institute of Scientific and Technological Research (TISTR)